COMBINING MULTIPLE COMPONENTS OF InfiniTEM® ELECTROMAGNETIC DATA TO BETTER REPRESENT SUBSURFACE ANOMALIES

ADAM MERCER

Combining multiple components of InfiniTEM® electromagnetic data to better represent subsurface anomalies

by

Adam Mercer

A thesis submitted to the

School of Graduate Studies

in partial fulfillment of the requirements for the degree of

Master of Science

Department of Earth Sciences

Memorial University of Newfoundland and Labrador

December 2012

St. John's Newfoundland and Labrador

ABSTRACT

Time-domain electromagnetic (TDEM) surveys rely on electromagnetic induction from a time varying magnetic field to produce recordable responses from conductive material in the subsurface. Interpretation of TDEM data is dependent on the location of a conductor in relation to the primary field of the transmitter and therefore can be very complicated. This is especially true for the InfiniTEM® figure 8 transmitter configuration where the same vertical conducting plate can produce a variety of signatures depending on its location relative to the transmitter loop. This study investigates the usefulness of the energy envelope processing technique to combine multiple components of InfiniTEM® survey data to remove the directional dependance on the primary field. The energy envelope involves adding the vertical and horizontal components responses with associated Hilbert transforms in quadrature to create a single profile peaking over the location of an anomaly. This approach provides a more intuitive contour map for interpretation.

ACKNOWLEDGMENTS

Attending graduate school has been a great opportunity, that would not have possible without the encouragement and support of many people. I have been very fortunate to attend a university with such high caliber faculty who are at the top their field. I would like to thank my advisor, Dr. Colin G. Farquharson, for his guidance and patience throughout. He has been a huge influence over the past three years and the driving force behind this project. I would also like to thank my co-supervisor, Dr. Charles Hurich. His expertise allowed me to persevere in some of the most challenging aspects of this project. A special thanks goes to my technical advisor Circé Malo-Lalande. Her knowledge and industry background made this project an extremely rewarding experience. I would also like to express my gratitude Abitibi Geophysics and the Natural Sciences and Engineering Research Council of Canada for their financial assistance. Without their support this project would not have been possible. I would also like to thank my family and friends for their encouragement throughout my university career.

TABLE OF CONTENTS

CHAPTER 5

CHAPTER 6

CHAPTER 7

LIST OF FIGURES

CHAPTER 1

INTRODUCTION

Like most geophysical methods, interpretation tools for electromagnetic (EM) data have greatly improved over the years. Processing techniques are being developed to isolate anomalies and characterize their response. This study will show the effectiveness of combining multiple components of time domain electromagnetic (TDEM) data to develop a consistent response that is easily interpretable

The technique used here, called the 'energy envelope', was initially investigated to introduce an alternative approach to processing airborne EM data (Smith and Keating, 1996). During an airborne EM survey, alternating flight paths on adjacent survey lines produce contrasting responses from the measured secondary field components of a conducting unit in the subsurface. The same is applies to measurements taken relative to the primary field in a surface TDEM survey. The energy envelope technique combines responses of the vertical and horizontal components with associated Hilbert transforms into one profile and removes the directional dependance on the primary field (see Figure 1.1). The energy envelope gives a single obvious peak directly over a conducting body, in contrast to the various side-lobes and cross-overs in the three-component profiles. This is very similar to the analytical method used on potential field data, e.g. magnetics, which removes any geographical dependance it might have in relation to regional magnetic trends (Bournas and Haydar, 2001).

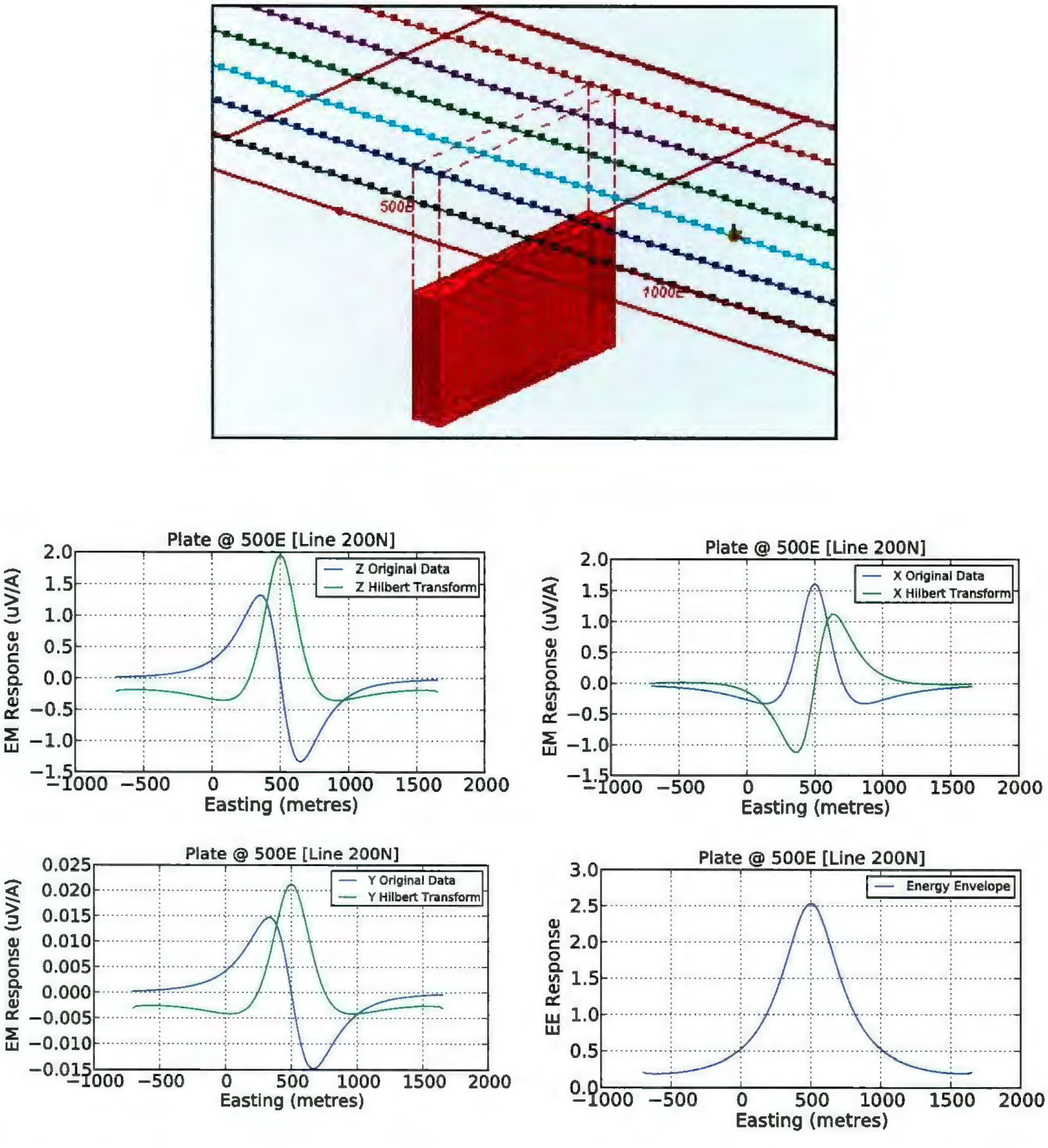

Figure 1.1. The *z*, *x*, and *y* component profiles of a conductive plate in a TDEM survey. Blue line indicates original profile and the green line represents the Hilbert transformed quantity of the original signal, as shown in label in upper right corner. Scale on top three graphs corresponds to EM Response measured in μV/A. Bottom right profile shows energy envelope profile using all components and scale corresponds to EE Response. Bottom scale indicates Easting position in metres. This example is described in full in Chapter 4.

An important aspect of TDEM surveys is the geometrical relationship of the primary field generated by the transmitter and the orientation of the desired target. The shape and location of the target define the optimum configuration of the transmitter loop and survey lines, which play an important role in the intensity and response from that target. A conductive body may produce a positive maximum, negative minimum or a cross-over in each of the *x*, *y* and *z* components depending on its location relative to the primary field.

A rectangular transmitting loop is most commonly used for TDEM surveys. It is easily deployable and can be positioned to optimize EM coupling with the conductive target to produce the strongest response. For deeply buried and steeply dipping conductors, the rectangle loop is limited because it has to be placed far from the target to maximize EM coupling direction, resulting in a relatively weak intensity of the primary field which in turn produces a weaker response from the target. This study will concentrate on the InfiniTEM® Figure 8 transmitter loop developed by Abitibi Geophysics and SOQUEM (see Figure 1.2). The InfiniTEM® is a new configuration that generates a strong horizontal primary field that is specifically designed to maximize coupling with steeply dipping and deeply buried base-metal targets. It was initially modeled after the Figure 8 loop of Macnae (1978), with a roving receiver taking measurements along survey lines inside the transmitting loop. This configuration consists of two rectangle loops connected in series with a variable spacing between them.

a.

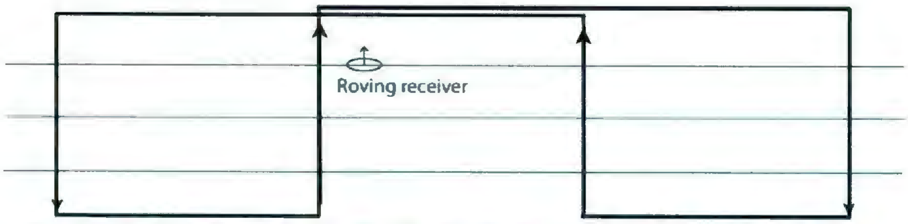

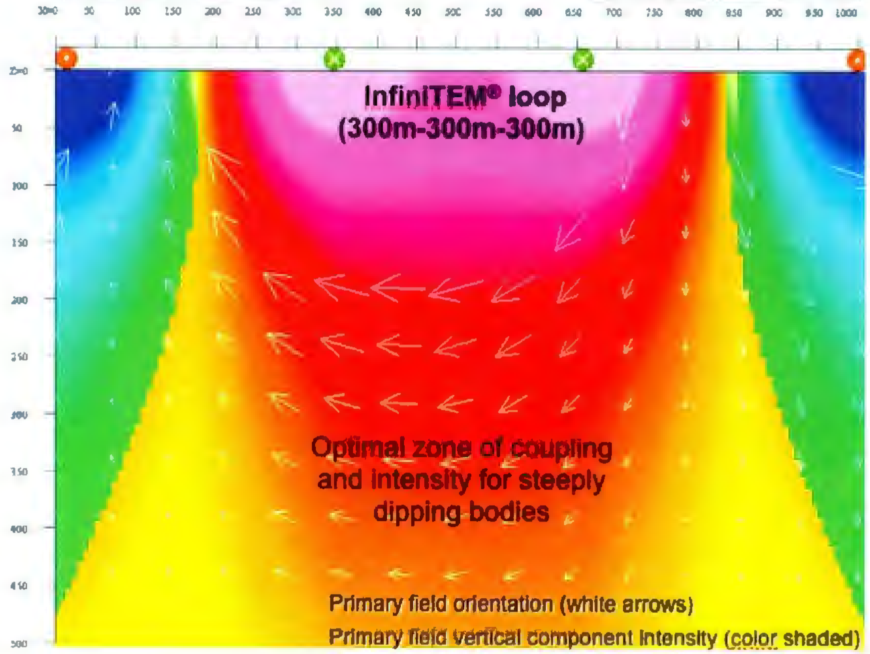

b.

Figure 1.2 (a). InfiniTEM® TDEM transmitter loop configuration. Black line indicates the transmitter loop and arrows show direction of the current path from the transmitter. Thin black lines show location of survey lines. (b). Cross section view of the primary magnetic field. Arrows indicate the direction of the primary magnetic field. Red/warm colors show positive polarity and blue/cool colors show negative polarity. The hue of the color indicates the strength of the field in that location (per. comm. Malo-Lalande).

A drawback of using dual loops with opposite polarities, as illustrated in Figure 1.2b, is that anomalous signatures can vary significantly throughout the survey area due to the change in primary field orientation. A conductive body with the same size and shape can produce different responses depending on its location within the transmitting configuration. The energy envelope technique provides the potential for a consistent response, regardless of the conductors location, and removes the directional dependance on the primary field. This study will show the effectiveness of this technique on InfiniTEM® survey data in a of variety synthetic and field examples.

Chapter 2 presents the time-domain electromagnetic method. Chapter 3 will introduce the InfiniTEM® system. In Chapter 4, a detailed description of the processing techniques used in the thesis is given and also includes a brief summary of the computer code that was written to implement the energy envelope technique for InfiniTEM® data. An extensive range of synthetic examples is provided in Chapter 5, illustrating the effectiveness of this technique with the InfiniTEM® configuration. These examples cover a variety of plate sizes, locations and orientations to exhibit the dexterity and also the limitations of the algorithm. Chapter 6 provides 4 examples of field data acquired from actual InfiniTEM® surveys that will show the benefits of using this approach in a variety of geological environments.

CHAPTER 2

THE TIME-DOMAIN ELECTROMAGNETIC METHOD

TDEM surveys are some of the most common and effective methods for base metal exploration. The TDEM technique relies on electromagnetic induction within a conductive medium to generate a recordable response from the subsurface (Nabighian & Macnae, 1987). The fundamental properties of this survey are best described through Maxwell's electromagnetic equations, in particular Ampère's, Faraday's Law, and Ohm's Law.

Ampère's Law $$\nabla \times \vec{H} = \vec{J} \tag{1}$$

Faraday's Law $$\nabla \times \vec{E} = -\frac{\partial \vec{B}}{\partial t} \tag{2}$$

Ohm's Law $$\vec{J} = \sigma \vec{E} \tag{3}$$

Where $\vec{H}$ is the magnetic field intensity, $\vec{J}$ is the current density, $\vec{E}$ indicates the electric field, and $\vec{B}$ indicates the magnetic field. For this study the quasi-static assumption is assumed valid where all time-variations in the TDEM method are relatively slow compared to the time for light to travel across the survey area (Grant and West, 1965).

In Time-domain surveys the current is cycled on and off at predetermined intervals. An example of the waveform used in the InfiniTEM® survey can be seen in Figure 2.1, which is also known as step function excitation (Nabighian & Macnae, 1987). As the transmitter current waveform varies, Ampére's Law implies there is a time-varying magnetic field (Figure 2.2).

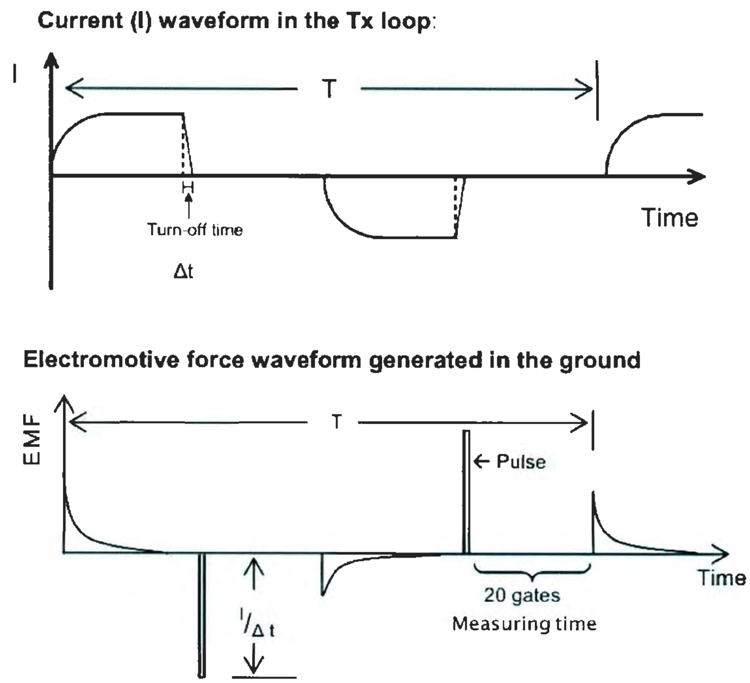

Figure 2.1. Top panel: diagram of the ramp frequency, turn on and off times used in typical TDEM systems including InfiniTEM®. Bottom panel: resulting EMF from the decay in the electric field (per. comm. Malo-Lalande).

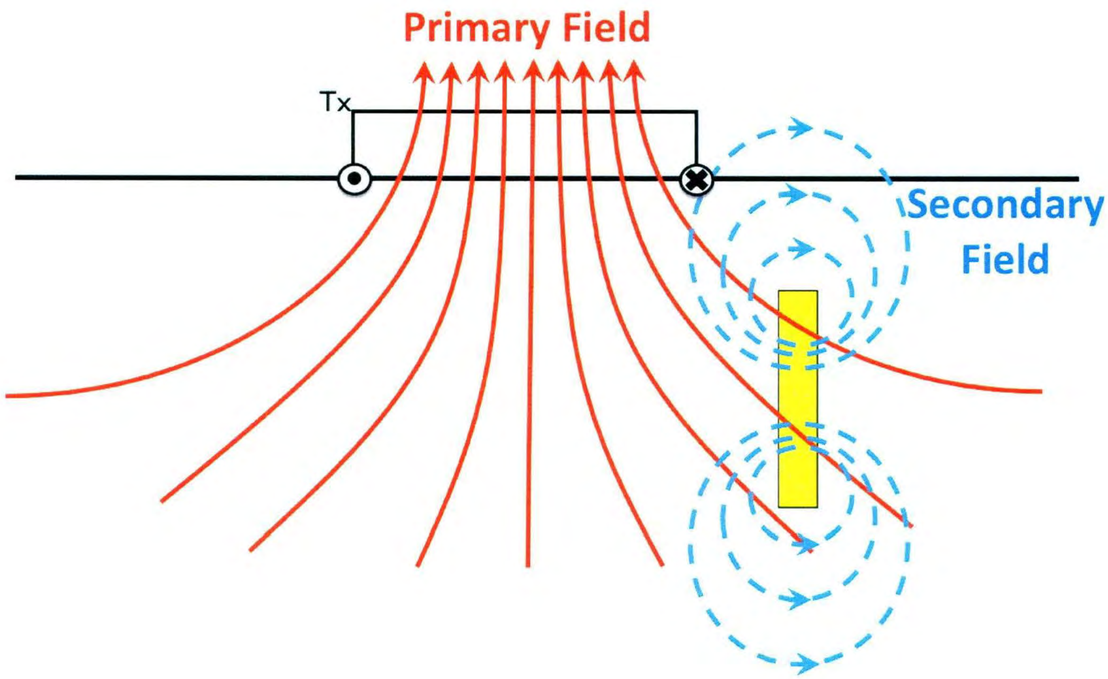

Figure 2.2. Cross section view of primary and secondary magnetic field direction of conventional square loop TDEM survey. Red and blues arrows indicate direction of primary and secondary magnetic field, respectively.

In order to simplify modelling and interpretation, the transmitter current is held constant for an established amount of time. This allows the currents generated by the switch on to decay by the time the current is turned off. The latter switch off gives rise to another time-varying magnetic field, which is what is normally measured and modelled. According to Faraday's Law, equation (2), the time varying magnetic field, $-\partial B/\partial t$, will induce an electric field, $\vec{E}$, that will interact with any conductive bodies in the subsurface. The induced electric field causes eddy currents to flow in a conductive body, as stated by Ohm's Law, equation (3), the magnitude of which are dependant on the conductivity, σ, of the body. The strength of the induced current also depends on the relative orientation of the inducing magnetic field and the conductive target, also known as 'coupling'. The strength of the coupling and induced current is greatest when the inducing field is perpendicular to the conductive body. These eddy currents generate a magnetic field by Ampère's Law, equation (1), which can be measured at the surface. Grant and West (1965) state that these current will initially be confined to the surface of the conductor but will immediately start to dissipate throughout the conductor due to Ohmic losses. The decreasing currents will have a decreasing magnetic field, which will induce smaller currents further inside the body. This process is described by Nabighian & Macnae (1987) as the inward diffusion of the current pattern and it will continue until generated currents have vanished. The secondary magnetic field produced from this process provides information pertaining to the size and conductivity of the subsurface conductor. The higher the 'quality' of the conductor the longer this diffusion process will take to dissipate.

A variety of receivers can be used in TDEM. The most common is a coil which records the time rate of change of the secondary field, i.e. dB/dt, at preset time intervals, called channels or gates, after the primary field is sharply terminated. By recording in the transmitter current off cycle and without the presence of the primary field, as for InfiniTEM®, it is much easier to decipher the considerably smaller secondary field. Since the receiver is not influenced by the field from the transmitter while taking a reading, its gain can be much higher and therefore the signal from greater depths can be detected. The transmitter pulse and measurements are repeated multiple times which then can be stacked to enhance the signal-to-noise ratio. The measurement of the rate of decay in the magnetic field produced by the eddy currents provides information pertaining to the conductivity of the bodies. A good conductor is characterized by an anomalous response throughout the later channels of the decay, where as the response of a poor quality conductor may be only visible over early time channels (Nabighian & Macnae, 1987). Their location and orientation are determined by the amplitude measured along some profile.

Figure 2.1 shows the primary magnetic field waveform generated by the transmitter (top panel) and the primary electric field (electromotive force) produced as the magnetic field changes with time (bottom panel). The top panel illustrates the time intervals during which the transmitter produces current, and how the current is reduced over a specific period of time (ramp time/time off). As the current is ramped down it produces a time varying magnetic field that gives rise to a primary electric field (induced electromotive force, EMF), as shown in the bottom panel. As previously stated, the electric field will produce eddy currents in the subsurface that decay over time. The magnitude and rate of decay of the secondary field of the eddy currents, which are dependant on the location, size, orientation and conductivity of the body, and are measured by the receiver.

Generally, as is the case for InfiniTEM®, large loop transmitter surveys are conducted by taking measurements at evenly spaced stations on picketed survey lines normal to the geological strike (see Figure 2.3)

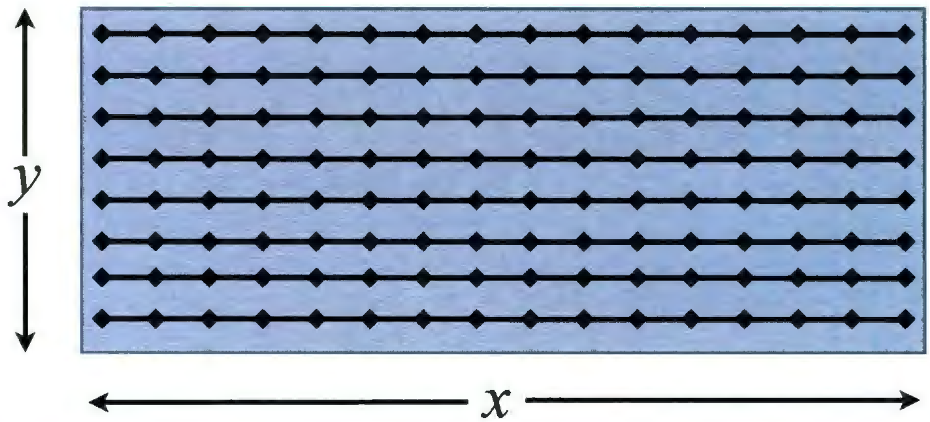

Figure 2.3. Illustration of typical TDEM survey design. Individual stations are indicated by black diamonds on each line. x and y directions shown by arrows on bottom and left hand side of Figure, respectively.

At each station, the decays of the three components of the secondary dB/dt are typically recorded, (see Figure 2.4 & 2.5), in relation to a local Cartesian coordinate system, with the x direction along the survey line, y perpendicular to the survey line, and z being vertical upward direction.

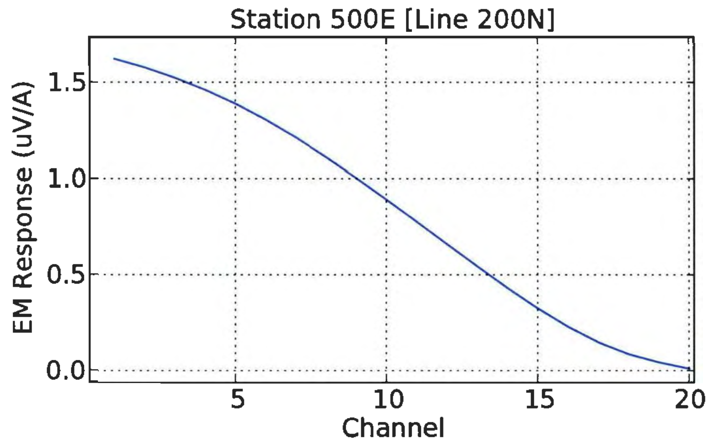

Figure 2.4. Example of x component decay of synthetic data at a single station measured in $\mu V/A$ as indicated by scale in left hand side of Figure. Bottom scale shows decay in relation to time channel in which it was recorded.

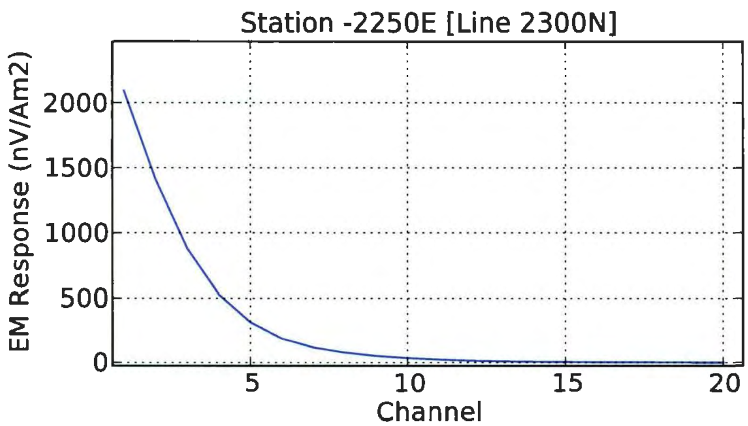

Figure 2.5. Example of x component decay of Field example 4 at a single station measured in nV/Am^2 as indicated by scale in left hand side of Figure. Bottom scale shows decay in relation to time channel in which it was recorded.

The measurements from each station are then combined to develop line profiles for each component. Qualitative interpretation of the subsurface is then based on comparison of the x, y and z component profiles of individual lines. These line profiles (see example in Figure 2.6) can then be combined to construct contour maps (see Figure 2.7) of the entire area. A table of the channel delay times is provided in APPENDIX 1.

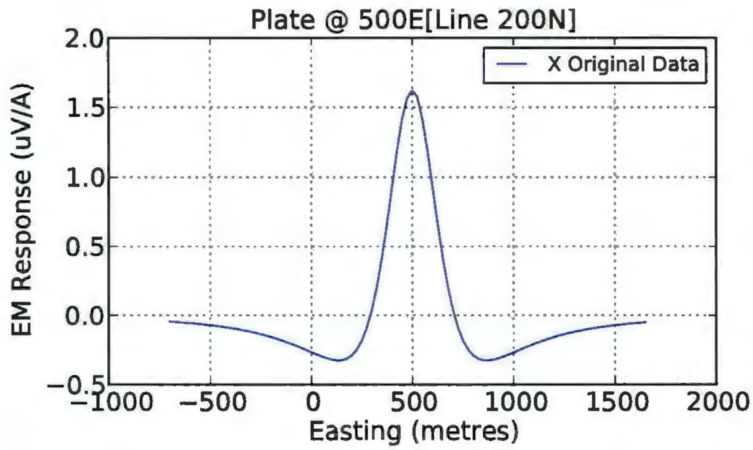

Figure 2.6. The x component profile of a vertical plate positioned at 500E. Blue line indicates original profile as shown in label in upper left corner. Scale corresponds to EM Response measured in μV/A. Bottom scale indicates Easting position in metres.

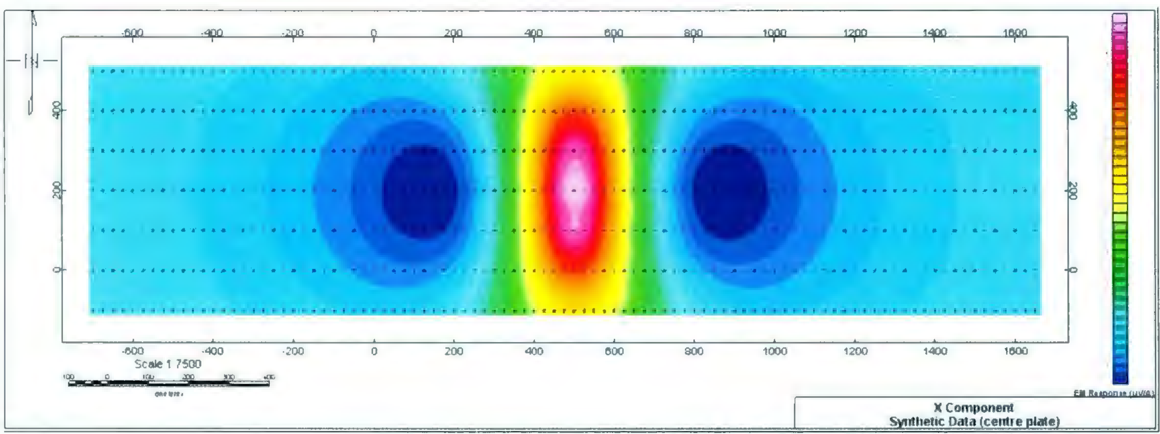

Figure 2.7. Color contour map of x components of InfiniTEM® survey. Scale on right side indicates EM Response measured in μV/A. North is oriented towards the top of the page and all relative locations are indicated by edge ticks.

CHAPTER 3

THE INFINITEM® SYSTEM

The shape and location of the transmitter loop and the configuration of survey lines are critical to the intensity of the response obtained from a subsurface conductive target (per. comm. Malo-Lalande). There are several varieties of transmitter loops that have been developed to better illuminate different shapes and sizes of conducting targets (Nabighian & Macnae 1987). Figure 3.1 provides several examples of different transmitter and receiver arrangements. For the purpose of this study we will concentrate on the configuration illustrated in panels *(e)* and *(f)*: *Large loop-single wire for transmitter* & *Large fixed transmitter loop with roving receiver*.

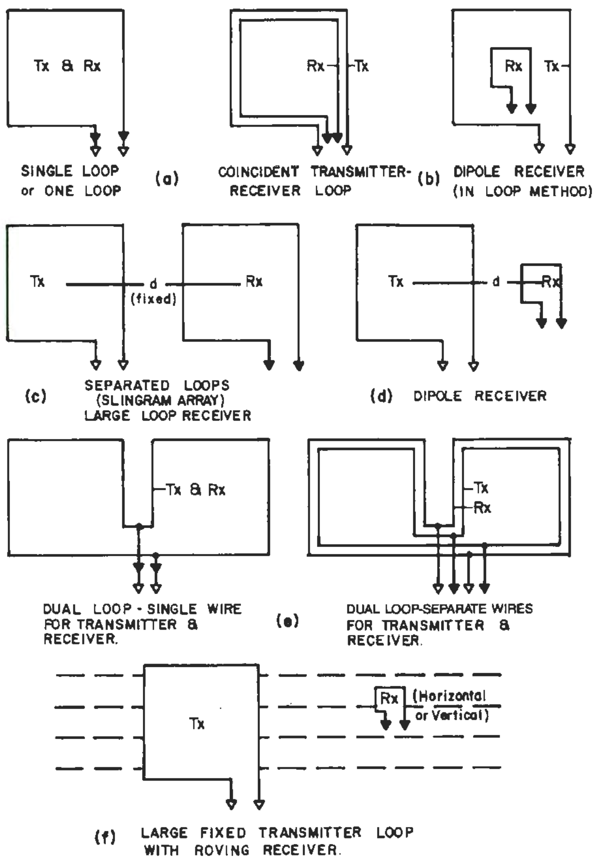

Figure 3.1. Examples of TDEM configurations. This study will focus on *(e)* and *(f)*; *Large loop-single wire for transmitter & Large fixed transmitter loop with roving receiver* (Nabighian & Macnae 1987).

The most common configuration used in base metal exploration is a single square fixed transmitter loop using a roving receiver, such as *(b)*, *(d)* and *(f)*. This set-up is very popular because it can be mobilized relatively quickly due to its simple shape. The location and direction of the primary field for this configuration can be seen in Figure 3.2.

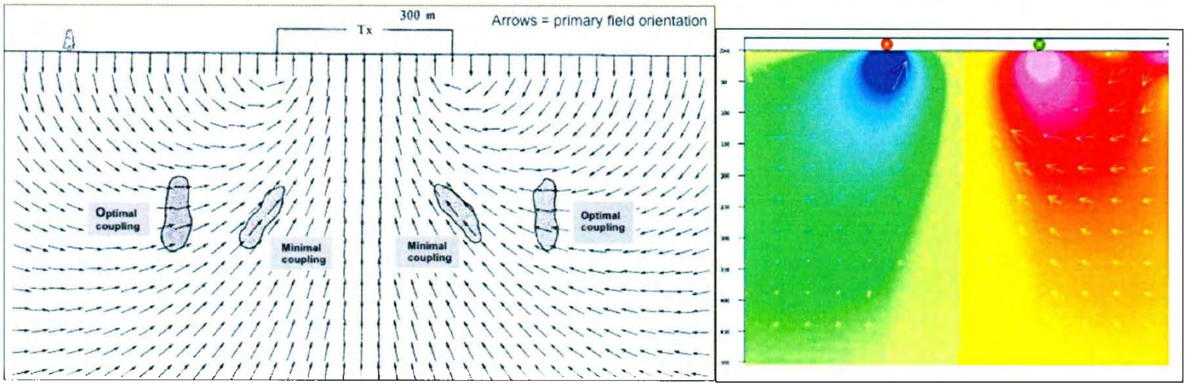

a. b.

Figure 3.2. Cross section view of primary magnetic field direction (a) and intensity (b) for conventional square loop TDEM survey. Arrows indicate direction of magnetic field, red/warm colors show positive polarity and blue/cool colors show negative polarity. The hue of the color indicates the strength of the field in that location. Panel (a) provides examples of optimal and minimal coupling situations (per. comm. Malo-Lalande).

The most critical aspect about designing the transmitter loop configuration is how the primary field interacts with any conducting bodies that may be in the subsurface. The angle at which the primary field crosses the body influences the strength of the induced currents in the body and thus the strength of the secondary field. In an ideal situation, the primary field will intersect the body orthogonally to its largest aspect and produce optimal coupling with the target (Figure 3.2 a). This will produce the strongest response for a given distance between transmitter and body. Conversely, if the primary field is parallel to the target it will produce minimal coupling and a very small and low amplitude response. So, if the target is believed to be horizontal the square transmitter loop can be placed directly over the estimated location of the body to produce optimal coupling. This is the ideal situation for a conventional square loop because the primary field will be vertical at the conductor, and the intensity of the primary field at the conductor will be strong. If the target is believed to be steeply dipping, the transmitter loop has to be placed off to one side of the target to ensure the primary field is horizontal at the target depth to maximize coupling. The drawback of using this type of configuration for a vertical target is that since the loop needs to be far away from the target the primary field intensity is dramatically reduced. It is difficult to determine the orientation of a target beforehand, but all available information must be taken into account to ensure the best configuration is used.

A great deal of established deposits are steeply dipping and sheet or cone like in structure, which makes them difficult to illuminate with a conventional square loop. The InfiniTEM® configuration developed by Abitibi Geophysics and SOQUEM consists of a distorted fixed Figure 8 loop (Figure 3.3 a) and uses a roving receiver. By using this configuration the orientation of the primary field is very different from that of the conventional square loop, and much stronger than that of just a single loop. This is an ideal configuration for investigating steeply dipping targets because the primary field is horizontal under the region between the two loops and will be normal to any steeply dipping targets in this region. This will optimize the coupling of the primary field with the target and increase the intensity of the response. InfiniTEM® measurements are taken using a roving receiver along survey lines across the entire configuration where the intensity of the primary field is the greatest.

a.

b.

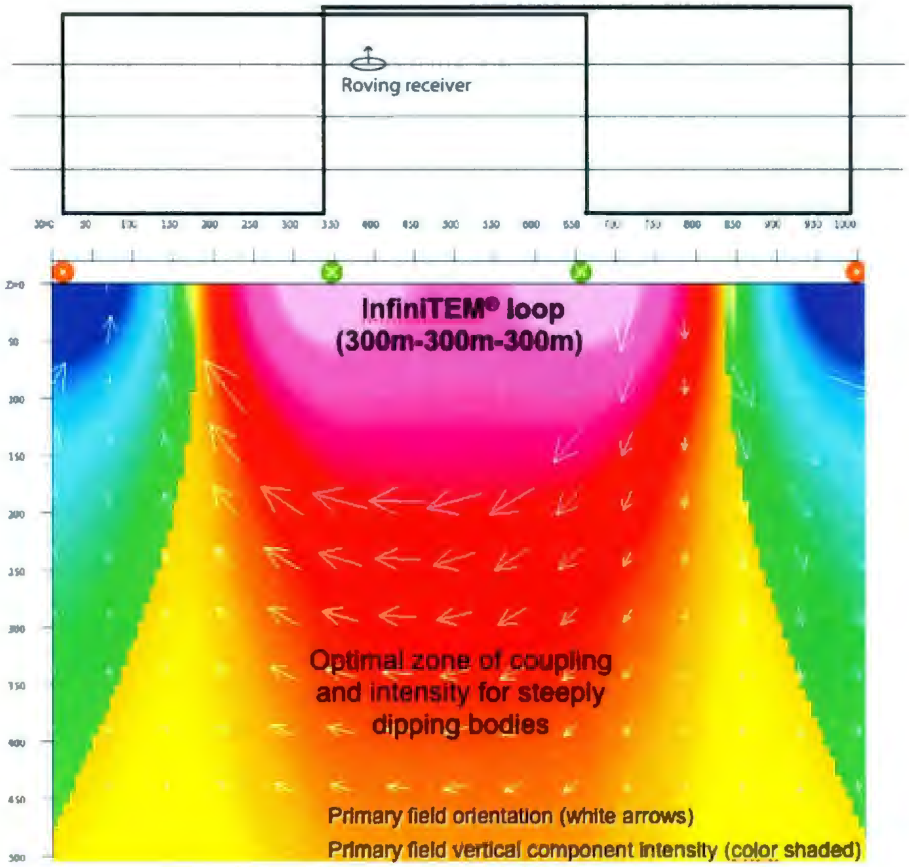

Figure 3.3 (a). InfiniTEM® TDEM transmitter loop configuration. Black line indicates the transmitter loop and arrows show direction of the current path from the transmitter. Thin black lines show location of survey lines. (b). Cross section view of the primary magnetic field. Arrows indicate the direction of the primary magnetic field. Red/warm colors show positive polarity and blue/cool colors show negative polarity. The hue of the color indicates the strength of the field in that location (per. comm. Malo-Lalande).

Generally, exploration for targets under conductive overburden is difficult because in conventional square loop geometries the primary field dissipates quickly in the overburden. As previously discussed for the conventional square loop configuration the primary field is vertical below the loop and therefore couples with the overburden. This causes the primary field to dissipate in the overburden and prevents the detection of currents from deeper conductive bodies. This is a common problem for surveys conducted in some areas of the Canadian Shield, specifically the Abitibi Greenstone Belt. For the InfiniTEM® configuration the primary field is vertical at the surface but horizontal a short distance below the surface (i.e. parallel to the overburden) which makes coupling with the overburden poor in the area between the loops. This poor coupling at the near surface preserves the primary field intensity for deeper targets and makes it possible to explore for deeper targets. Through extensive field testing Abitibi Geophysics and SOQUEM determined the distance between the two loops should not be greater than twice the width of either loop (per. comm. Malo-Lalande). This ensures sufficient distance for the superposition of the primary fields of both lobes to give a suitable horizontal primary field while providing adequate field intensity. This allows for the target to be centred between the two lobes where the primary field is the strongest and thus produce a much higher amplitude response.

Typical loop dimensions for the InfiniTEM® survey (size varies depending on location) are: 400m (loop width), 400m (loop separation) and 400m (second loop width), with the length of both loops at 800m (up to 1200m). There are generally at least 7 survey lines 100m apart, or 4 at 200m apart. Measured values are typically given in nV/Am^2, that is, values for the time derivative of the secondary magnetic field (*dB/dt*) normalized by transmitter loop current and receiver coil effective area.

CHAPTER 4

PROCESSING TECHNIQUES

When processing TDEM survey data there can be a number of peaks and troughs on each component profile that make the response of a conductor complicated to interpret. The z and x components have larger amplitude because of their orientation to the primary field and are the principle indicators of the location of an anomaly. The y component has a much lower amplitude but is used to determine lateral changes in anomalous structures orthogonal to the strike of the survey lines

The following chapter will illustrate how the same plate can produce different signatures depending on its location relative to the primary field from the transmitter, and how the energy envelope processing technique of Smith and Keating can simplify interpretation by combining all three components into one response. The motivation of applying this technique to InfiniTEM® data originated from airborne EM surveys, where a similar problem of different anomalous signatures was apparent. The algorithm developed for this project is modelled after this technique and uses a similar approach for combining the component's responses with their associated Hilbert transforms.

4.1 RESPONSES OF DISCRETE CONDUCTORS

Figures 4.1a) to 4.1d) shows synthetic data for the InfiniTEM® configuration over a vertical plate in a homogenous non-conductive half-space at different locations relative to the transmitter loop. All profiles correspond to a synthetic plate with dimensions 400m by 200m by 50m. The data was modeled using EMIT Maxwell EM imaging software with InfiniTEM® transmitter loop with dimensions: 400m (loop width), 400m (loop separation) and 400m (second loop width). A 25m station separation was used on 2375m lines. The top panels on each page show the location of the plate (the large red rectangle in lower portion of each panel) with respect to the survey grid (parallel multi coloured lines cutting across panel). The Figure 8 transmitter loop is indicated by the red lines under the survey grid. The red arrows in the vertical plane show the direction of the magnetic field produced by the transmitter. The blue and green axes indicate distance in metres. The bottom panels show profiles of the *z*, *x* and *y* components for the corresponding plate locations. The magnetic field and component profiles are shown for the survey line 200N.

As is shown in Figure 4.1, a peak on one component will align with a zero crossover on another component directly above the conductive body. Also, depending on its location relative to the transmitter loop, the same plate-like conductor can generate very different responses. In Figure 4.1(a) the plate lies outside the whole configuration and and in this case a negative to positive crossover on the *z* component profile correlates with a negative peak on the *x* component.

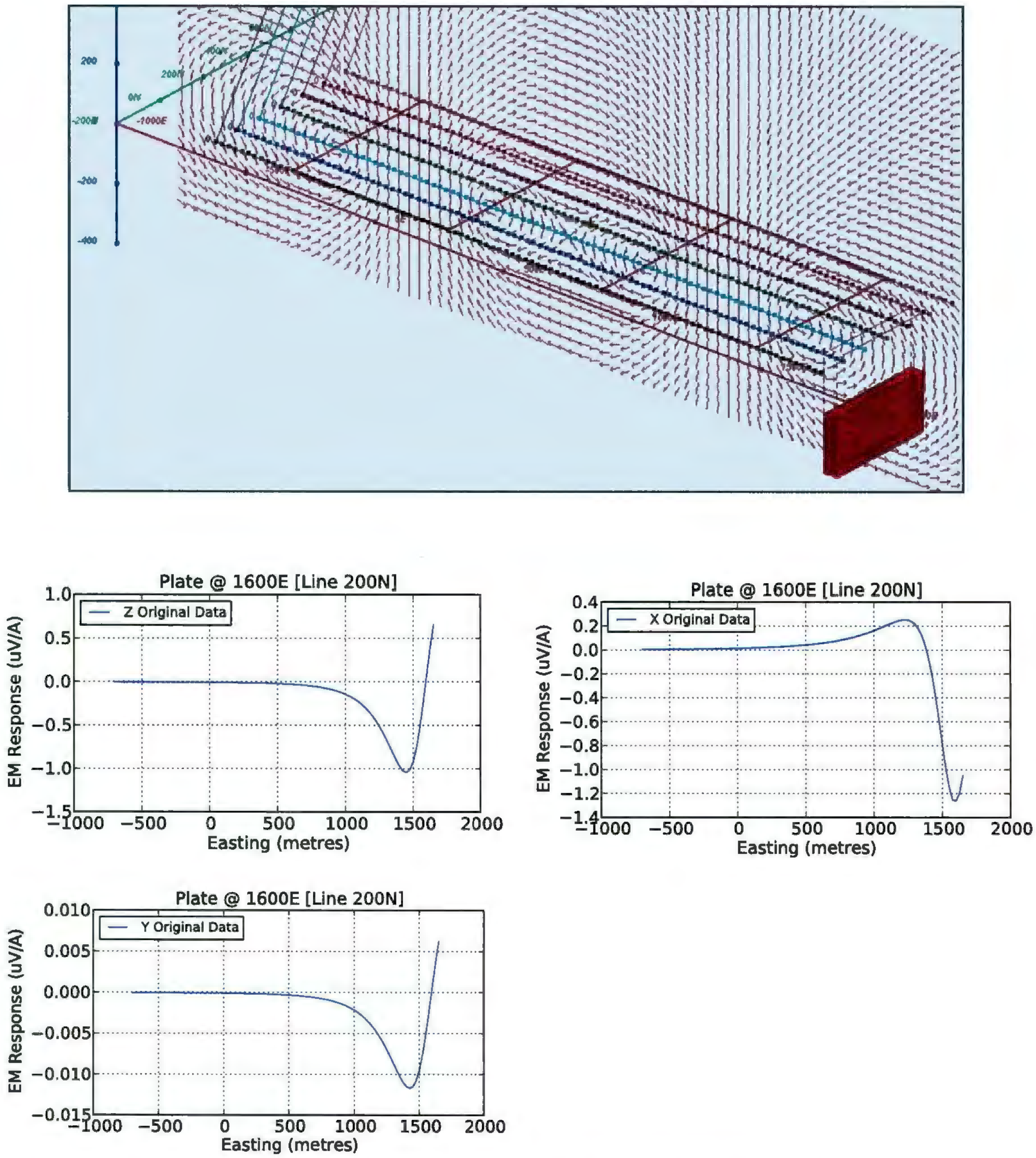

Figure 4.1. (a) The z, x, and y component profiles of a vertical plate positioned at 1600E. Blue line indicates original profile as shown in label in upper left corner. Scale on three graphs corresponds to EM Response measured in μV/A. Bottom scale indicates Easting position in metres.

As the plate moves to the centre of the right loop, Figure 4.1(b), the correlation changes to a negative peak on the *z* with a positive to negative crossover on the *x*.

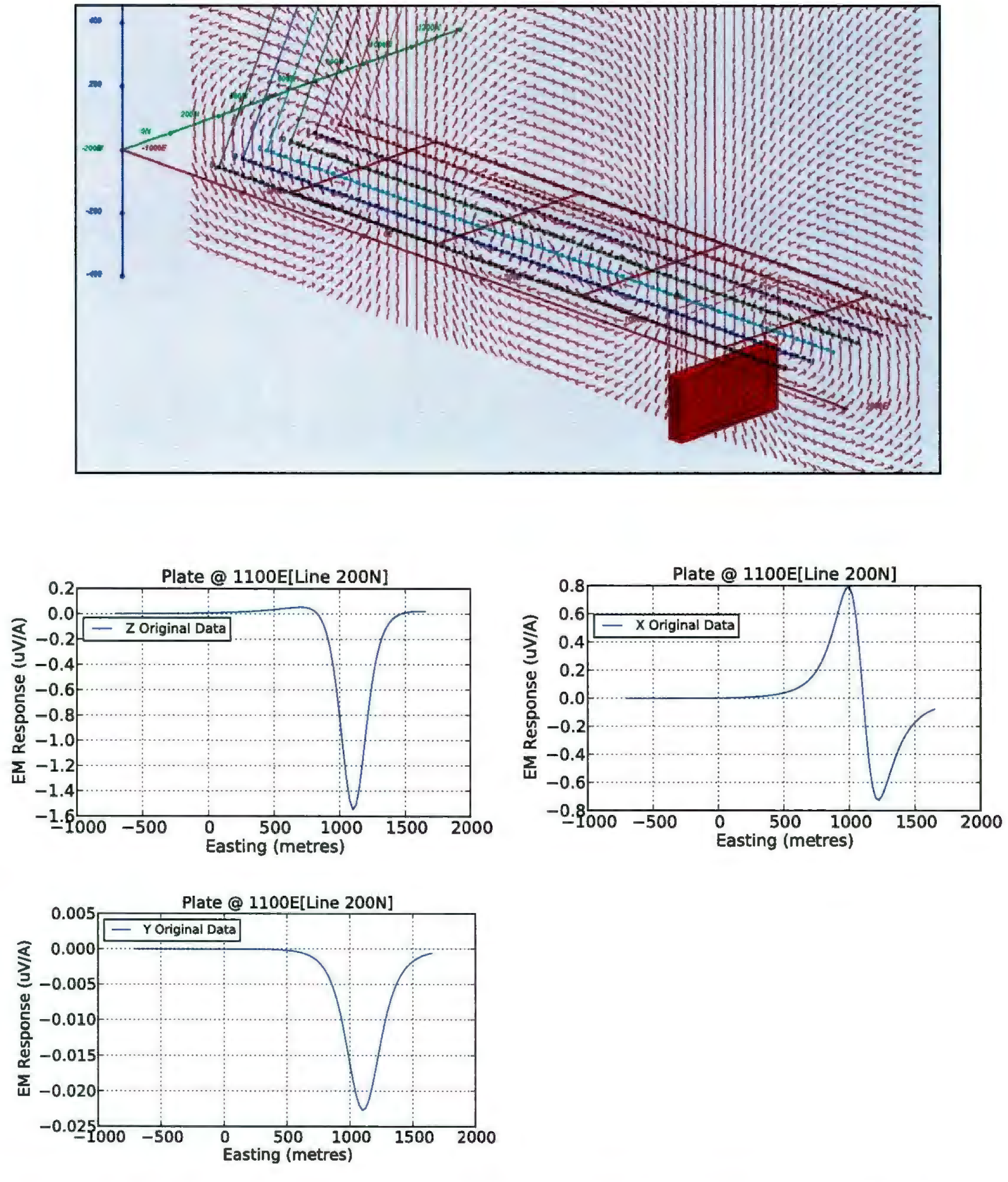

Figure 4.1. (b) The *z*, *x*, and *y* component profiles of a vertical plate positioned at 1100E. Blue line indicates original profile as shown in label in upper left corner. Scale on three graphs corresponds to EM Response measured in μV/A. Bottom scale indicates Easting position in metres.

Figure 4.1(c), with the plate in between the two loops, shows a positive to negative crossover on the *z* correlated with a positive peak on the *x*.

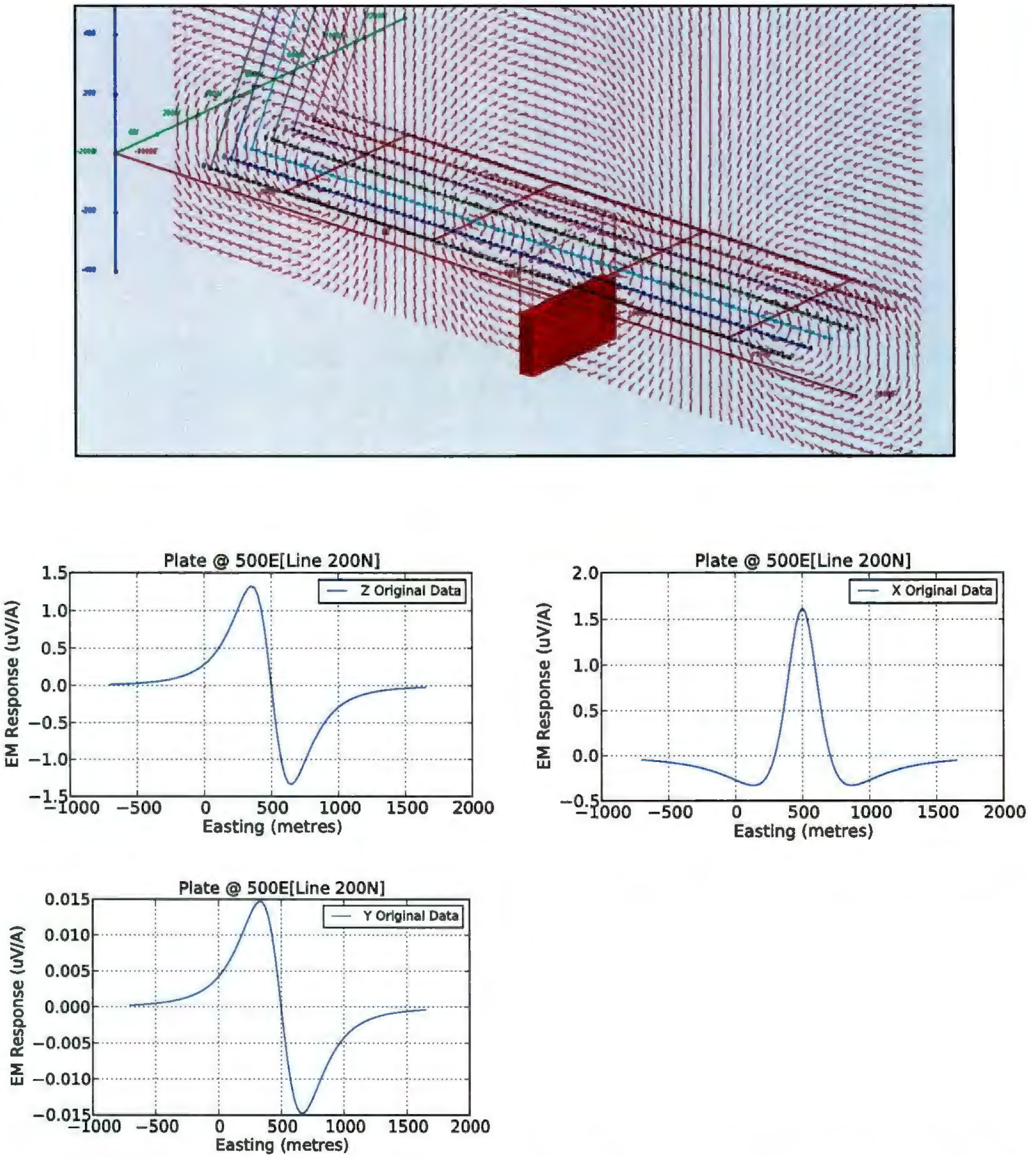

Figure 4.1. (c) The *z*, *x*, and *y* component profiles of a vertical plate positioned at 500E. Blue line indicates original profile as shown in label in upper right corner. Scale on three graphs corresponds to EM Response measured in μV/A. Bottom scale indicates Easting position in metres.

In Figure 4.1(d), the plate lies in the the centre of the left loop and again shows a similar response to the other examples but with a much different shape. The z component shows a positive peak and corresponds to a negative to positive crossover in the x component.

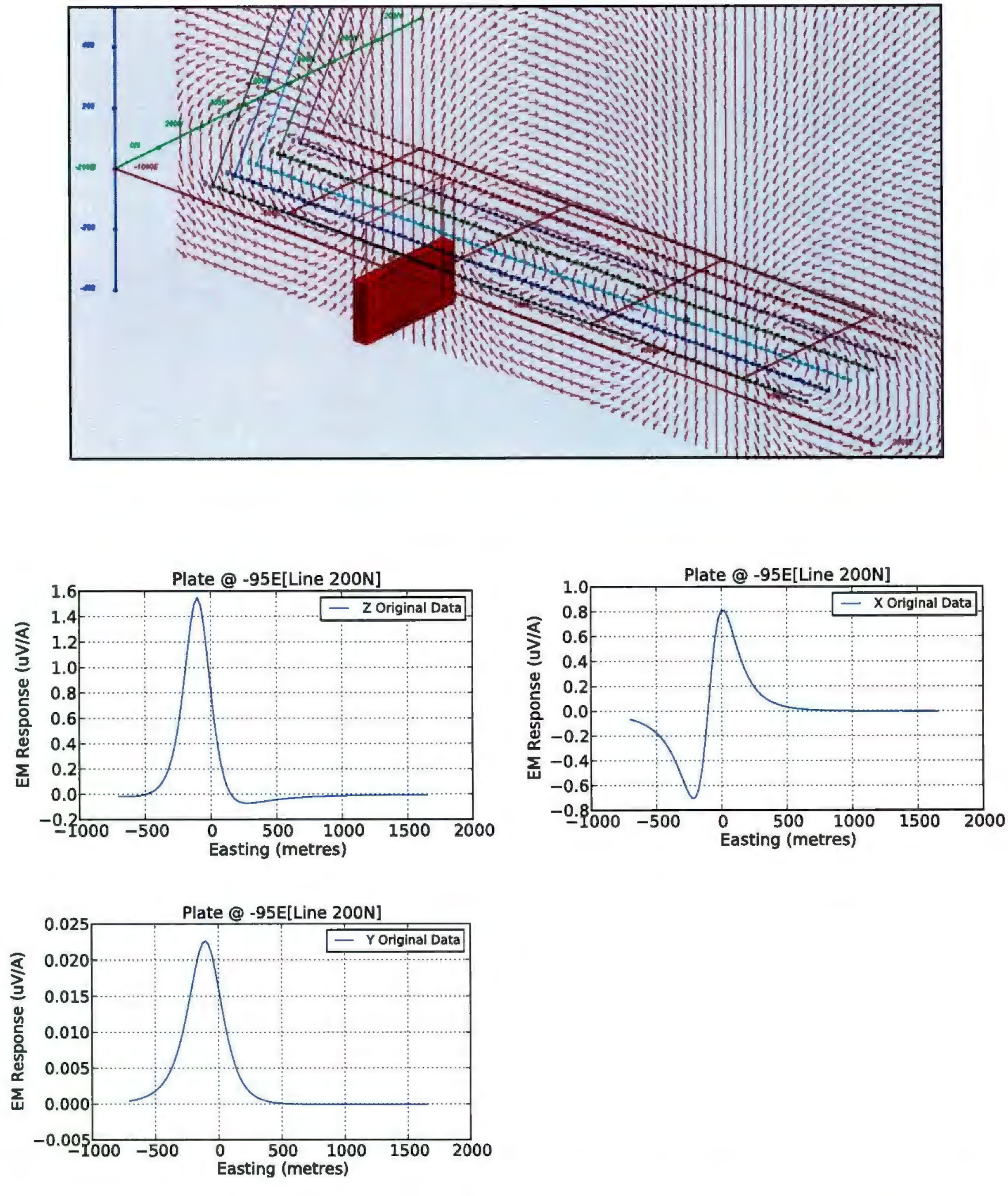

Figure 4.1. (d) The z, x, and y component profiles of a vertical plate positioned at -95E. Blue line indicates original profile as shown in label in upper right corner. Scale on three graphs corresponds to EM Response measured in μV/A. Bottom scale indicates Easting position in metres.

As discussed in Chapter 3 the response of a conductive body is dependant on its interaction with the primary field. So, when processing InfiniTEM® data it is critical to keep the direction of the primary field in perspective because it is the key to correctly assigning the shape and position of the conductor. Although the individual components have different anomalous signatures depending on the relative locations of the transmitter loop and conductor, the summation of all three components will have a much more similar signature.

Color contour maps can be developed by combining the profiles of survey lines, see for example Figure 4.2. However, because interpretation relies on comparison of peaks and zero crossover points they are not as intuitive as maps of, for example, potential field data, where an anomaly will show a single positive response on one map. As for individual line profiles these maps are created from separate x, y, and z components which are analyzed and compared to determine the location of any conductors. Similar problems arise when targets become apparent in various areas on the survey grid. The anomalies from different locations produce very different responses because of the variable coupling situation, so it is imperative to relate them to the direction of the primary magnetic field to ensure correct interpretation. By using the energy envelope to combine profiles, a conductive plate will produce a single positive anomaly regardless of its location relative to the primary field.

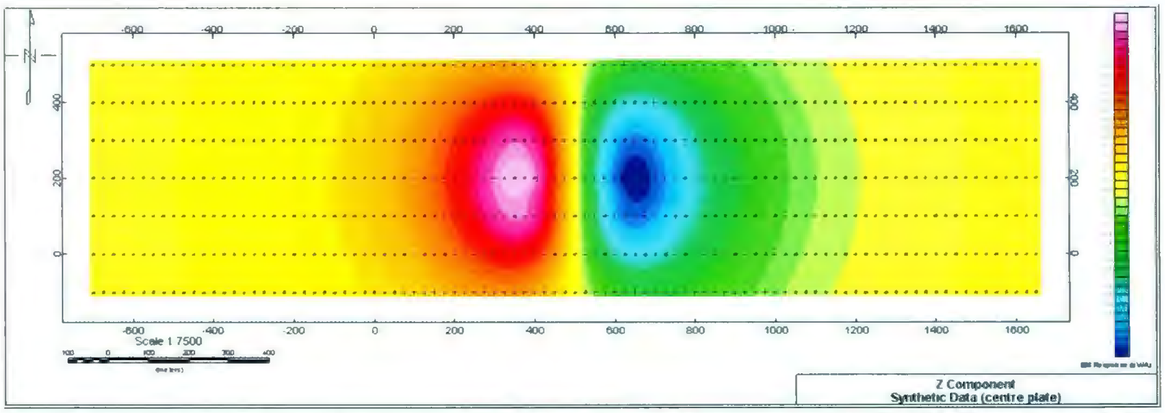

Figure 4.2. An example of the z component of an InfiniTEM® anomaly located in the centre lobe (Figure 4.1c) on a color contour map. The anomaly is indicated by negative (blue) to positive (pink) crossover.

4.2 HILBERT TRANSFORM

The Hilbert transform (HT) is used in complex signal processing as a means of transforming a signal into its analytical representation (Diniz, Silva, Netto, 2002). It uses the Fourier transform (FT) to transform the signal into the frequency domain so the amplitude and phase components can be accessed separately. A consequence of the HT is that when applied it produces a 90° phase shift of the data, where the direction of the phase shirt is dependent on the sign of the signal (-90° for positive values and +90° for negative), and is the primary role of the HT in this study. By operating on the amplitude and phase information separately the amplitude is unaffected by this phase shift. An inverse FT is then used to bring the transformed quantity back to the real domain.

Evidence of this phase shift can be seen when the HT is applied to a sine function. The HT of the sine function is cosine, with no change in amplitude, Figure 4.3 (the HT in this Figure was calculated using a subroutine within Python and will be discussed in more detail in Section 5.11). The original real function and its Hilbert transformed counterpart are called HT pairs, and can be combined these to create what is known as the analytical signal, which will be discussed in the next section.

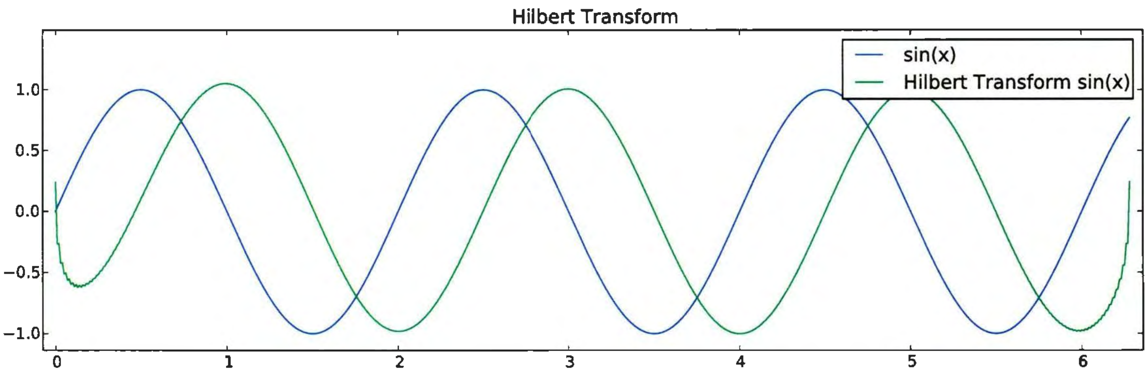

Figure 4.3. Profile of sine function, blue line, and Hilbert transform of that sin function, green line. This profile was generated using Python.

Using a FT to perform the HT on an unmodified, finite signal superimposes oscillations on the signal. The FT transform produces these oscillations from its inability to reproduce the truncated edges of the signal with a infinite sinusoid. These oscillations are then carried back to the spatial domain after the phase shift with the inverse FT. To avoid these oscillations we can extrapolate the data before the HT is performed. This will be discussed later when dealing with the edge effects resulting from performing the HT.

4.3 ANALYTIC SIGNAL

The analytic representation of a signal makes it possible to manipulate that signal as a complex number and facilitates a variety of processing techniques that are particularly useful in geophysics. The analytical signal, $f_A(x)$, of a real one-dimensional signal is defined as (Gabor, 1946):

$$f_A(x) = f(x) + if_H(x) \tag{4}$$

Where $f_H(x)$ is the Hilbert transform of the original signal, $f(x)$. From the analytical representation the 'envelope' of the signal can be calculated.

$$|f_A(x)| = \sqrt{f^2(x) + f_H^2(x)} \tag{5}$$

The envelope can be used to estimate the total amplitude at a particular point in the signal and is a common tool when processing oscillating arrays.

The analytic signal is also used in processing static magnetic data (Bournas and Haydar, 2001) and is very similar to the energy envelope used in this study. The initial response of a magnetic anomaly is dependent on its location relative to the Earth's magnetic field. Two bodies with the same size, shape and mineral concentration will produce different signatures if located in different regions on the globe.

Nabighian (1972) shows that the absolute value of the analytic signal of a 2-D source provides a consistent response independent of the angles of inclination and declination of the magnetic field, *M.*

The 2-D analytical signal for magnetic anomalies can also be computed in the frequency domain, its real part being the horizontal derivative of the field and its imaginary part being the vertical derivative, both being Hilbert transforms of each other (Debeglia and Corpel, 1996). Nabighian (1972) uses this relationship to extend the analytic signal, $|A(x,y)|$, from two dimensions to three, which makes it more applicable to other potential field data.

$$|A(x,y)| = \sqrt{\left(\frac{\partial M}{\partial x}\right)^2 + \left(\frac{\partial M}{\partial y}\right)^2 + \left(\frac{\partial M}{\partial x}\right)^2} \qquad (6)$$

The response will show a positive, bell shaped symmetric peak with its maximum correlated to magnetized contrasts. The use of the absolute value of the analytical signal is that its shape over magnetic structures is independent of the earth's ambient magnetic field and of the direction of the magnetization of the source material, while it's amplitude remains unchanged. This is useful in establishing source characteristics without having to make assumptions on the direction of a body's magnetization, especially in areas where information on remanent magnetization of the observed anomalies in not known (Roest et al., 1992). The peak amplitude of the analytical signal along with the width of the amplitude curve can be related to the depth of the target. The derivatives of the signal also show these properties and can be used to locate contacts and to estimate their locations (Nabighian, 1974).

The analytic signal is similar to the energy envelope as it removes a directional dependancy of the field. The two have a similar goal but have different mathematical approaches because of the particular data being processed.

4.4 THE ENERGY ENVELOPE PROCESSING TECHNIQUE

The energy envelope (EE) technique was initially described by Smith & Keating (1996) to aid with the interpretation of airborne EM data. Certain airborne EM surveys are conducted by flying a plane with a transmitter loop wrapped around the plane and a receiving coil suspended beneath and behind the plane. Measurements are taken flying over adjacent survey lines in opposite directions (see Figure 4.4).

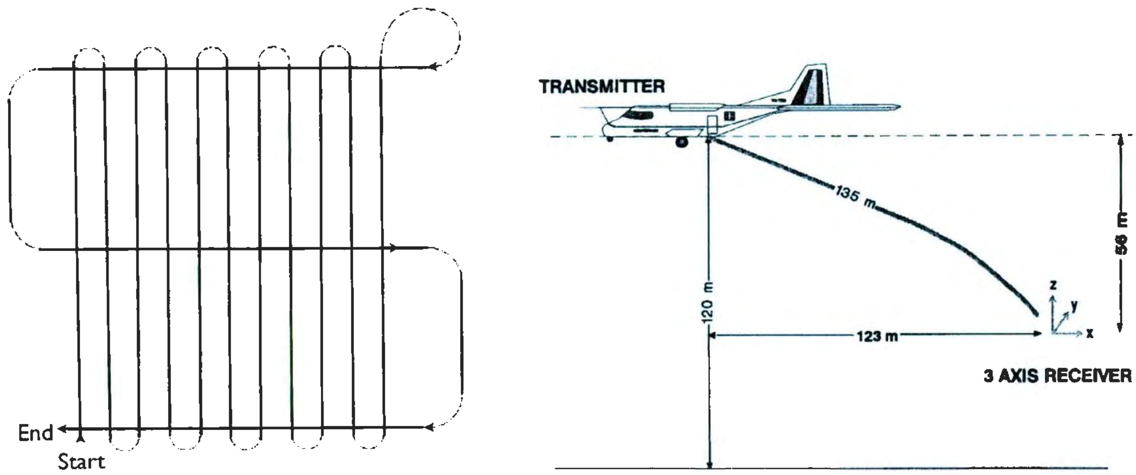

Figure 4.4. Illustration of a flight pattern from an airborne EM survey (Smith and Keating, 1996).

As the survey is conducted, the orientation of the transmitter-receiver pair relative to any conductor switches directions for each line therefor producing opposite responses on alternating lines. This complicates processing, but Smith & Keating (1996) use the energy envelope approach to create a simplified signature of the data. The EE applies a Hilbert transform to the three components of the data and combines them into a single quantity:

$$EE = \sqrt{V_x^2 + \bar{V}_x^2 + V_y^2 + \bar{V}_y^2 + V_z^2 + \bar{V}_z^2} \qquad (7)$$

where V is the voltage recorded after the transmitter is turned off, $\bar{V}$ denotes the Hilbert transform of the quantity, and the subscripts denote the component. The energy envelope is effectively a measure of the total amount of response in all three components. These quantities are functions of position along a profile. For airborne EM data the EE produces a response that is less dependent on flight direction.

Figure 4.5 illustrates how each component and its Hilbert transform affects the shape of the energy envelope. Solely using the x, y, and z components, top right panel, produces a symmetric bell curve with a large base width and low amplitude. This is not ideal because the profile would illuminate a large portion of the grid and not isolate the anomalous area in the centre. The middle and bottom panels show how the y component influences the overall shape of the profile. Both examples produce very similar profiles since the y component and Hilbert Transform quantity have such low amplitudes compared to the x and y. It is important to include the y component because it contains information pertaining to lateral changes in anomalous structures orthogonal to the strike of the survey lines (per. comm. Malo-Lalande).

$$\sqrt{z^2 + x^2 + y^2}$$

$$\sqrt{z^2 + \bar{z}^2 + x^2 + \bar{x}^2}$$

$$\sqrt{z^2 + \bar{z}^2 + x^2 + \bar{x}^2 + y^2 + \bar{y}^2}$$

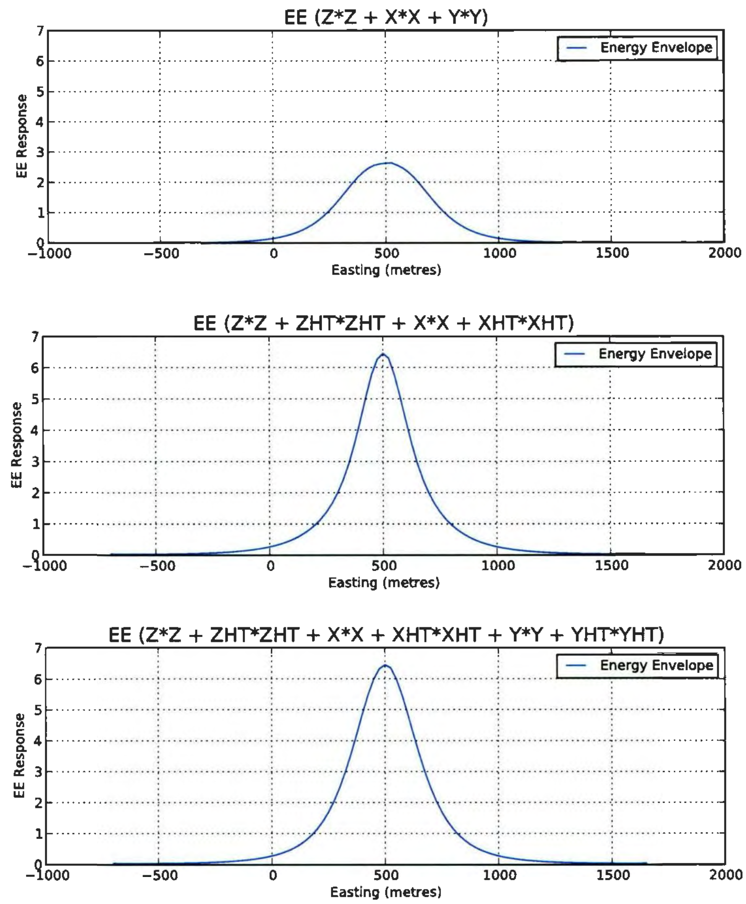

Figure 4.5. Examples of developing energy envelope equation and associated equations used. Blue line indicates profile of calculated data. All data correspond to synthetic plate positioned at 500E (see Figure 4.1c).

In this study the energy envelope is investigated to develop a more intuitive response for InfiniTEM® data that is not dependent on the location of the target in relation to the transmitter loop. To test the effectiveness of these techniques on TDEM data a synthetic model will initially be used.

The response of a single plate in a homogenous half space, see Figure 4.1, will give a better understanding of how well these methods correlate to the original component profiles. Noise will also be added to the synthetic data to evaluate how these techniques react in a non-ideal situation. The single profile will be easier to interpret than comparing all three components at one time and will better represent any anomalies in the subsurface. This profile can also be used to asses the effect of the individual components on the response. By analyzing how the response changes when one component is removed we can develop a better understanding of how changes in different components affect the shape of the profile. This new response will also make contour maps more intuitive and easier to analyze. Instead of having to compare crossover points and peaks of different components on separate maps to determine the location of anomalies, one can concentrate on a single map which indicates the actual size and location of the target. This will be especially useful for anyone who has limited knowledge of TDEM theory because the anomaly will resemble more of a bullseye instead of zero crossover. For more experienced interpreters it will make initial analyses much quicker and provide an extra piece of information when comparing individual components.

4.5 THE ENERGY ENVELOPE FOR INFINITEM® DATA

The code in this study was created by the author using the Python programming language. The algorithm was modeled after the energy envelope processing technique described by Smith and Keating (1996) for airborne electromagnetic surveys.

Python was chosen because of its extensive library of mathematical subroutines, ability to manipulate arrays, ease of syntax error resolution, and built in plotting capabilities.

The subroutine packages used in the algorithm consist of NumPy, SciPy, and matplotlib. NumPy is the principle/core computing package in Python. It is required for basic mathematical functions, array control, random number generation, and plays a key role in other scientific libraries. SciPy controls a variety of more advanced applications and relies on specific tools located in the NumPy library. The Hilbert transform used in the EE algorithm is located in SciPy. The code itself is included on the following 5 pages.

Before importing, the data from the *x*, *y*, and *z* components are arranged in 3 respective .txt files. Each line within the files contains succeeding stations on individual survey lines. As each .txt file is imported into the EE program it is extrapolated with forty cells containing zeros, twenty at the beginning and at the end (see Section 5.9). The Hilbert transform quantity of each extrapolated component is then calculated using the scipy.signal.signaltools.hilbert module located in SciPy. The extrapolated components files are then converted into arrays to correspond to the format of the Hilbert transformed results.

The six arrays are now combined using the energy envelope equation to produce the consistent response of the three components. Finally, the extrapolated cells are removed from the EE and the final result is ready for interpretation, with profiles generated using the Matplotlib library.

```
import numpy
from numpy import *
import scipy
from scipy import *
import matplotlib
from matplotlib import *
import pylab
from pylab import *
from scipy.signal.signaltools import hilbert


infile = open ('z.txt')

array_1 = ['']
i = 0
line = infile.readline()
array_1 = array_1 + [0,0,0,0,0,0,0,0,0,0,0,0,0,0,0,0,0,0,0,0,0,0,0]
while len(line) != 0:
   line = line[:-1]
   parts = line.split('        ')
   array_1.append(double(parts[0]))
   i = i + 1
   line = infile.readline()
array_1 = array_1[1:]
array_1 = array_1 + [0,0,0,0,0,0,0,0,0,0,0,0,0,0,0,0,0,0,0,0,0,0,0]
double(array_1)
print array_1

result_1 = scipy.signal.signaltools.hilbert(array_1)
print result_1.imag


infile = open ('x.txt')
array_2 = ['']
i = 0
line = infile.readline()
array_2 = array_2 + [0,0,0,0,0,0,0,0,0,0,0,0,0,0,0,0,0,0,0,0,0,0,0]
while len(line) != 0:
   line = line[:-1]
   parts = line.split('        ')
   array_2.append(double(parts[0]))
   i = i + 1
   line = infile.readline()
array_2 = array_2[1:]
array_2 = array_2 + [0,0,0,0,0,0,0,0,0,0,0,0,0,0,0,0,0,0,0,0,0,0,0]
double(array_2)
print array_2

result_2 = scipy.signal.signaltools.hilbert(array_2)
print result_2.imag
```

```
infile = open ('y.txt')

array_3 = ['']
i = 0
line = infile.readline()
array_3 = array_3 + [0,0,0,0,0,0,0,0,0,0,0,0,0,0,0,0,0,0,0,0,0]
while len(line) != 0:
   line = line[:-1]
   parts = line.split('      ')
   array_3.append(double(parts[0]))
   i = i + 1
   line = infile.readline()
array_3 = array_3[1:]
array_3 = array_3 + [0,0,0,0,0,0,0,0,0,0,0,0,0,0,0,0,0,0,0,0,0]
double(array_3)
print array_3

result_3 = scipy.signal.signaltools.hilbert(array_3)
print result_3.imag


array_1=array(array_1)
array_2=array(array_2)
array_3=array(array_3)


EE = ((((array_1)*(array_1))+((result_1.imag)*(result_1.imag))+((array_2)*(array_2))+((result_2.imag)*
(result_2.imag))+((array_3)*(array_3))+((result_3.imag)*(result_3.imag)))**(0.5))
print(EE)


EE=list(EE)

del EE[0]
del EE[0]
del EE[0]
del EE[0]
del EE[0]
del EE[0]
del EE[0]
del EE[0]
del EE[0]
del EE[0]
del EE[0]
del EE[0]
del EE[0]
del EE[0]
del EE[0]
del EE[0]
del EE[0]
del EE[0]
del EE[0]
del EE[0]
```

```
L = len(EE)

del EE[L-1]
del EE[L-2]
del EE[L-3]
del EE[L-4]
del EE[L-5]
del EE[L-6]
del EE[L-7]
del EE[L-8]
del EE[L-9]
del EE[L-10]
del EE[L-11]
del EE[L-12]
del EE[L-13]
del EE[L-14]
del EE[L-15]
del EE[L-16]
del EE[L-17]
del EE[L-18]
del EE[L-19]
del EE[L-20]
print(EE)

ee=str(EE)

outfile = open('EE.txt','w')
for row in ee:
   outfile.write('%5.6s'%row)
   outfile.write('\n')
outfile.close()
```

```
#array_1
fig = plt.figure()
ax = plt.subplot(111)
t=linspace(-700,1650,95)
ax.plot(t,array_1, label='Z Original Data')
ax.plot(t,result_1.imag, label='Z Hilbert Transform')
title('Plate @ 1100E [Line 200N]')
xlabel(('Easting (metres)'))
ylabel('EM Response (uV/A)')
ax.legend(loc='upper left', bbox_to_anchor=(0, 1.0))
grid(True)
show()

# array_2
fig = plt.figure()
ax = plt.subplot(111)
t=linspace(-700,1650,95)
ax.plot(t,array_2, label='X Original Data')
ax.plot(t,result_2.imag, label='X Hilbert Transform')
title('Plate @ 1100E [Line 200N]')
xlabel(('Easting (metres)'))
ylabel('EM Response (uV/A)')
ax.legend(loc='upper left', bbox_to_anchor=(0, 1.0))
grid(True)
show()

# array_3
fig = plt.figure()
ax = plt.subplot(111)
t=linspace(-700,1650,95)
ax.plot(t,array_3, label='Y Original Data')
ax.plot(t,result_3.imag, label='Y Hilbert Transform')
title('Plate @ 1100E [Line 200N]')
xlabel(('Easting (metres)'))
ylabel('EM Response (uV/A)')
ax.legend(loc='upper left', bbox_to_anchor=(0, 1.0))
grid(True)
plt.show()

# EE = Energy Envelope
fig = plt.figure()
ax = plt.subplot(111)
t=linspace(-700,1650,95)
ax.plot(t,EE_1, label='Energy Envelope')
title('Plate @ 1100E [Line 200N]')
xlabel(('Easting (metres)'))
```

```
ylabel('EE Response')
ax.legend(loc='upper left', bbox_to_anchor=(0, 1.0))
grid(True)
show()
```

CHAPTER 5

SYNTHETIC EXAMPLES

Multiple examples involving a conductive plate in a variety of positions, depths, orientations and sizes are provided and show the dexterity of the energy envelope technique. All profiles correspond to a synthetic vertical plate in a homogeneous half space of zero conductivity with dimensions 400m by 200m by 50m, unless stated otherwise. All profiles were modeled using EMIT Maxwell EM imaging software with an InfiniTEM® transmitter loop with dimensions: 400m (loop width), 400m (loop separation) and 400m (second loop width). A 25m station separation was used on 2375m long lines. All profiles shown correspond to Line 200N on the survey grid.

5.1 VERTICAL PLATE LOCATED IN CENTRE LOBE

As previously discussed, conductors of the same size and shape at different locations on the InfiniTEM® survey grid can produce different x, y and z component profiles. This deviation makes properly identifying any anomalies difficult and requires an experienced processor. The following examples will illustrate how the energy envelope technique simplifies the response of any conductor into a consistent profile.

Figure 5.1 displays a plate at 500E and its associated x, y and z profiles with Hilbert transform quantities. This location provides the strongest coupling with a vertical plate of any area on the survey grid and produces the most conventional response with positive to negative crossover on the z and a positive peak on the x. The EE profile clearly exhibits a positive bell shape curve directly over the location of the conductor.

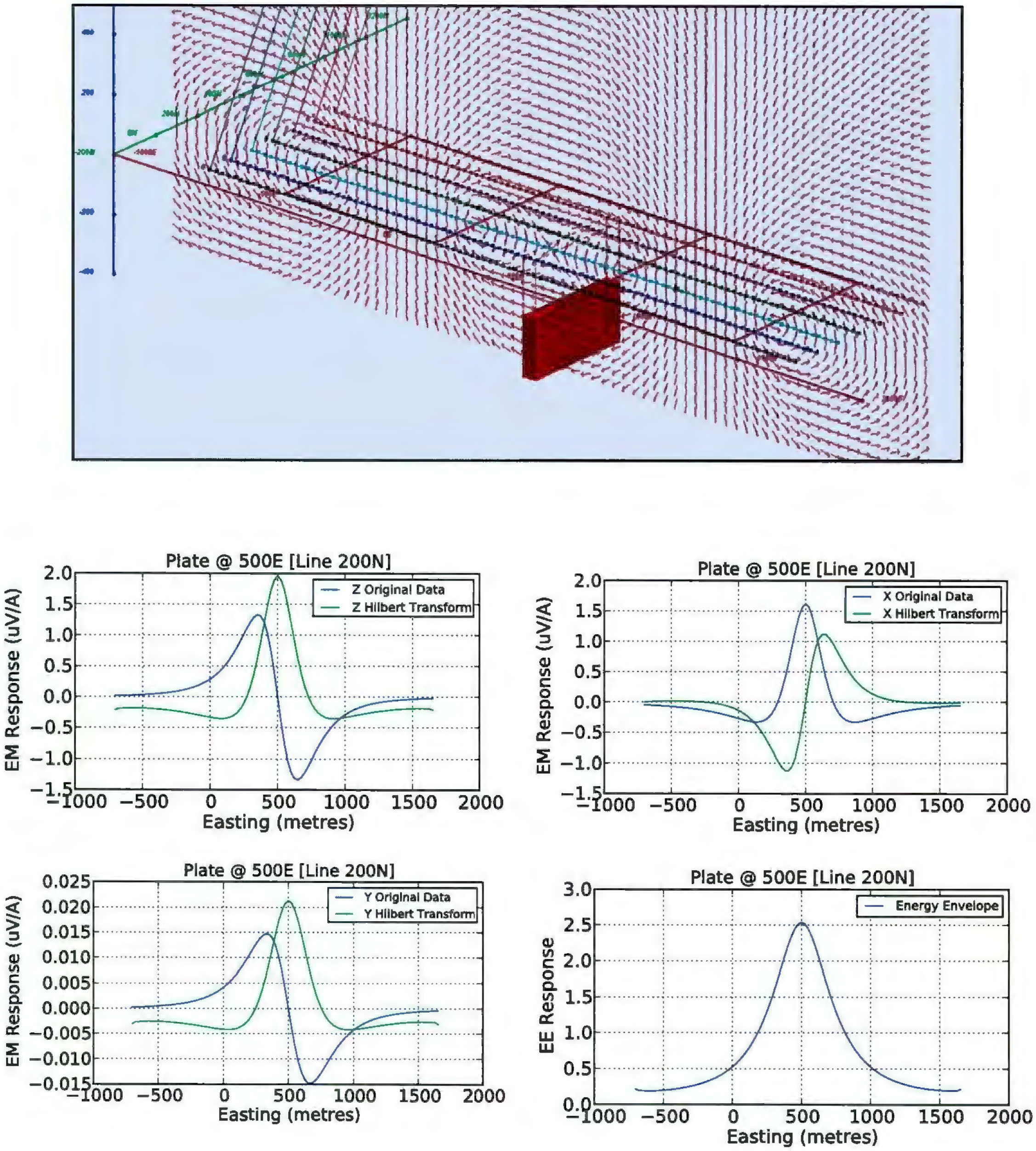

Figure 5.1. The z, x, and y component profiles of a vertical plate positioned at 500E. Blue line indicates original profile and the green line represents the Hilbert transformed quantity of the original signal, as shown in label in upper right corner. Scale on first three graphs corresponds to EM Response measured in μV/A. Bottom right profile shows energy envelope profile using all components and scale corresponds to EE Response. Bottom scale indicates Easting position in metres.

5.2 VERTICAL PLATE LOCATED IN LEFT LOBE

The next example, Figure 5.2, examines the same plate but located at -95E. Although the component profiles changed to a positive peak on the *z* and a negative to positive crossover on the *x,* the EE response remained a positive peak directly over the target. The primary field from the transmitter intersects parallel to the target producing a minimum coupling scenario and results in a weaker response from the conductor (see Figure 3.2). Although the EE response has a reduced amplitude, it still produces a predominant profile that is easily distinguishable.

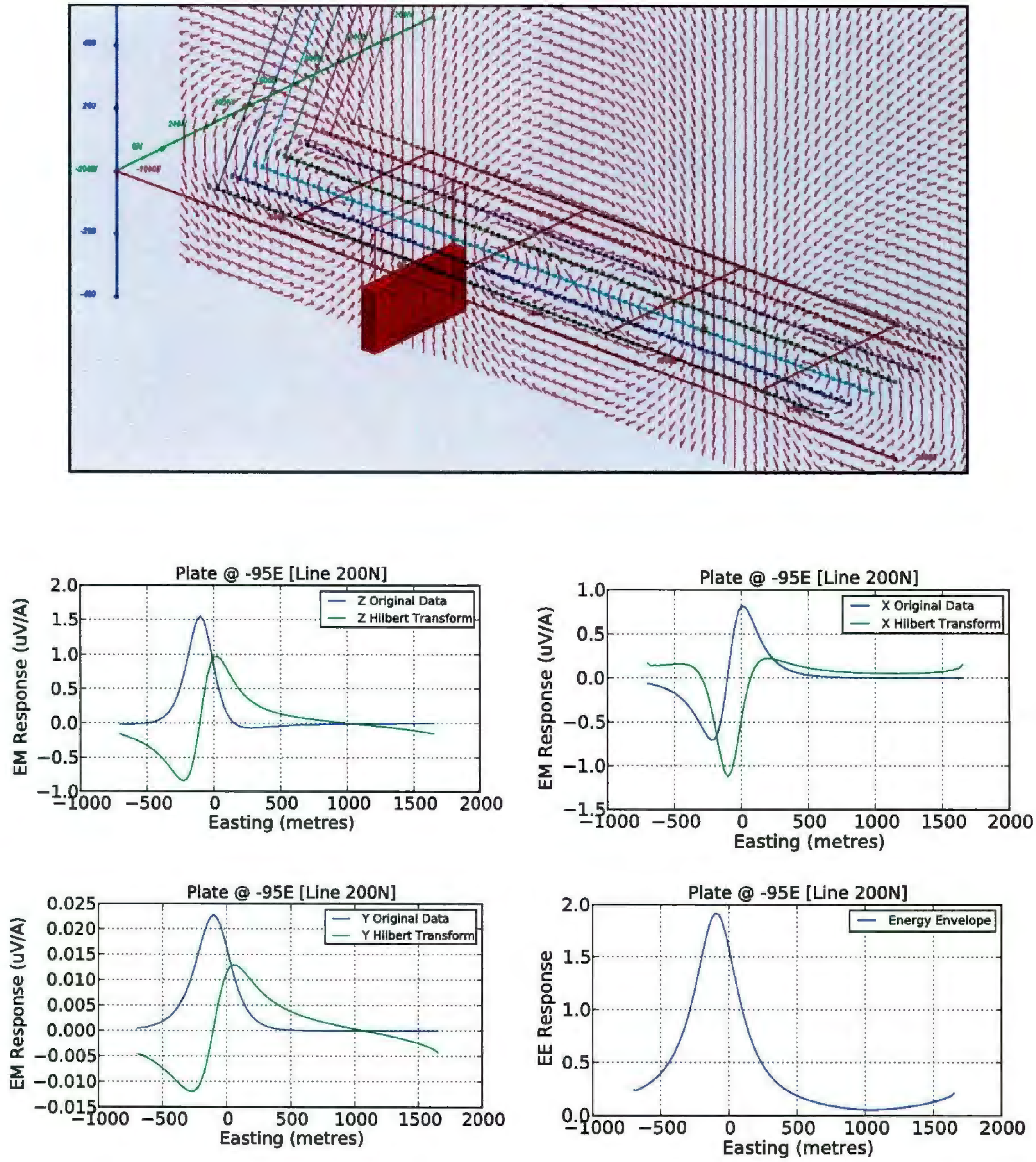

Figure 5.2. The *z*, *x*, and *y* component profiles of a vertical plate positioned at -95E. Blue line indicates original profile and the green line represents the Hilbert transformed quantity of the original signal, as shown in label in upper right corner. Scale on first three graphs corresponds to EM Response measured in μV/m. Bottom right profile shows energy envelope profile of all components and scale corresponds to EE Response. Bottom scale indicates Easting position in metres.

5.3 VERTICAL PLATE LOCATED IN RIGHT LOBE

The same conductor when located at 1100E produces yet another set of unique component profiles, Figure 5.3, a negative peak on the z and a positive to negative crossover on the x. The plate is once again subjected to a minimal coupling situation which results in a weaker secondary field. As in the previous examples the EE produces a positive peak directly over the target and proves its effectiveness regardless of the shape of the component profiles.

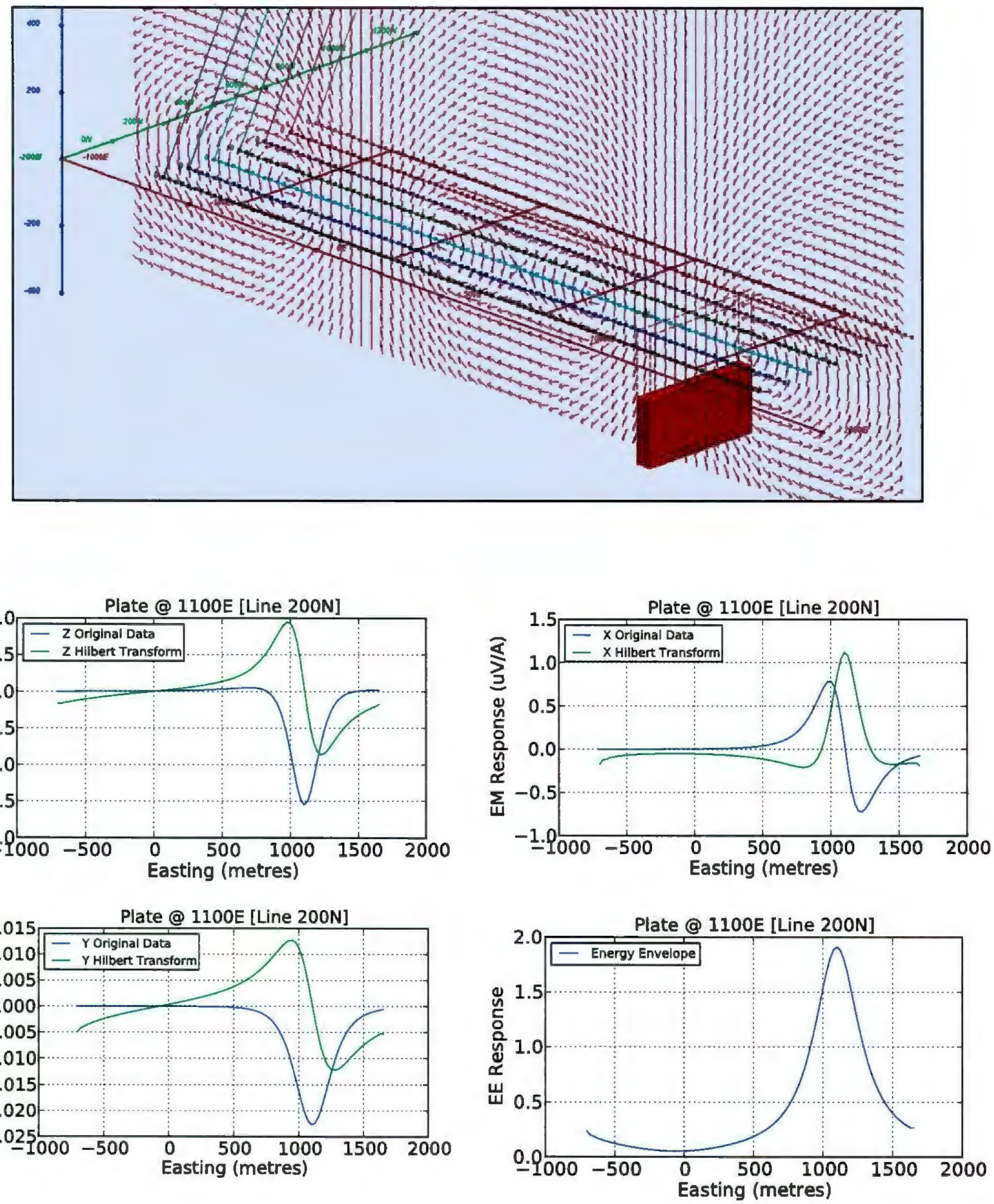

Figure 5.3. The z, x, and y component profiles of a vertical plate positioned at 1100E. Blue line indicates original profile and the green line represents the Hilbert transformed quantity of the original signal, as shown in label in upper left corner. Scale on first three graphs corresponds to EM Response measured in μV/m. Bottom right profile shows energy envelope profile of all components and scale corresponds to EE Response. Bottom scale indicates Easting position in metres.

5.4 25 DIFFERENT POSITIONS OF THE VERTICAL PLATE

Figure 5.4 shows the responses for 25 different positions of a vertical plate on a survey grid with the same dimensions and depth. Each plate was modeled individually but all plots are shown here to compare amplitudes. The colored profiles indicate the amount of energy envelope response each individual plate generates. The total response from the plates is dependent on the strength of the primary field in that area and the coupling that the field has with the plate. The centre of the InfiniTEM® transmitter loop is designed to have a strong, horizontal primary field at depth that optimizes coupling with steeply dipping targets. The four highest amplitudes for plates at -400m, 205m, 800m and 5m, are generated from plates located directed below wires from the transmitter loop. This is a common occurrence in TDEM and is known as the wire effect and was expected in the EE profiles (per. comm. Malo-Lalande). Areas located directed below the wires of the transmitting loop are exposed to the strongest primary field because of their locality to the transmitting current. The EE algorithm proved very effective in all plates modeled within 100m of the InfiniTEM® transmitter loop. Plates lying 100m outside the transmitting loop are exposed to a weaker primary field and produce lower amplitude responses. Due to the nature of the Hilbert transform used in the EE, low amplitude signals are more subject to edge effects and require further processing (discussed in Section 5.9). Although further processing was needed, these plates still showed the same shape response and could be identified.

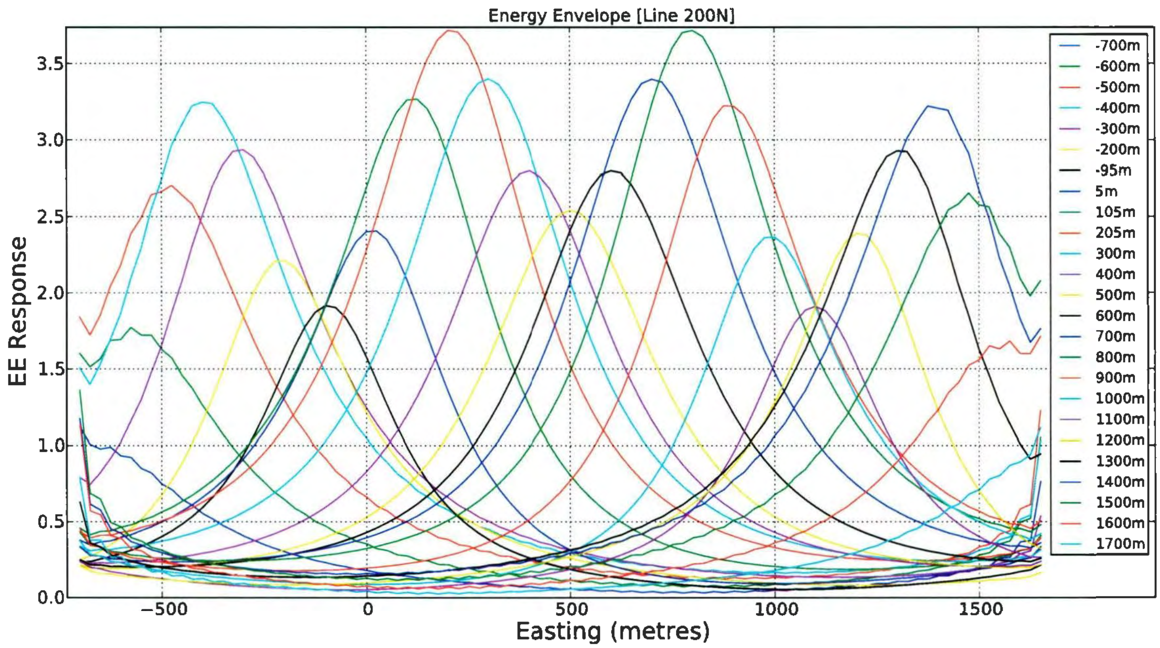

Figure 5.4. Energy envelope profiles for 25 vertical plates, 200m below the surface. Legend shows location of plates, indicated by different colors, relative to Easting position on survey grid. Scale on left side corresponds to total amount of energy envelope response. Only profiles from Line 200N are shown. Bottom scale indicates Easting position in metres.

5.5 SINGLE VERTICAL PLATE, CENTRAL LOCATION, DIFFERENT DEPTHS

In this section the effect of increasing the plate depth on the EE response is illustrated. The dimensions and conductivity of the plate are the same as in previous sections. Figure 5.5 shows profiles of 10 vertical plates of varying depths positioned at the 500 m Easting position. The most shallow plate modeled lies 50m under the surface with successive plates at 50m intervals directly below until reaching 500m depth. Responses show the same symmetrical bell shape directly over the target at all depths. Similar to conventional TDEM surveys, the plates modeled closer to the surface produced the larger amplitudes. Responses producing amplitudes lower then 1 EE response, i.e. depths 350m - 500m, show signs of edge effects which were removed with further processing. Another characteristic that the EE profiles show that is similar to conventional TDEM is the relationship that amplitude and half width have with the depth of the plate. As the depth of the target increases the ratio between the amplitude and half width decreases. This ratio can be used to determine a general depth for the target and can be seen in Figure 5.6.

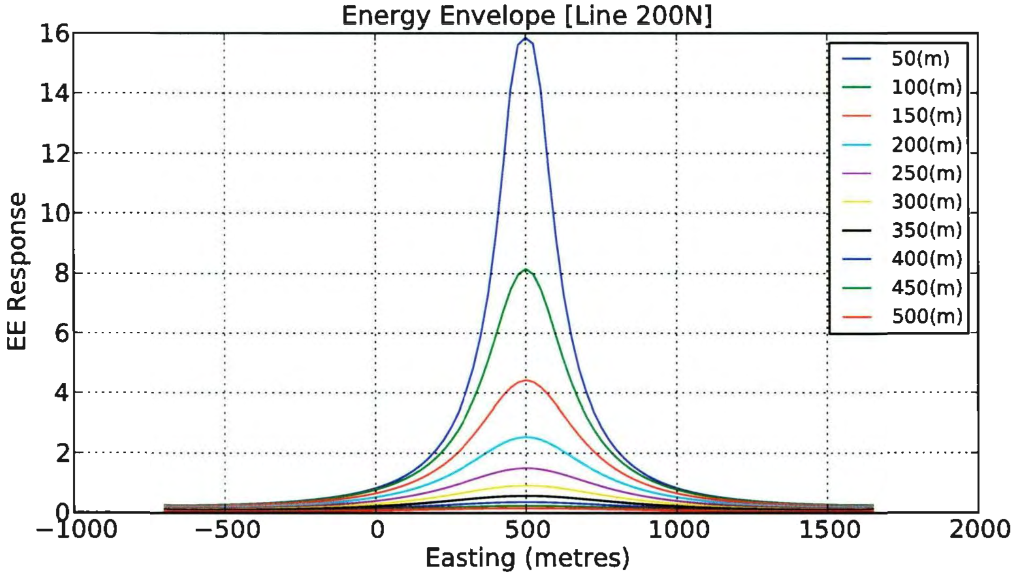

Figure 5.5. Energy envelope profiles for 10 vertical plates of various depths. Legend shows depths of plates, indicated by different colors, directly below the 500m Easting position. Scale on left side corresponds to total amount of EE Response. Only profiles from Line 200N are shown. Bottom scale indicates Easting position in metres.

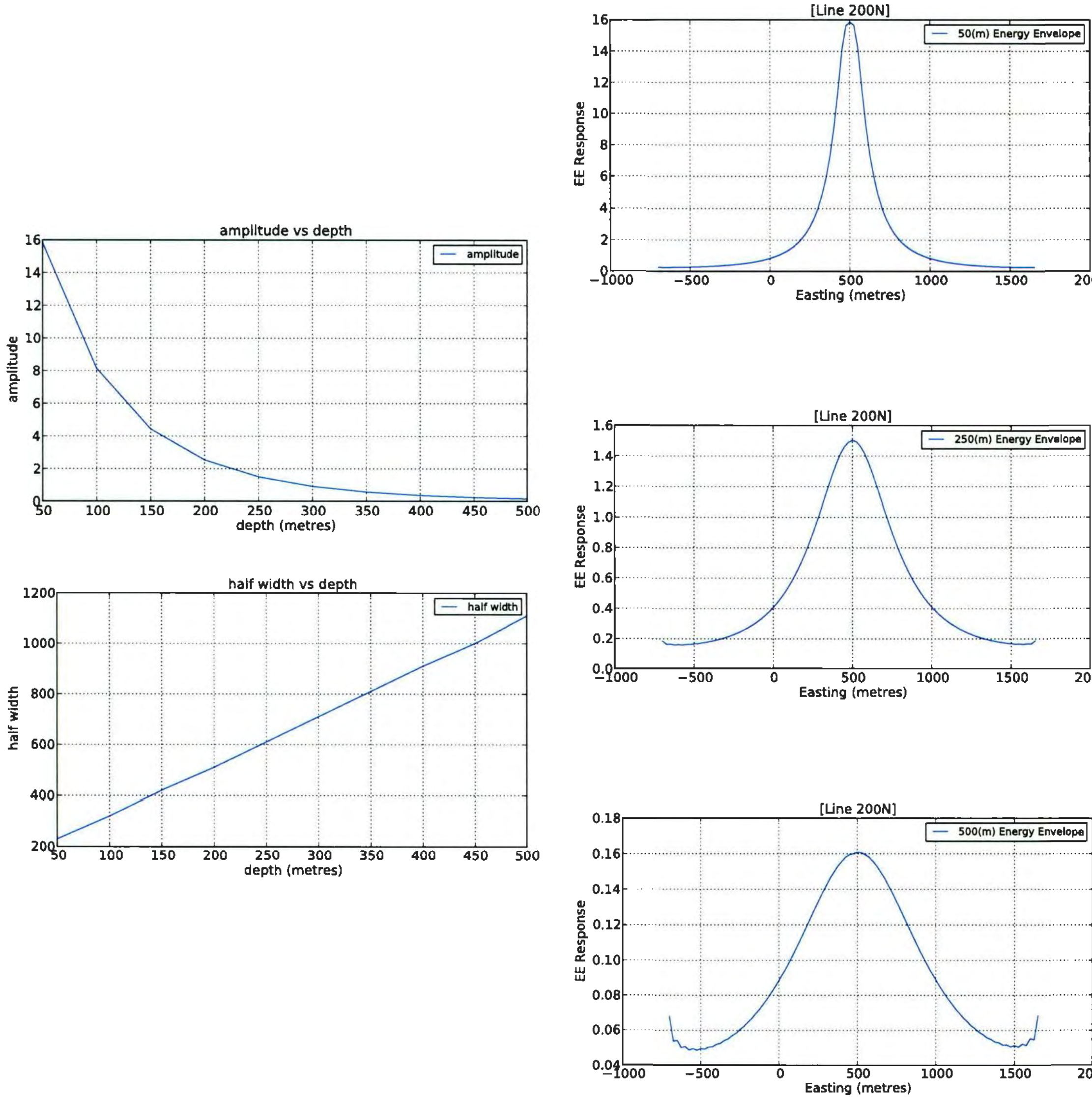

Figure 5.6. Right panels: energy envelope profiles of three plates at different depths; 50m, 250m and 500m respectively. Energy Envelope profile of all components and scale corresponds to EE Response. Bottom scale indicates Easting position in metres. Left panels shows amplitude vs depth profile on top and half width vs depth on bottom.

5.6 SINGLE PLATE, DIFFERENT DIPS

As a conductor's vertical orientation changes from 90° its coupling with the primary field also changes. This interaction can produce positive or negative effects depending on the specific scenario. Figure 5.7 a & b show the same plate, with its top position remaining at 200m depth, in a variety of Easting positions but with a different vertical orientation, dipping 30° and 60° to the West respectively. 200E and 1400E in Figure 5.7a have higher amplitudes, showing nearly twice the amplitude as the other positions, and is directly related to their coupling with the primary field. Figure 5.7b shows a dramatic increase in amplitude in plates at -100E, 200E, 1100E and 1400E, as compared to the vertical plates in Figure 5.4, produced by a more optimal coupling with the primary field in those particular positions. It is critical to keep this relationship in perspective when correctly assigning the quality of an anomaly.

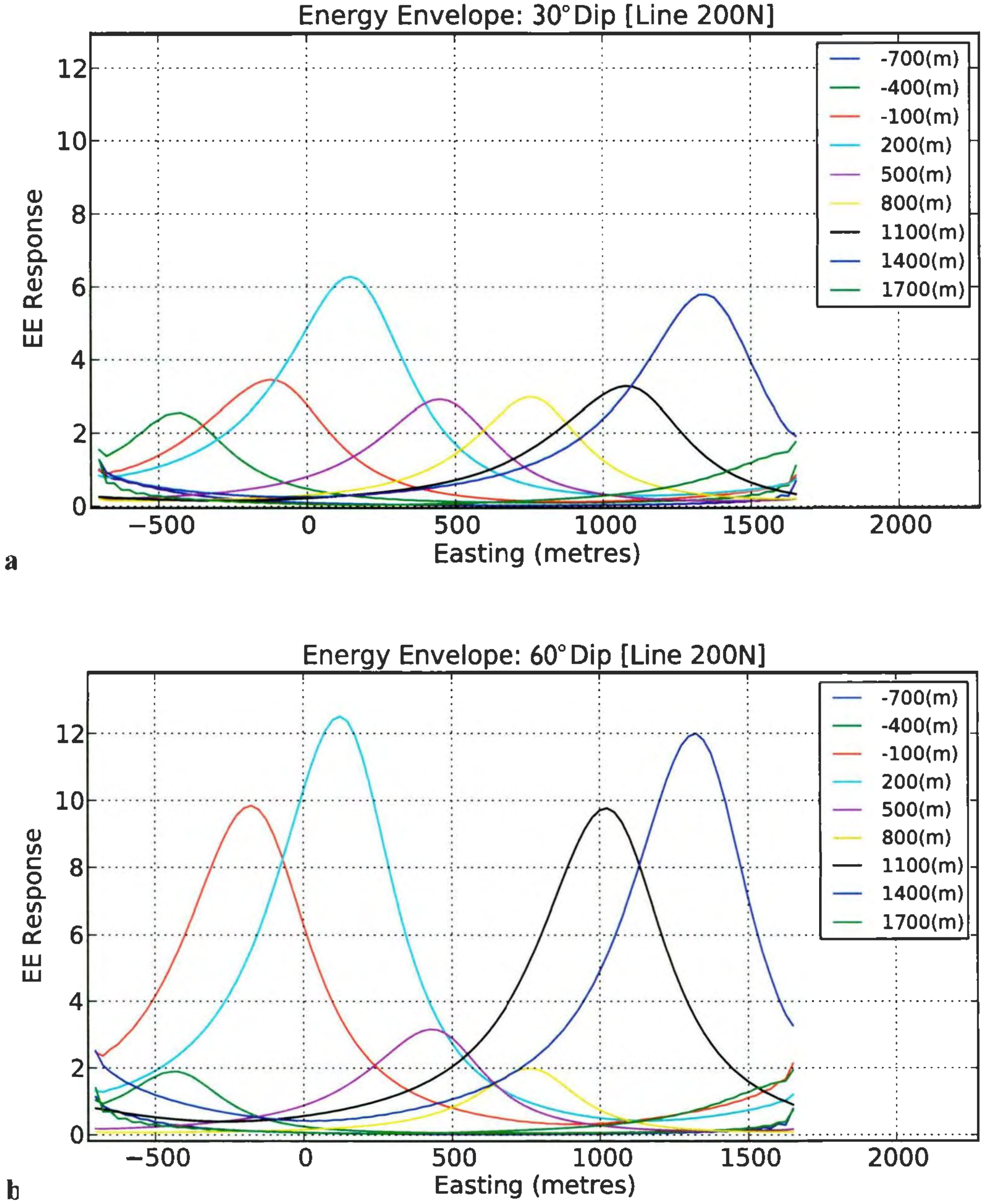

Figure 5.7 a&b. Energy Envelope profiles for 9 plates dipping at 30° and 60° respectively, 200m below the surface. Legend shows location of plates, indicated by different colors, relative to Easting position on survey grid. Scale on left side corresponds to total amount of EE Response. Only profiles from Line 200N are shown. Bottom scale indicates Easting position in metres.

Figure 5.8a&b provides an example of a plate in 8 different vertical orientations, ranging from 10° to 80° dipping to the west, shown in Figure 5.8a. With the plate's top Easting position remaining at 500E, there is not a significant amount of migration in the EE profile. This shows that even with a change in amplitude produced by different coupling scenarios the EE profiles still peaked directly over the most shallow portion of the conductor. As the dip is decreased the EE profile produces a more shallow flank towards the direction of the dip of the plate. This increase of amplitude and asymmetry shows that the EE produces a higher response when the body is close to the surface and can be used to indicate dip direction.

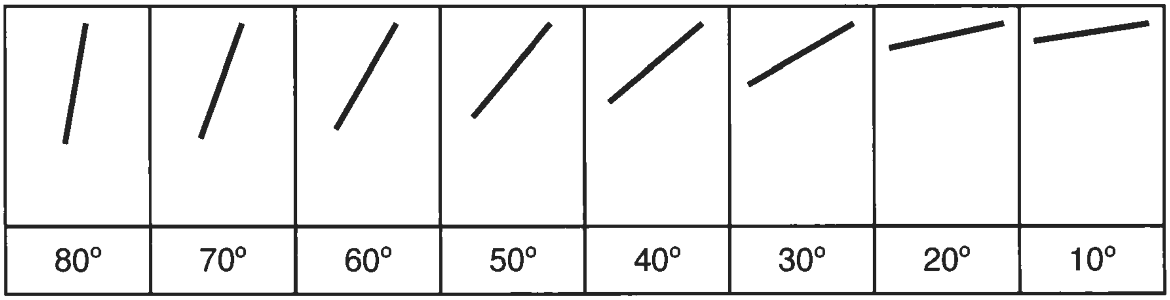

a.

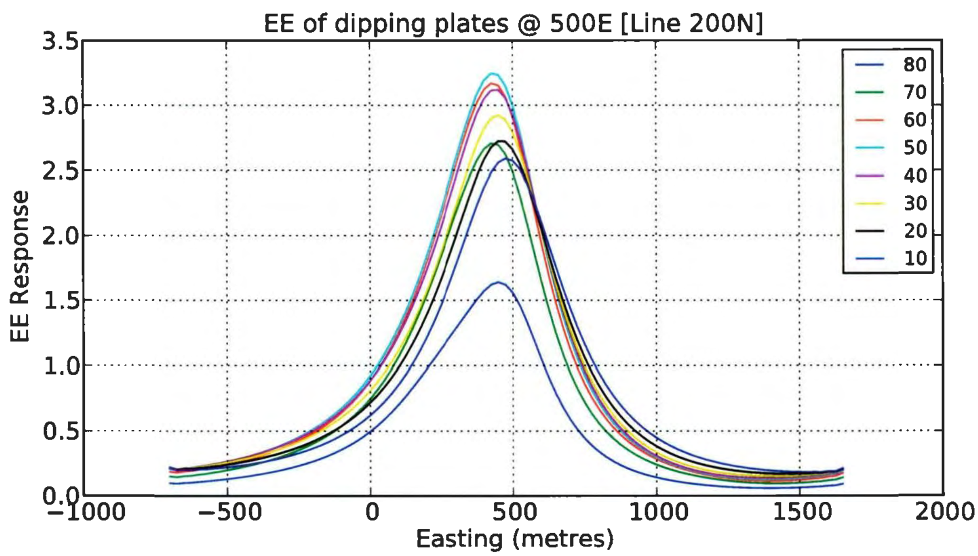

b.

Figure 5.8 a&b. Energy Envelope profiles for 8 plates dipping 200m below the surface. Legend shows dip of plates, indicated by different colors. Scale on left side corresponds to total amount of EE Response. Bottom scale indicates Easting position in metres. Only profiles from Line 200N are shown.

5.7 SINGLE VERTICAL PLATE WITH DIFFERENT THICKNESS

To investigate the effect of the thickness of a conductor on the EE, 7 plates were modeled with successively increasing widths, ranging from 50m to 350m, Figure 5.9. As the plate's width becomes greater than 200m the EE response begins to peak at the outside edges of the conductor leaving a trough in the centre of the profile. This becomes more evident as the width is increased and is also apparent in the components profiles which have distorted away from their conventional shape. This is due to the orientation of the secondary field produced by the plate where the edge of the plate produces a higher response than the centre, and is a common response for long horizontal plates.

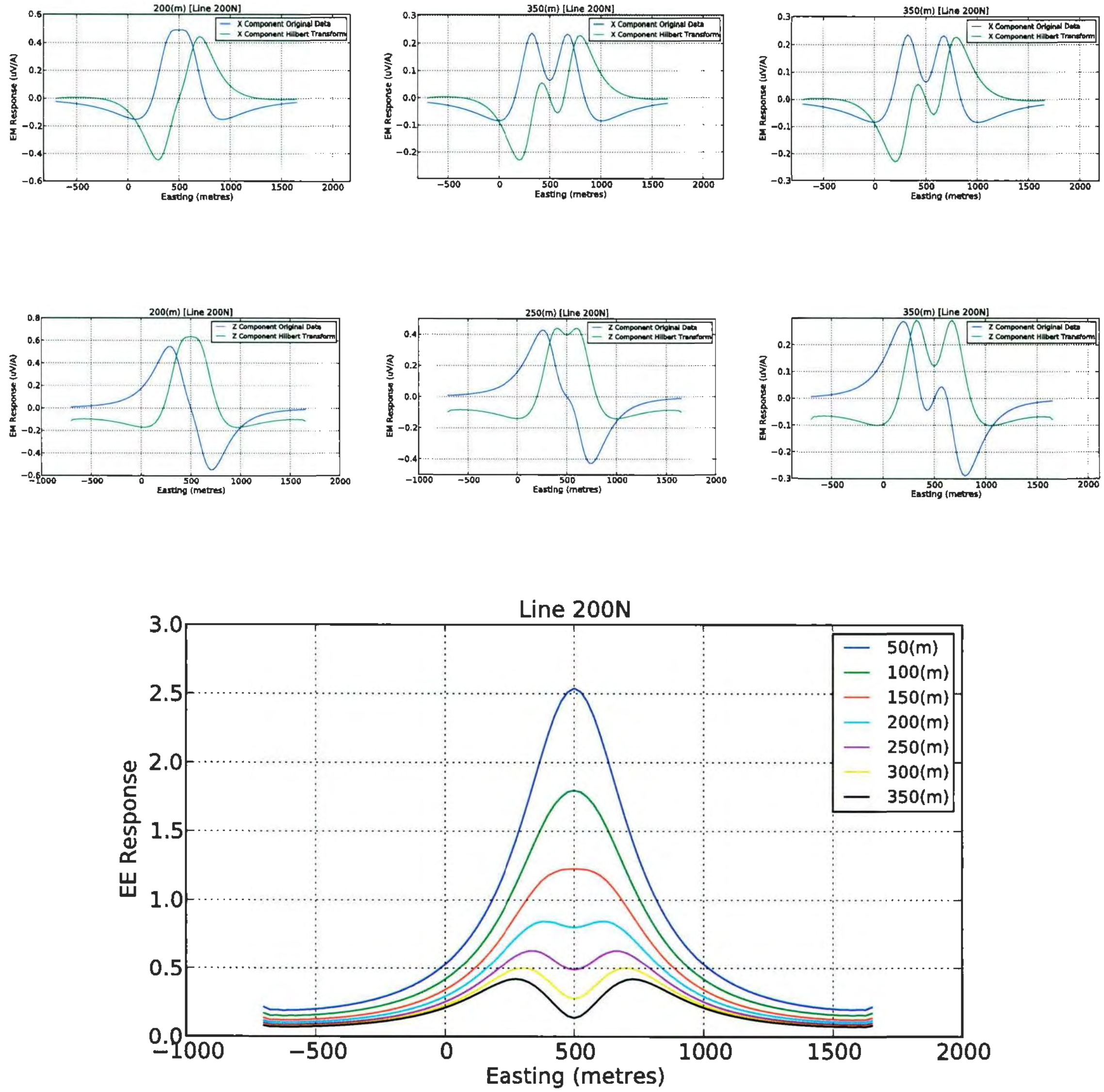

Figure 5.9. The x and z component profiles of a vertical plate positioned at 500E with different thickness. Blue line indicates original profile and the green line represents the Hilbert transformed quantity of the original signal, as shown in label in upper right corner. Scale on top six graphs corresponds to EM Response measured in μV/m. Bottom profile shows energy envelope profile of all components and scale corresponds to EE Response. Bottom scale indicates Easting position in metres.

5.8 SINGLE VERTICAL PLATE WITH GAUSSIAN DISTRIBUTED NOISE

Random noise was added to a synthetic *dB/dt* example to investigate the EE algorithm's effectiveness in realistic situations. A set of random numbers was created using the random number generator in SciPy with a mean of 0 and a standard deviation of 0.1, left panels of Figure 5.10, and was added to all three components. Due to the low amplitude of the y component, the random noise distorted its original shape and the HT quantity. The z and x components retained their basic shape. The EE does show effects of the added noise with a number of low amplitude spikes evident on the profile. However the overall shape is consistent with previous examples with a positive peak directly over the conducting plate.

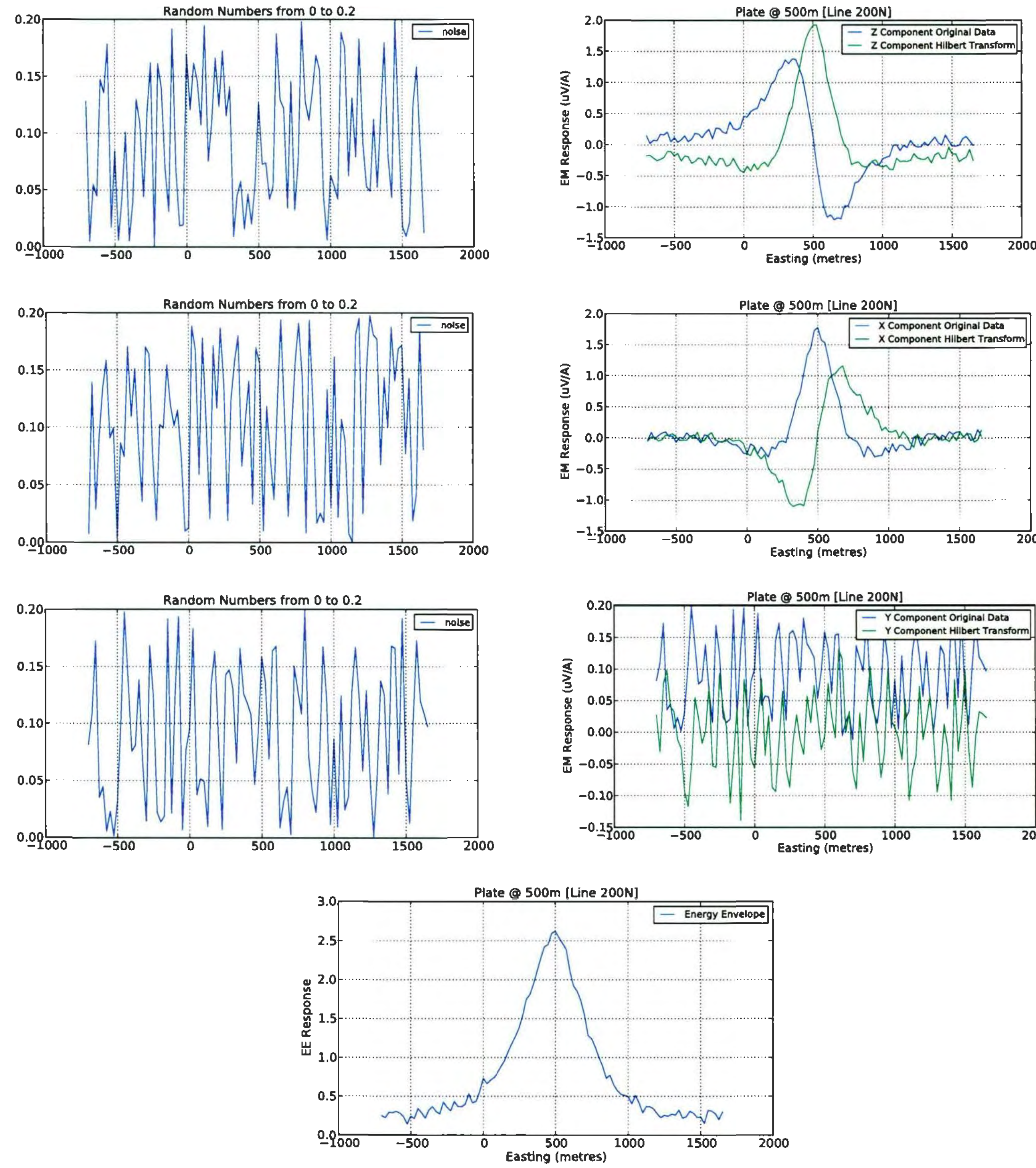

Figure 5.10. Top right three panels show the z, x, and y component profiles of a vertical plate positioned at the 500E with random noise added. Blue line indicates original profile and the green line represents the Hilbert transformed quantity of the original signal, as shown in label in upper left corner. Scale on the three graphs on the right corresponds to EM Response measured in μV/A. Bottom profile shows energy envelope profile of all components and scale corresponds to EE Response. Bottom scale indicates Easting position in metres. Top left three panels show the amount of noise added the each individual component.

5.9 EDGE EFFECTS AND SOLUTIONS

Edge effects are a common problem when using the Hilbert transform for data analysis and frequently cause processing issues for the end points of a signal. Endpoints are troublesome because the FT used by the HT treats them as if they were part of a periodically repeating array. If the signal abruptly terminates or does not extend to zero the FT produces oscillations, Figure 5.11. Also, as the plate moves away from the transmitting loop it is exposed to a weaker primary field, thus producing a lower amplitude response, which is more susceptible to edge effects. Previous examples given were exposed to a sufficiently strong primary field that these effects were not pronounced.

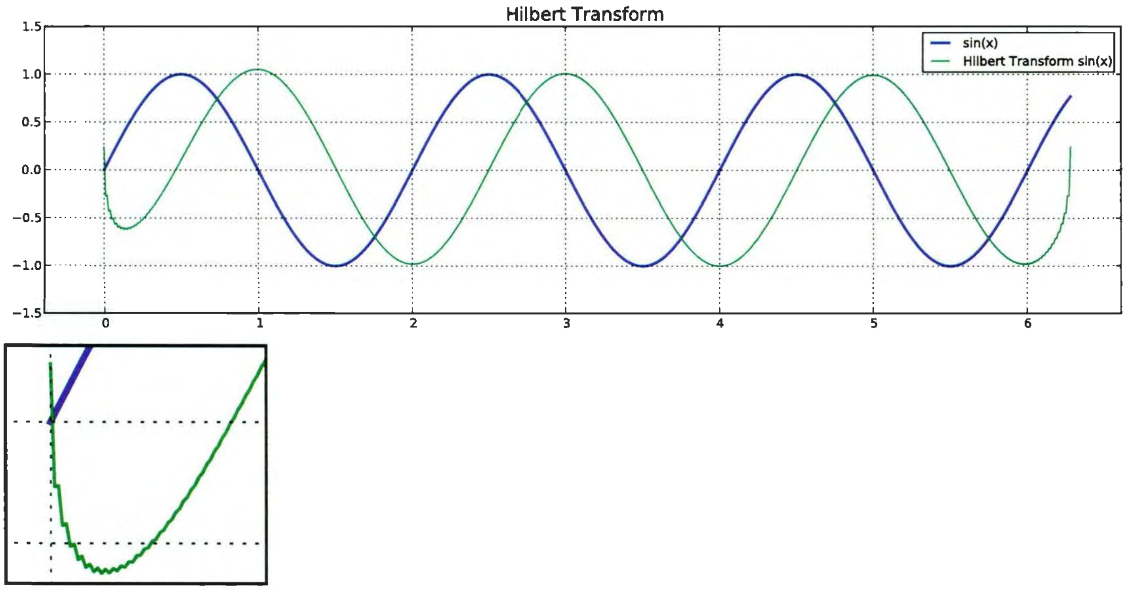

Figure 5.11. Example of results, green profile, from a Hilbert transformed sine function, blue profile. Edge effects are visible in the insert panel.

As seen in Figure 5.12 the EE from a plate at -700E, shows a positive artifact on the right side that is an edge effect produced by the HT. This is a serious problem when using the technique for exploration purposes because the appearance of a positive peak may lead a processor to believe that there is an anomaly in that area. The severity of these effects becomes greater as the amplitude of the signal is reduced.

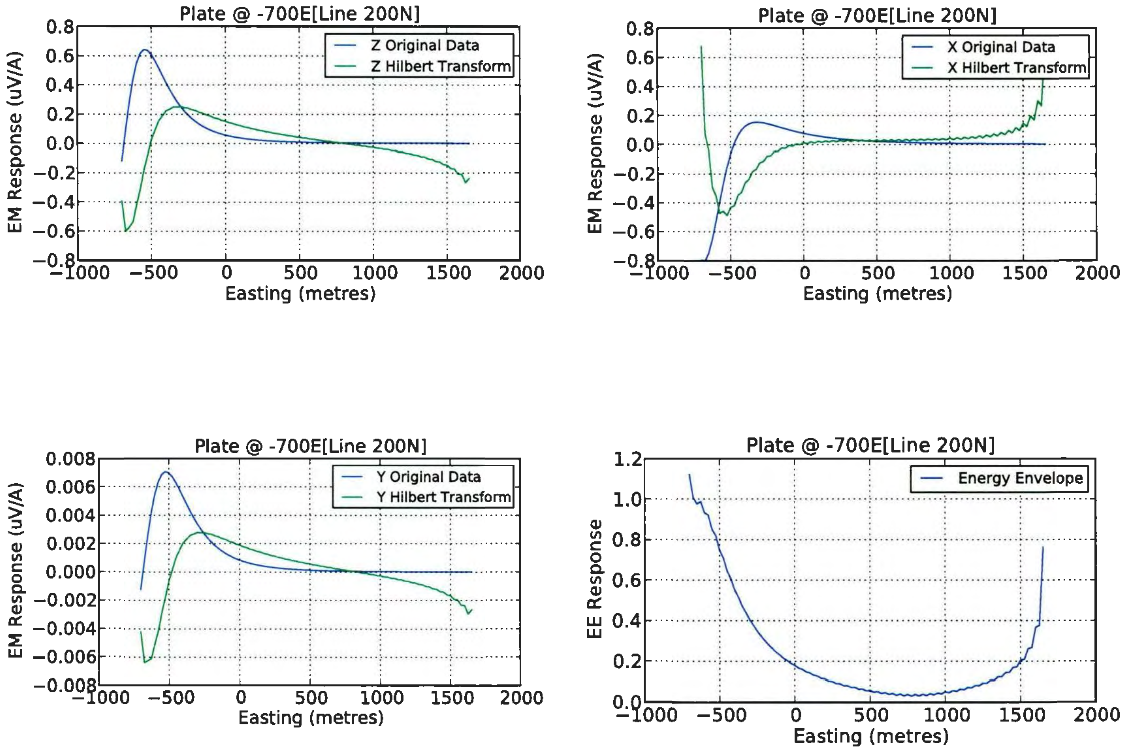

Figure 5.12. The *z*, *x*, and *y* component and EE response profiles of a vertical plate positioned at -700E. Blue line indicates original profile and the green line represents the Hilbert transformed quantity of the original signal, as shown in label in upper right corner. Scale on first three graphs corresponds to EM Response measured in µV/m. Bottom right profile shows energy envelope profile of all components and scale corresponds to EE Response. Bottom scale indicates Easting position in metres.

Extrapolating the data beyond the end points is a practical solution for edge effects. Common techniques used to achieve this include extrapolating with trigonometric functions, linear predictions and repetition of the original signal. The effectiveness of trigonometric functions and linear predictions to reduce the severity of edge effects are explored in this section.

As discussed, the FT is less accurate towards the end points of an array. Extending the data to zero creates a larger sampling window and draws the end point away from the edge and reduces the severity of the oscillations produced by the FT. 20 data points were added to extrapolate the data.

Variations of a sinusoidal curve were used to model a trigonometric function to extrapolate the data and extend its end points to a zero value extremum. This was achieved using 1/4 and 1/2 of one complete period of a standard sine curve. The end point of the extrapolated data, adjacent to the signal, was scaled to be equivalent to the value of the last available point of the signal.

Figure 5.13 shows the extrapolation using a 1/4 sin curve. The function provides a simple curve that allows the data to decay to zero gradually. This approach produced a reduction in the amplitude of the edge effects, left hand side of figure, which made the target's response much more predominant. Although this generated favorable results, it did not completely remove the artifacts on the most easterly side of the figure. Without a conductive body there should be a zero response on the energy envelope profile in that area. This shows that the extrapolating function is effective but not ideal.

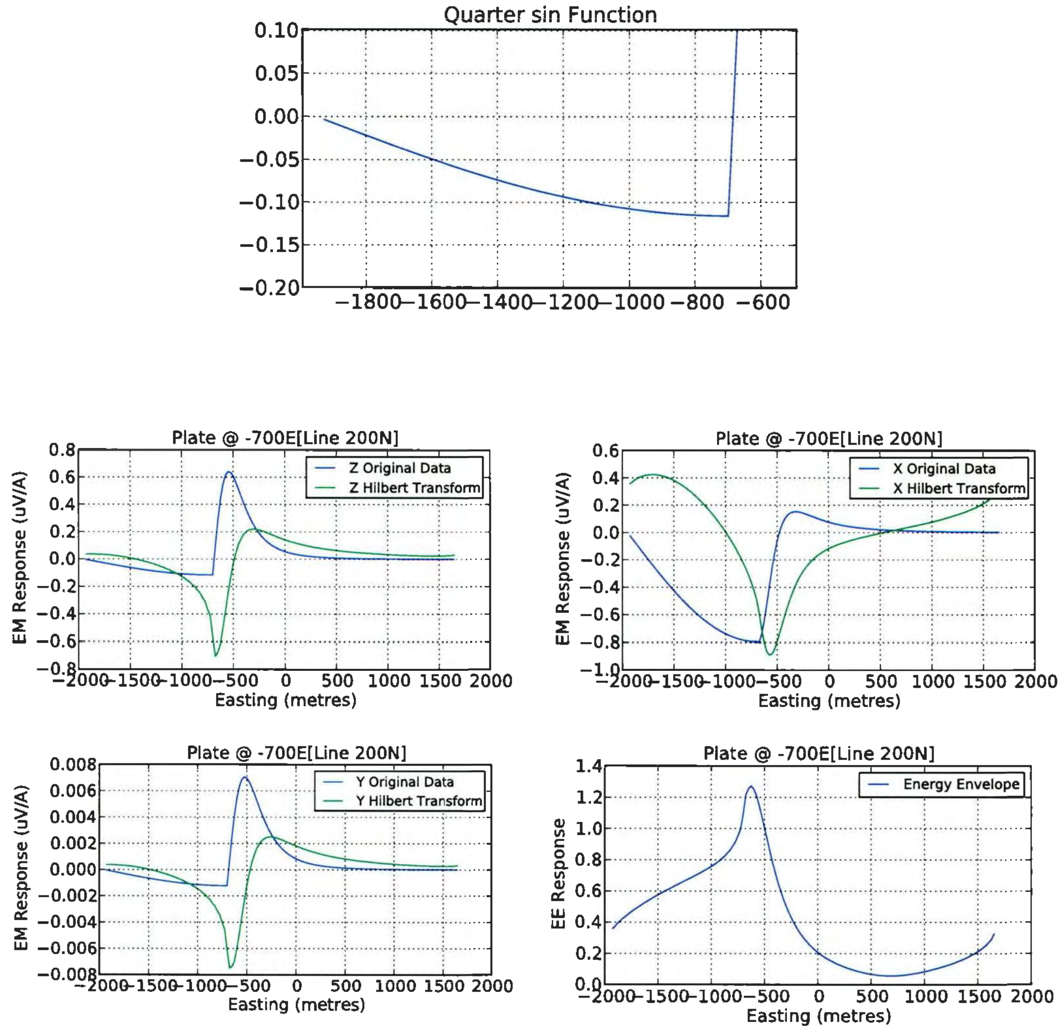

Figure 5.13. The z, x, and y component and EE response profiles of a vertical plate positioned at -700E. Top profile shows extrapolating function used. Blue line indicates original profile and the green line represents the Hilbert transformed quantity of the original signal, as shown in label in upper right corner. Scale on z, x, and y graphs corresponds to EM Response measured in μV/m. Bottom right profile shows energy envelope of all components and scale corresponds to EE Response. Bottom scale indicates Easting position in metres.

The next extrapolating function tested was a 1/2 sine curve, Figure 5.14. This provided a more gradual decay before reaching zero. As seen in the lower right panel the edge effect amplitude has been reduced more than the previous example, but still remains evident.

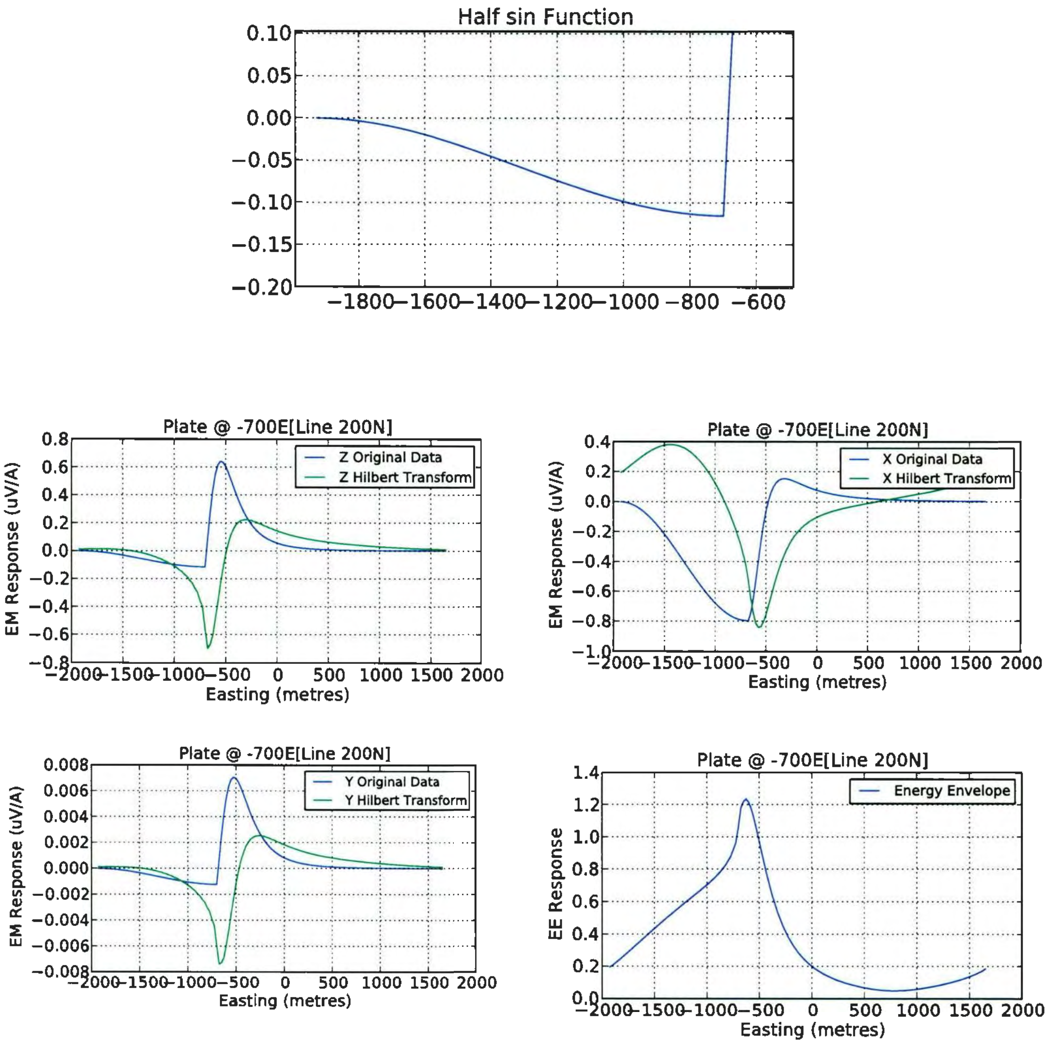

Figure 5.14. The z, x, and y component and EE response profiles of a vertical plate positioned at -700E. Top profile shows extrapolating function used. Blue line indicates original profile and the green line represents the Hilbert transformed quantity of the original signal, as shown in label in upper right corner. Scale on z, x, and y graphs corresponds to EM Response measured in μV/m. Bottom right profile shows energy envelope of all components and scale corresponds to EE Response. Bottom scale indicates Easting position in metres.

The final example simply uses a set of repeating zeros to extend the signal, Figure 5.15. This approach can be preformed very quickly without having to match the endpoint of the signal to the extrapolation function. By directly adding a set of zeros to the signal the response from the target is centered and the FT is capable of producing an accurate correlation for the HT. Using this method proved successful and removed the apparent edge effects from the response. Considering the ease with which the process was implemented and the positive results that were produced, using zeros to extend the sample window will carried out in the energy envelope algorithm for all field examples.

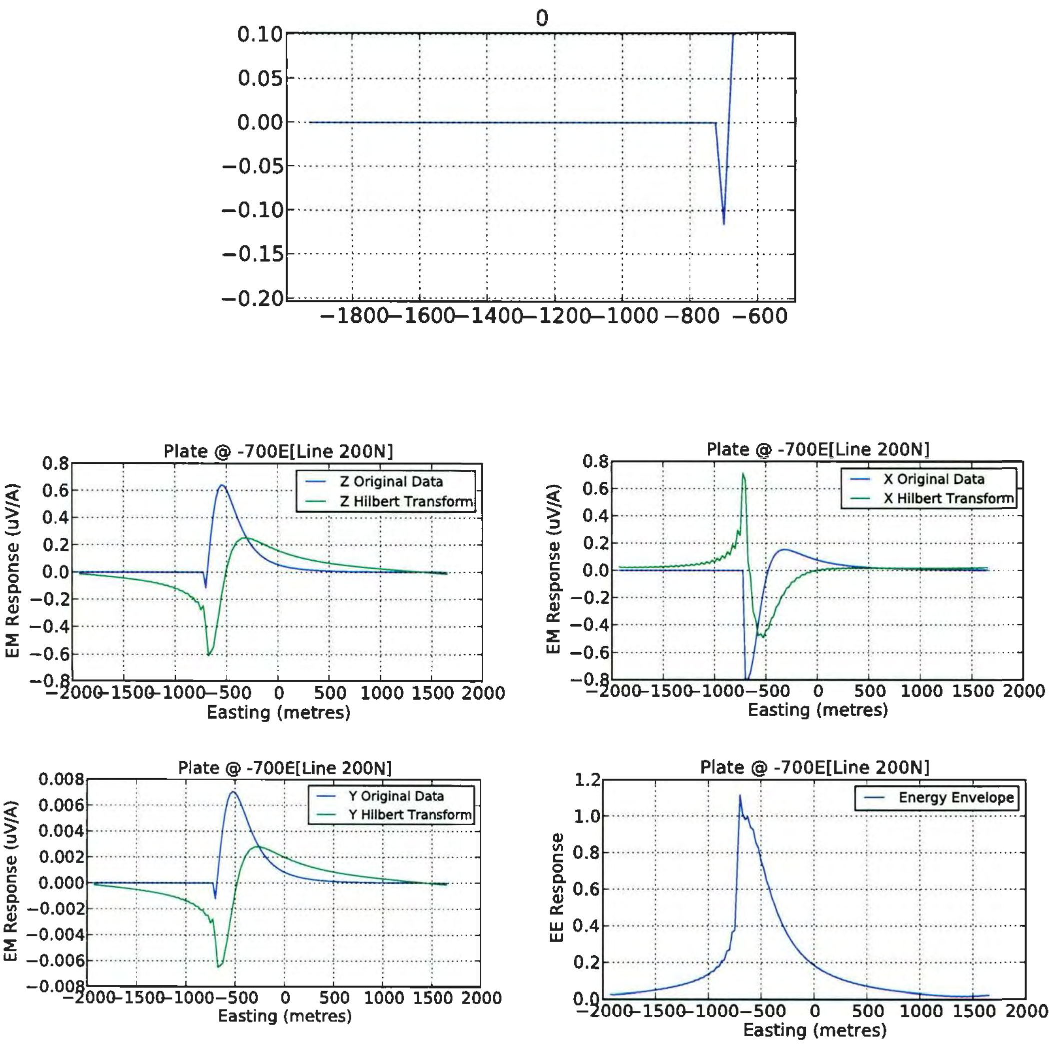

Figure 5.15. The z, x, and y component and EE response profiles of a vertical plate positioned at -700E. Top profile shows extrapolating function used. Blue line indicates original profile and the green line represents the Hilbert transformed quantity of the original signal, as shown in label in upper right corner. Scale on z, x, and y graphs corresponds to EM Response measured in μV/m. Bottom right profile shows energy envelope of all components and scale corresponds to EE Response. Bottom scale indicates Easting position in metres.

5.10 CONTOUR MAPS

Color contour maps for TDEM are developed by combining the profiles of multiple survey lines. Interpretation is consistent with analyzing individual lines where anomalies are indicated by a zero crossover point on one component and a positive or negative peak on another. Figure 5.16 shows an example of a full contour map generated from the same synthetic data used in previous examples, Figure 5.1, where the plate is centred at 500E in an InfiniTEM® transmitter loop. Seven 2.375 km lines with a spacing of 100m were used in creating the survey grid.

The conducting plate is shown on the *z* and *x* component contour maps by the positive to negative crossover on the *z* and the positive peak on the *x*. Although this may seem evident to the experienced EM geophysicist, without previous knowledge in TDEM theory it would be difficult to understand and interpret these particular maps. The EE clearly shows the location of the conductor and more closely resembles conventional contour maps where anomalies are indicated by positive peaks.

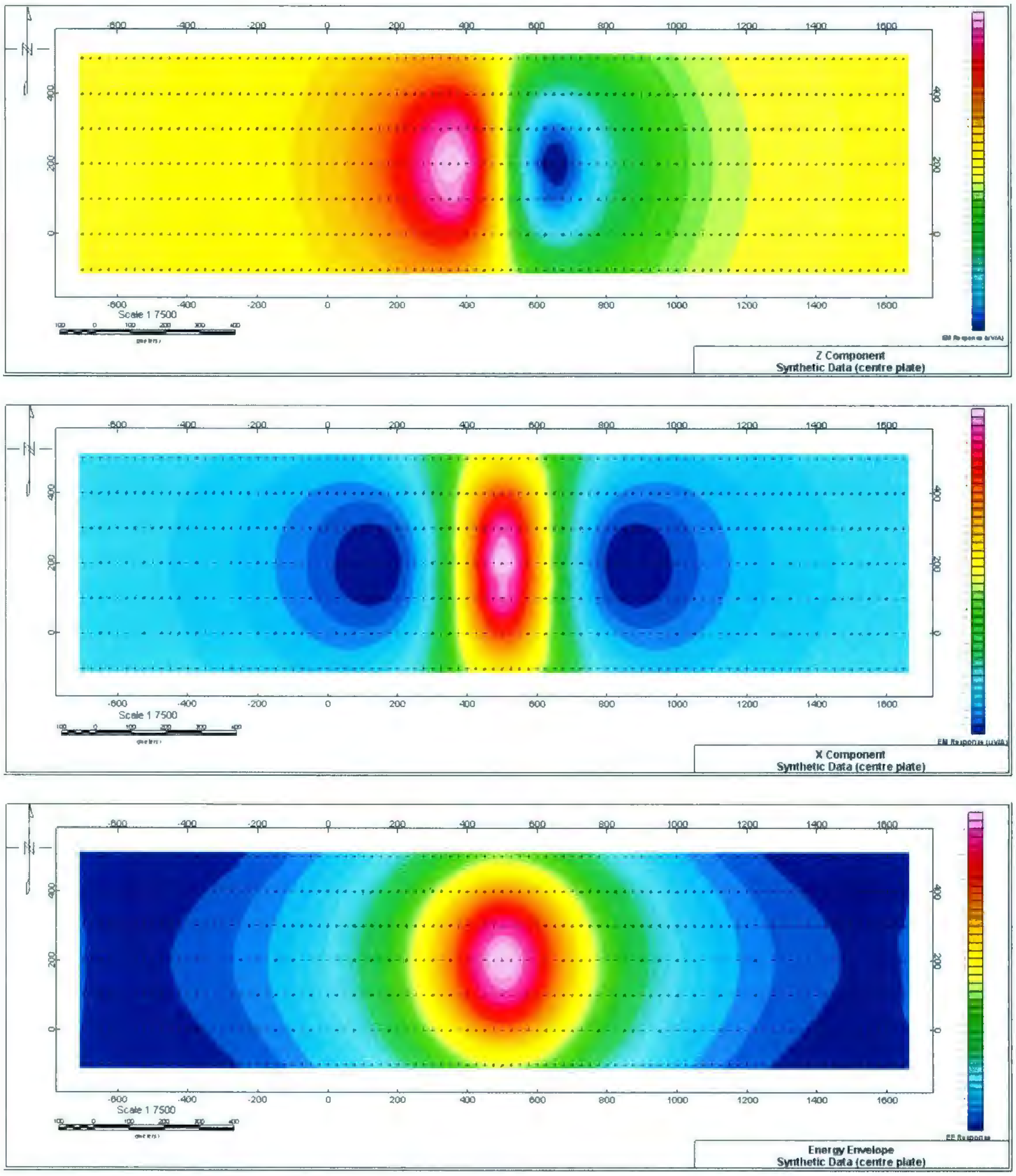

Figure 5.16. Color contour maps of z and x components and EE of InfiniTEM® survey. Scale on right side indicates EM Response measured in μV/A. Bottom contour map shows energy envelope response of all components and scale corresponds to EE Response. North is oriented towards top of page and all relative locations are indicated by edge ticks.

CHAPTER 6

FIELD EXAMPLES

Four field examples were chosen to show the versatility of the EE algorithm in a variety of geological settings. These examples were selected based on the different challenges they pose during processing. The examples consist of two zinc exploration targets in conductive carbonate hosts, a folded VMS deposit in a sedimentary environment, and a complicated graphitic fault system holding uranium.

All data were recorded using a Geonics 3D-3 surface coil receiver. A Geonics TEM57MKll transmitter and TEM67 power module were used to control the different current levels for each particular survey. Tables of channel delay times for each survey are provided in APPENDIX 1. The field measurements were normalized to nV/Am^2 according to the intensity of the transmitting loop and effective surface area of the receiver coil. Maps were generated using Geosoft Oasis Montaj. Larger maps are provided in APPENDIX 2.

6.1 FIELD EXAMPLE 1

This zinc exploration target consisted of a sphalerite unit in a conductive carbonate host. A large, conductive anomaly extending across the survey grid toward the lower extremities of the area displays the presence of a deeply buried semi-massive to massive sulphide mineralization zone in a conductive background. The exact location of the survey area can not be provided due to confidentiality restrictions.

The contour maps from Figure 6.1 show a total of 9.35 km from an InfiniTEM® survey with loop dimensions of approximately 400m – 600m – 400m. A 25m station interval was used on 12 survey lines of 100m spacings. A 14A current was used with a 6.25Hz repetition rate. A low repetition rate was used in this example to allow the eddy currents from the conductive carbonate to migrate into the non-conductive sphalerite sulphide lens.

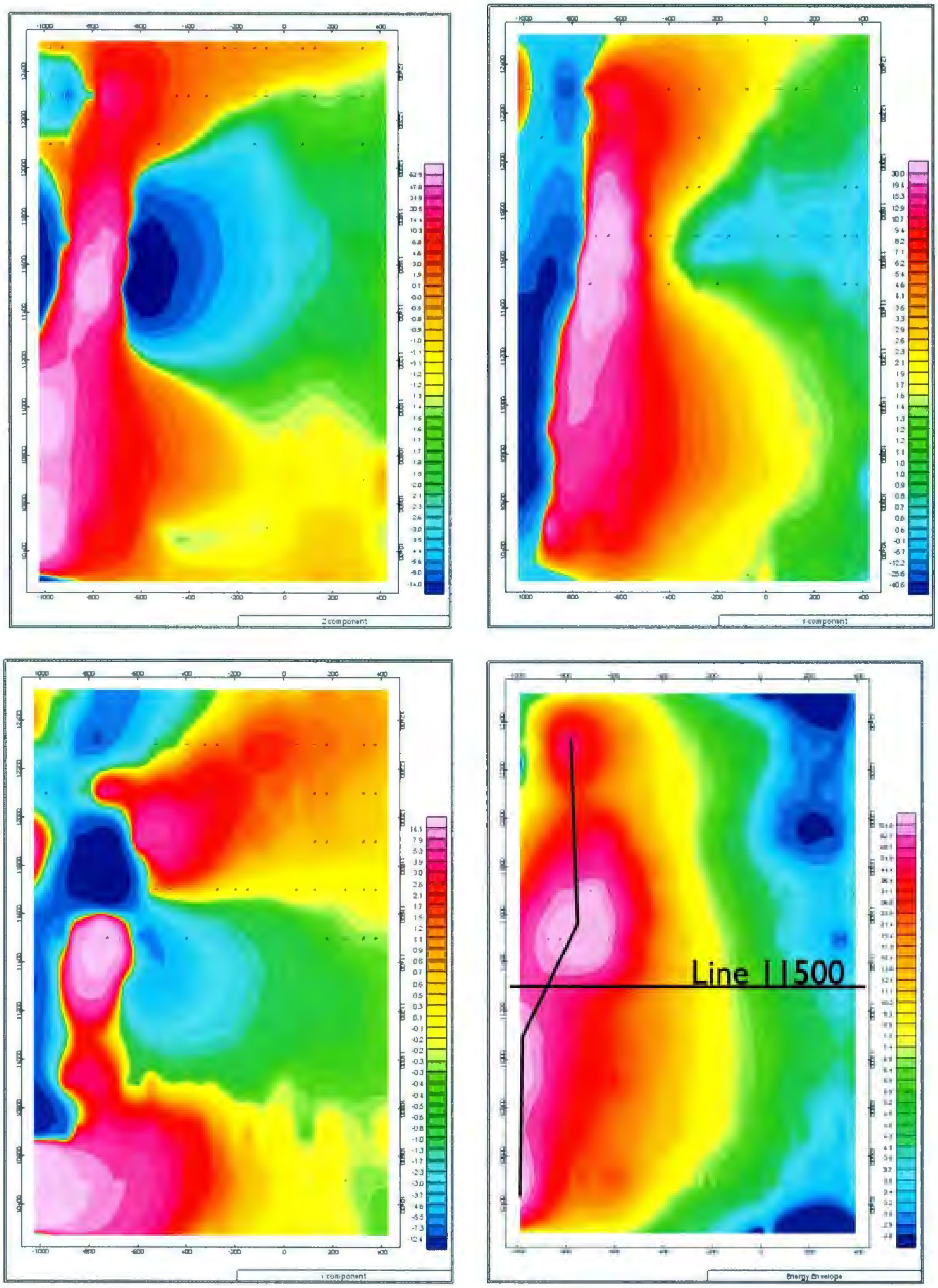

Figure 6.1. Color contour maps of z, x, and y components of InfiniTEM® survey. Scale on right side indicates EM Response measured in nV/Am². Bottom right contour map shows energy envelope response of all components and scale corresponds to EE Response. All relative locations are indicated by edge ticks.

Using the conventional x and z components alone to locate opened ended anomalies is sometimes difficult because the process relies on correlating specific points on both profiles that are not always available. In any exploration survey it is ideal to have the survey grid positioned directly over the desired target. Logistical problems and other unforeseen events do not always make this possible so it is important to have a dependable processing tool that can easily locate the anomaly even when the grid location is not optimal.

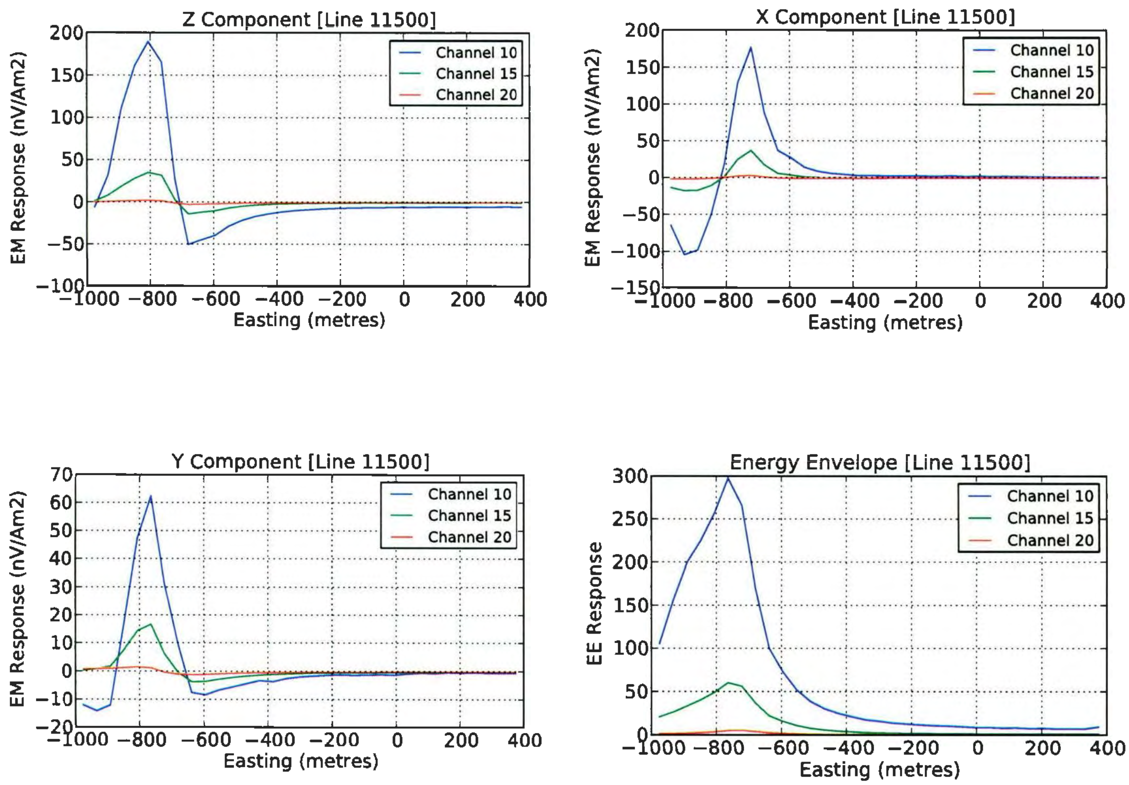

Figure 6.2. The z, x, and y component and energy envelope profiles for Field example 1. Blue, green and red line indicates channel 10, 15 and 20 respectively, as shown in label in upper right corner. Scale on top three graphs corresponds to EM Response measured in nV/Am^2. Bottom right profile shows energy envelope using all components.

The z and x components in Figure 6.2 show a response for the anomaly at -800m with a positive peak on the z component and a negative to positive crossover on the x component. This anomalous response is clearly visible in the EE profile in the bottom right hand panel at the same location.

The EE contour map clearly exhibits an open ended anomaly striking to the southwest with the most western portion lying outside the surveyed area, which is consistent with the components response, Figure 6.1. This is indicated by the black line in the centre of the bright pink area trending to the southern portion of the contour map. The anomaly's signature indicates that the source plunges to the south while its conductance and dimensions decreases northward. Presence of anomalous signature in the north indicates that the source has a great depth extent, but unfortunately prevents identifying the location of the conductor's northern boundary.

The clear and pronounced signature in the EE contour map confirms the effectiveness of the algorithm in this example.

6.2 FIELD EXAMPLE 2

This property is located in the Frotet-Evans Greenstone belt, in northwestern Quebec area. It is composed primarily of two volcanic units separated by a sedimentary unit of siltstone, mudstone and wacke. The two volcanic units are composed of thick basalt and andesite with minor layers of rhyolite, pyroclastic and volcaniclastic rocks. Extensive drilling for EM targets has occurred on the property yielding positive results for copper, gold, zinc and silver.

13.7 kine km were surveyed in the field area to further define the geometry of potential conductors such as semi-massive to massive sulphide mineralization zones associated with base metals. Stations were recorded at 25m intervals on 9 survey lines of 100m spacings. 25A was transmitted over a 30 Hz repetition rate.

Mineral deposits form in a variety of shapes and sizes. Folds and antiforms are common in geological exploration and can be challenging to map without previous knowledge of the area. These types of formation are especially complicated for TDEM because they produce unique secondary fields that are specific to that particular shaped structure. Figure 6.3 provides an example of the complications that can arise during interpretation. Over 20 plates were needed to accurately model the formation. Without the use of forward modeling it would be extremely difficult to identify the conductors producing the response. The energy envelope will help produce a more intuitive representation of the component's response.

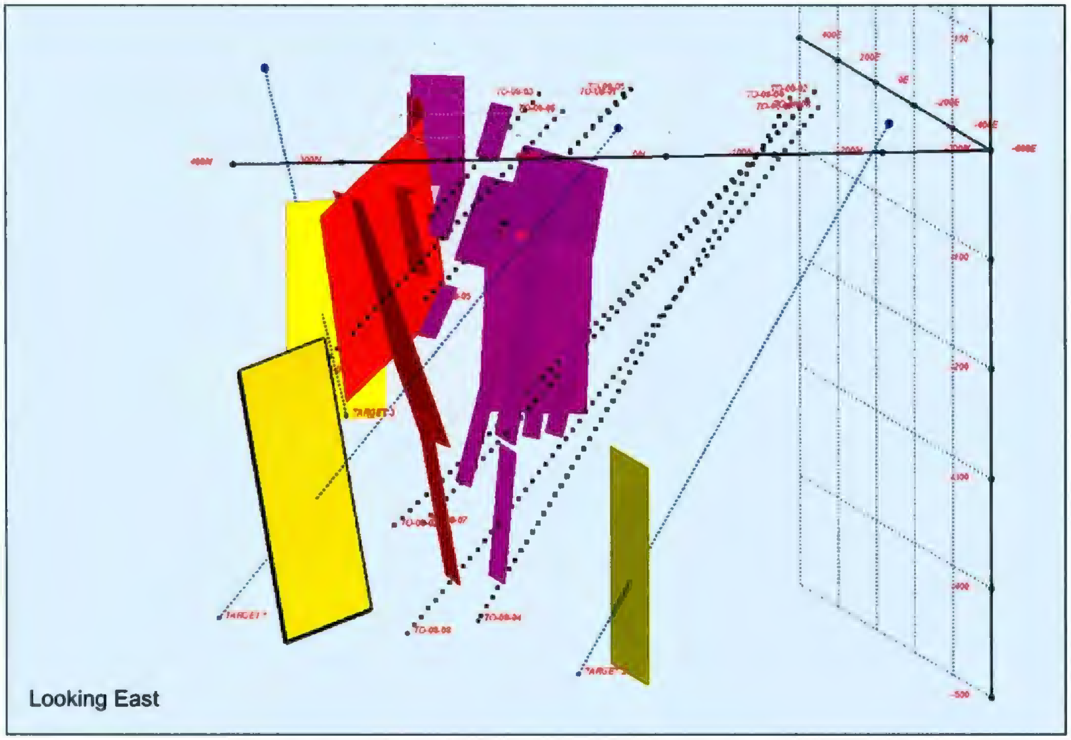

Figure 6.3. Forward model created with EMIT Maxwell software for Field example 2 oriented towards the East. Large multicolor boxes indicate location of modelled anomalies. Dotted blue and black lines show locations of exploration drill holes (per. comm. Malo-Lalande).

From the contour maps, shown in Figure 6.4, an open-ended anomaly is apparent to the west with varying conductance, indicated by the change in the level of EM response. The structure also appears to be delineated by a fault towards the east with its quality changing along its conductive axis. It is extremely difficult to determine the exact shape of the unit from the component contour maps. The EE contour map on the other hand distinctly shows a folded conductive unit with its hinge line oriented to the east, indicated by black lines on the contour map. The total response for EE produced a much more intuitive map of this area that is easily interpretable.

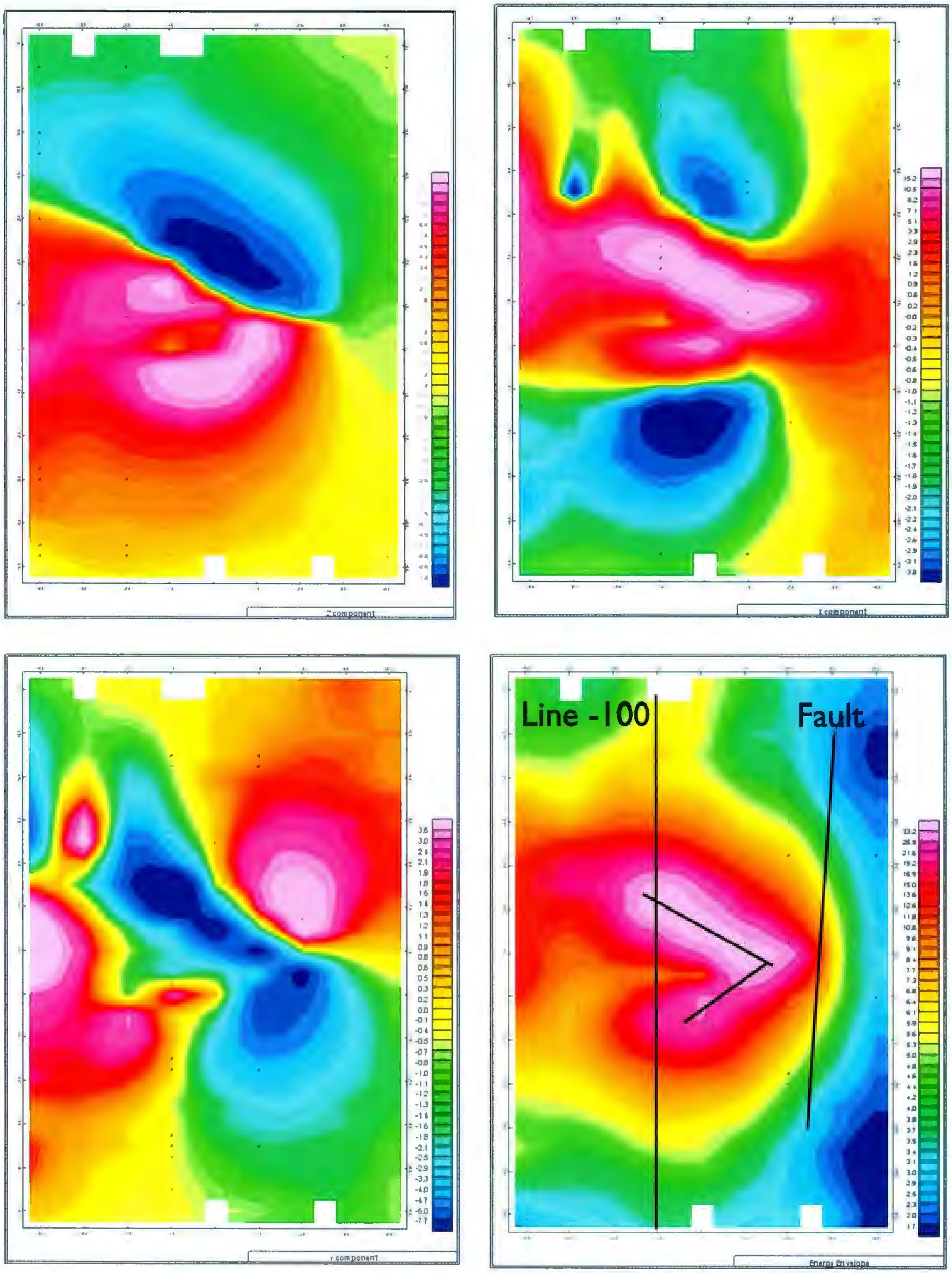

Figure 6.4. Color contour maps of z, x, and y components of InfiniTEM® survey. Scale on right side indicates EM Response measured in nV/Am^2. Bottom right contour map shows energy envelope response of all components and scale corresponds to EE Response. All relative locations are indicated by edge ticks.

The z and x components still display an anomalous response but it is difficult to determine the exact shape of the structure. Two positive to negative cross overs at 0m and 210m on the z component can be correlated to two positive peaks on the x (see Figure 6.5). Although it is possible to identify these signatures on the components profiles, the EE provides a more pronounced response that can be easily identified without further interpretation.

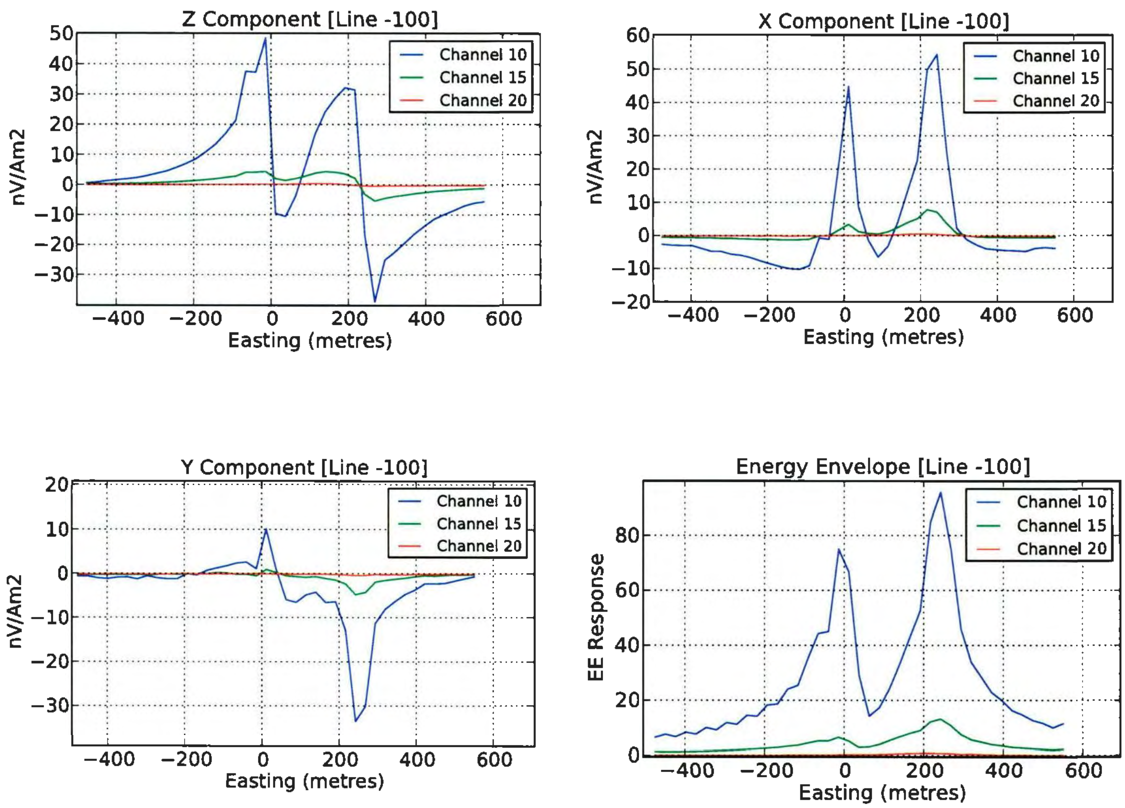

Figure 6.5. The z, x, and y component and energy envelope profiles for Field example 2. Blue, green and red lines indicate channel 10, 15 and 20 respectively, as shown in label in upper right corner. Scale on top three graphs corresponds to EM Response measured in nV/Am^2. Bottom right profile shows energy envelope using all components.

6.3 FIELD EXAMPLE 3

A total of 17.4 line km of InfiniTEM® survey were acquired in Northern Quebec, with a 25m station interval on 25 lines of 100m spacing. 20A was transmitted over a 30 Hz repetition rate. The survey detected numerous anomalous features that correspond to a graphitic horizon indicated by a dominant lateral continuity, good source conductance and thin geometry which helped indicate a large fault system. These properties correlate and show good indication of the primary exploration target, uranium. The uranium mineralization discovered on the property is a metasedimentary deposit belonging to the Lake Harbour Group. The main mineralization is located along contacts between ductile highly deformed paragneisses, marbles and pegmatites. Other information and the exact location of the survey area can not be provided due to confidentiality restrictions.

When surveying a very large area it is sometimes necessary to move the transmitter loop several times to cover the entire grid. This avoids trying to use a larger loop area which results in a weaker primary field. The survey in Figure 6.6 required moving the InfiniTEM® loop 3 times to cover the 2.5 km area. Orientating the lines perpendicular to the strike allows the measured z and x components to produce a constant profile of the secondary field over the large area. This can be seen in the large linear response from the anomaly indicated by a zero cross over on the z component and the positive peak on the x component extending North to South on both contour maps (see Figure 6.6).

This anomaly provided a substantial test for the EE technique for it required producing a consistent profile over a large area while using data from multiple transmitter loop locations. The EE generated a distinct profile for the anomaly for the entire span of the grid and provided a unique perspective on areas that produced the strongest responses. A smaller anomaly is also apparent in the Eastern portion of the grid at Line 200N. This anomaly was not as pronounced in the components contour maps and is more distinguishable with the EE technique.

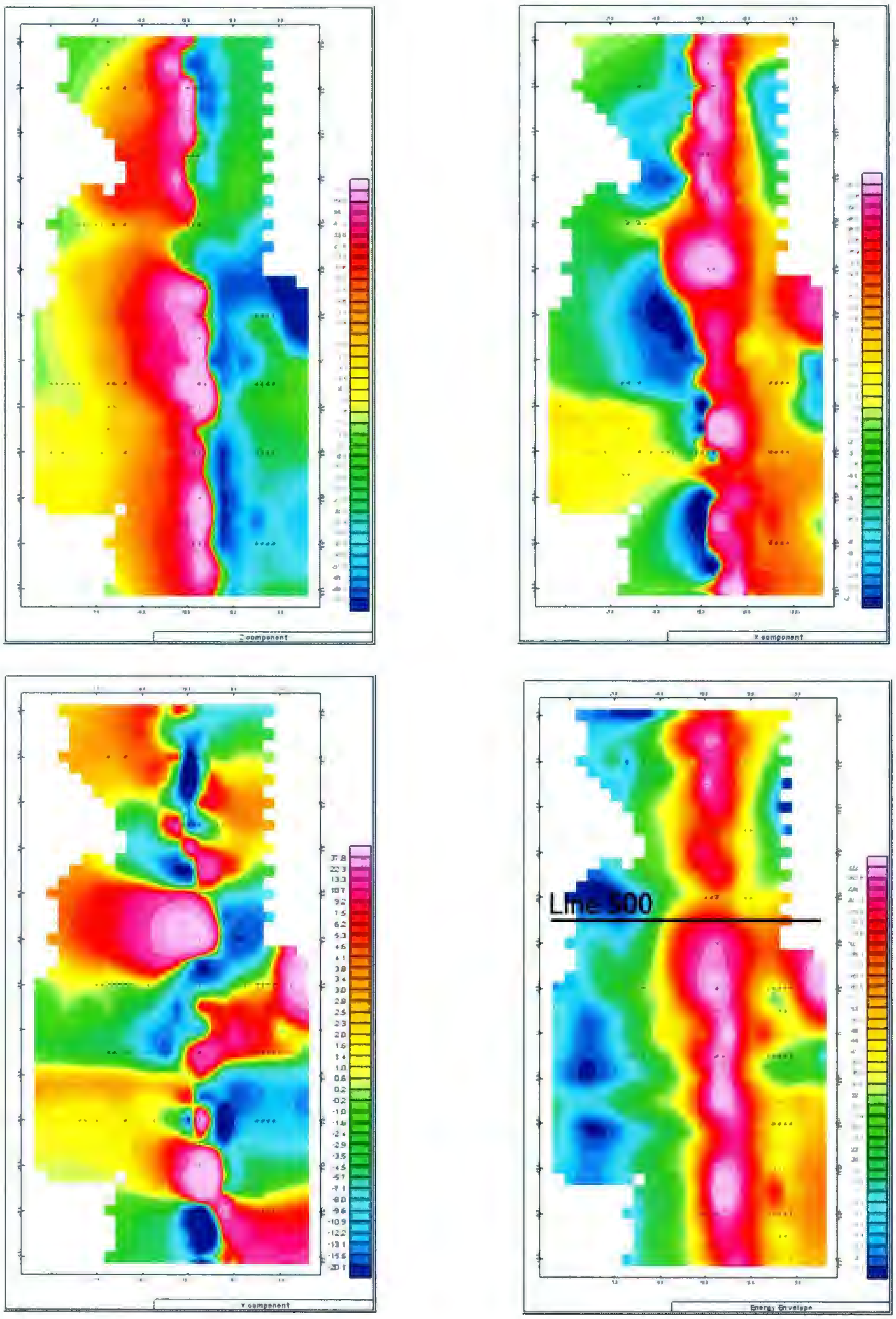

Figure 6.6. Color contour maps of *z*, *x*, and *y* components of InfiniTEM® survey. Scale on right side indicates EM Response measured in nV/Am². Bottom right contour map shows energy envelope response of all components and scale corresponds to EE Response. A relative locations are indicated by edge ticks.

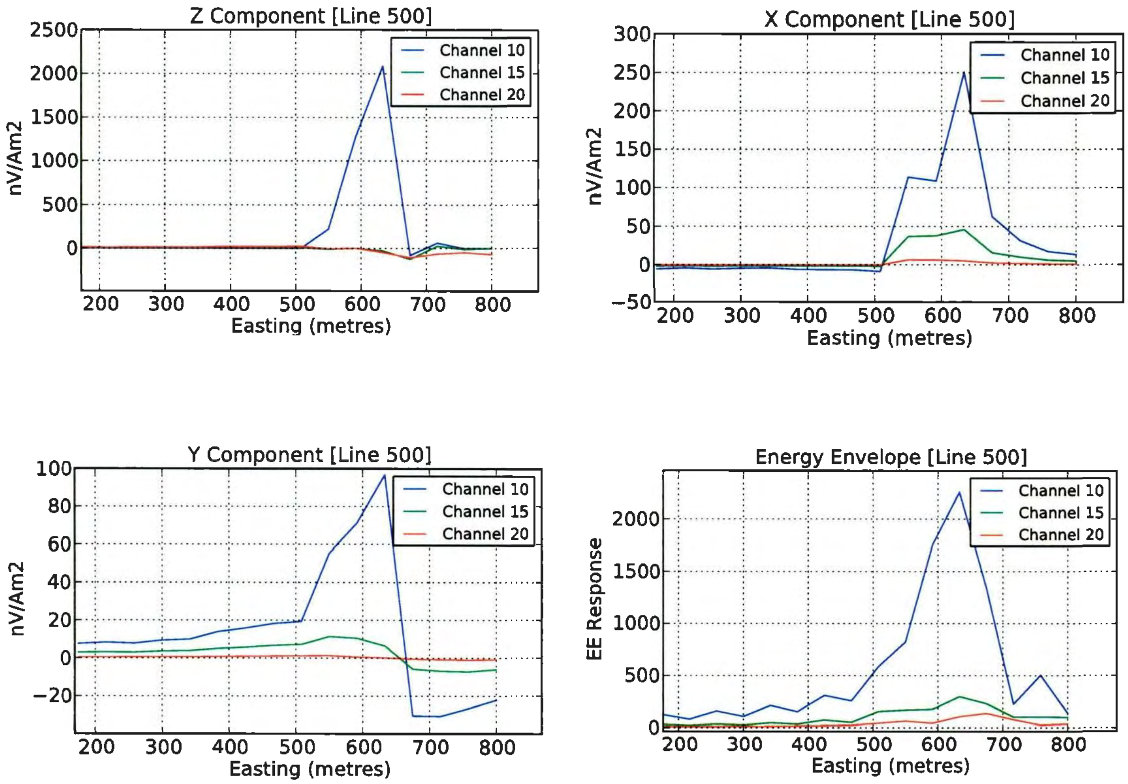

Figure 6.7. The z, x, and y component and energy envelope profiles for Field example 3. Blue, green and red line indicate channel 10, 15 and 20 respectively, as shown in label in upper right corner. Scale on top three graphs corresponds to EM Response measured in nV/Am^2. Bottom right profile shows energy envelope using all components.

FIELD EXAMPLE 4

Figure 6.8 shows results of a survey containing two distinct anomalies, one in the centre and the other in the lower southwest portion of the grid. A smaller response anomaly is also apparent located in the west portion of the grid. A total of 28.2 line km of InfiniTEM® survey was acquired with a grid consisting of N-S lines with spacings of 100m or 200m apart and a 50 m station interval. The InfiniTEM® loops (approx. 400m – 600m – 400m) were used to transmit a current of 14A with a 6.25 Hz repetition rate, common for zinc exploration in conductive environments. Other information and the exact location of the survey area can not be provided due to confidentiality restrictions.

As in previous examples TDEM surveys containing multiple anomalies tend to complicate processing as there are many secondary fields in the area which make them difficult to correctly identify. Although the z and x components yield anomalous signatures, the many high and low portions make the contour maps problematic to interpret. The combined component response of the EE eliminates this problem and produces an easily interpretable map and clearly identifies any anomalous responses in the area.

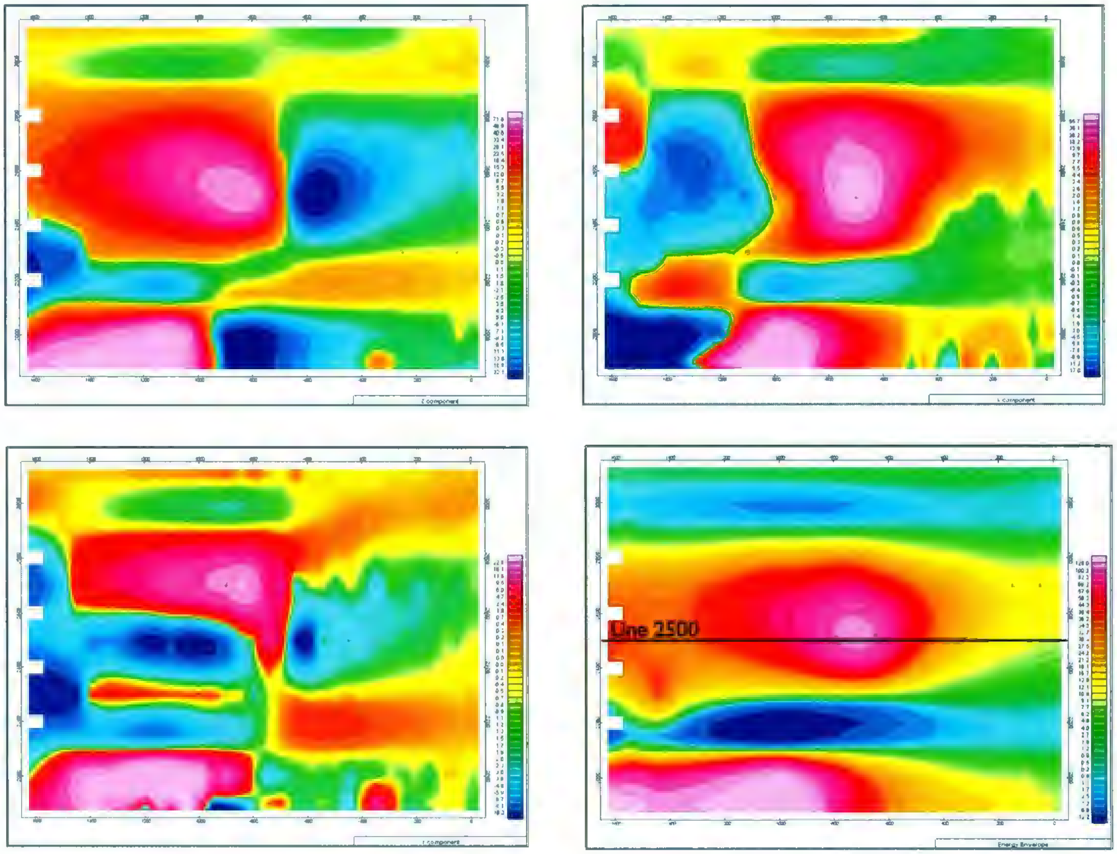

Figure 6.8. Color contour maps of z, x, and y components of InfiniTEM® survey. Scale on right side indicates EM Response measured in nV/Am^2. Bottom right contour map shows energy envelope response of all components and scale corresponds to EE Response. All relative locations are indicated by edge ticks.

The two large anomalies are characterized as good conductors, most likely associated with base metal mineralization. Both dip towards the west, which can be seen by the gradual slope on the west flank of the components profiles, as well as the energy envelope (see Figure 6.9).

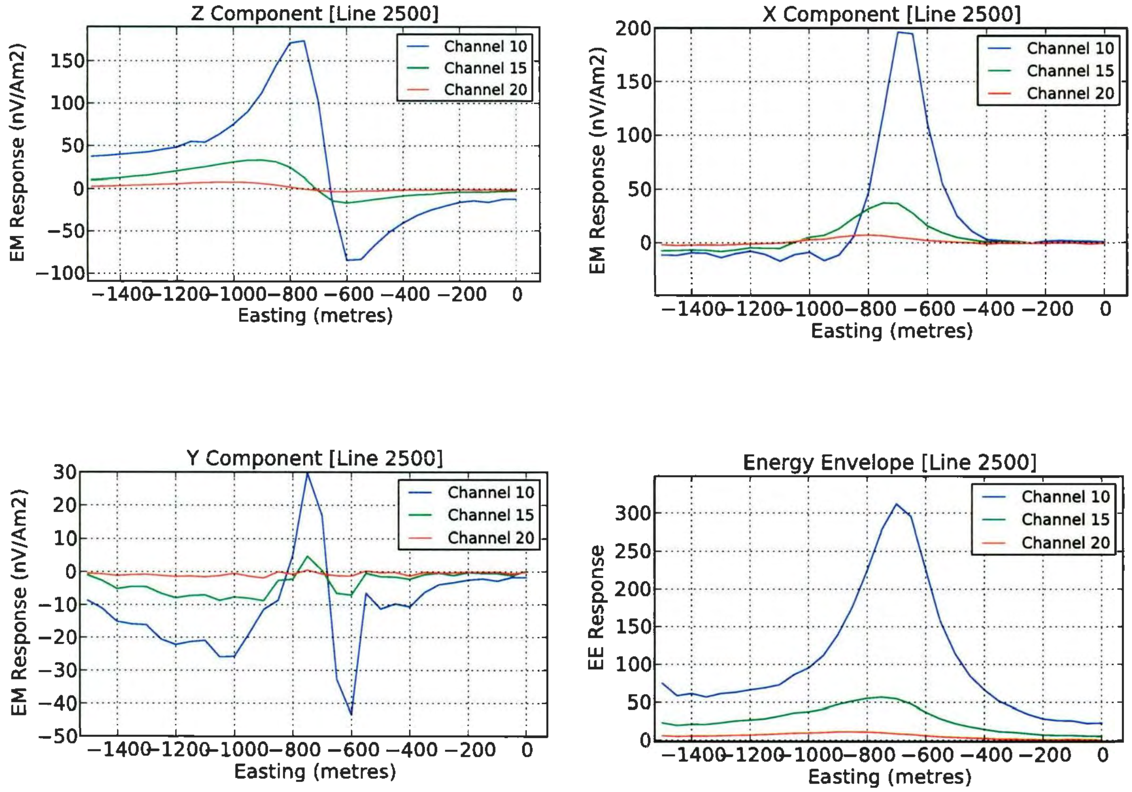

Figure 6.9. The z, x, and y component and energy envelope profiles for Field example 4. Blue, green and red lines indicate channel 10, 15 and 20 respectively, as shown in label in upper right corner. Scale on top three graphs corresponds to EM Response measured in nV/Am^2. Bottom right profile shows energy envelope using all components.

Through forward modeling the three anomalous signatures can be correlated with the plate locations in Figure 6.10. The lower amplitude response in the western plate can be attributed to its smaller size and proximity to the larger anomalies which yield larger base widths in their signatures. The energy envelope contour map is consistent with the results of the model and provides a clear perspective of the anomalies in the area.

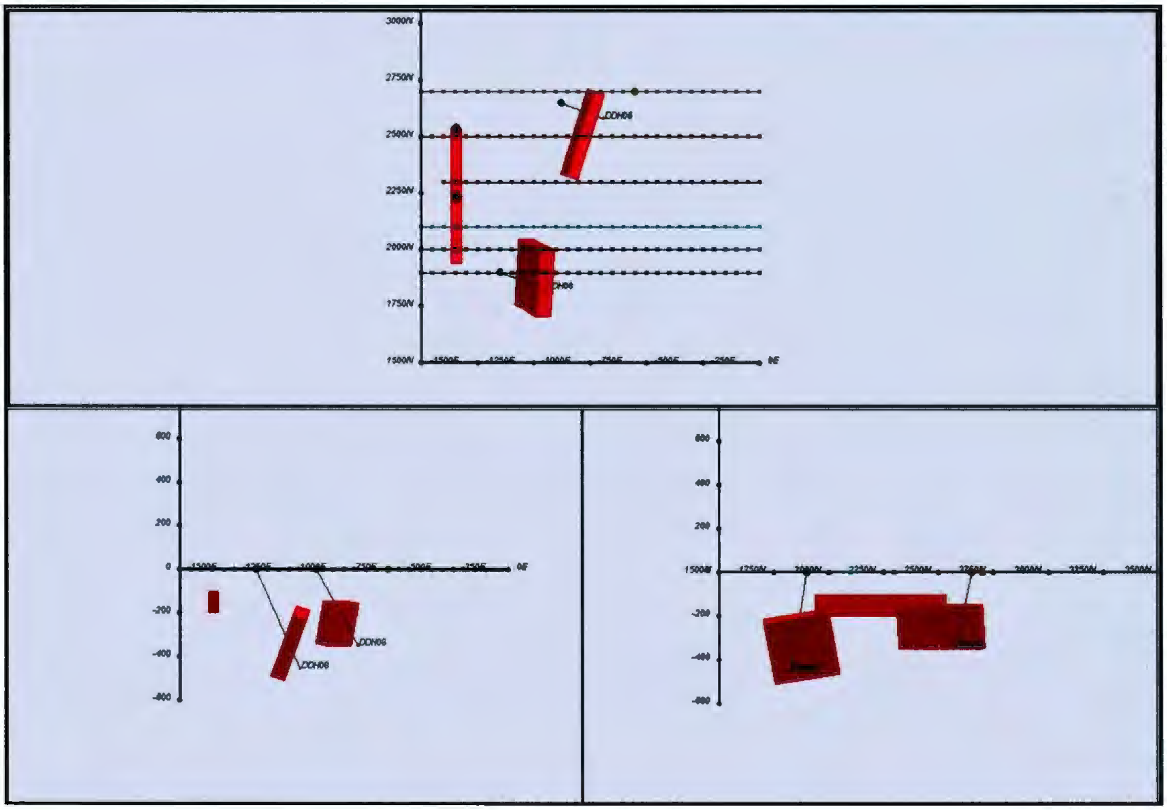

Figure 6.10. Forward model created with EMIT Maxwell software for Field example 4. Top panel shows top view of survey grid, bottom left panel is plane view looking South, bottom right is plane view looking East. Multicolored lines show survey lines and station locations. Large red boxes indicate location of modelled anomalies.

CHAPTER 7

CONCLUSION

TDEM is a widely used tool in base metal exploration. An anomaly's response can be complicated to interpret because of its dependancy on the primary field from the transmitter. This is especially so for the InfiniTEM® configuration where the same conductive vertical plate can produce a variety of signatures depending on its location. The goal of using the energy envelope in this study was to isolate the response and produce a more viable consistent signature that can be identified easily.

The Python code created to calculate the energy envelope is a fast and efficient algorithm that can produce reliable results in a variety of scenarios. It corrects for processing artifacts from limitations in the Hilbert transform and makes potential exploration targets located on the edge of survey areas more prominent.

Through numerous synthetic examples of a conductive plate in a variety of positions, depths, orientations and sizes, the energy envelope showed a consistent response regardless of the shape of the individual component profile.

Although combining the components together with their Hilbert transform counterparts produces a different method for interpreting TDEM data, the EE still holds common attributes with the original data that can be useful for determining conductance quality as well as certain orientation parameters. The half width and angle of the profile sides can provide information pertaining to the depth and dip of a conductive unit.

Due to the properties of the Fourier transform when calculating the Hilbert transform the energy envelope can produce edge artifacts towards the edge points of the signal. These can be more severe with lower amplitude data. By extrapolating the data beyond the sampled window these effects can be reduced. Doing this will make anomalous signatures produced by conductive bodies outside the surveyed area more detectable, as well as weaker or lower amplitude responses.

Producing colour contour maps for TDEM data is not as common as it is for other geophysical methods due to the interpretation practices of comparing peaks to zero crossover points in different components. However, the EE data provides a intuitive map that can be easily interpreted. This can be extremely beneficial when mapping geological formations across survey grids with a changing primary field.

Testing the EE on professionally acquired field data provided the most critical assessment of the algorithms' efficiency. The EE proved effective in a variety of geological environments with its consistent response providing an accurate representation of the different formations. The ability of the EE to detect horizontal and lateral changes in an anomalies response over large areas is its most beneficial characteristic.

The energy envelope is therefor a valuable processing tool for TDEM. Through an number of examples the algorithm showed consistent and accurate results. Its simple, straight forward profile provides an intuitive representation of the electromagnetic response in a given area.

APPENDIX 1

Channel decay times used for all synthetic data in Chapters 1-5 and field examples in Chapter 6.

Synthetic Data (30Hz)		
Channel	**Delay Time (ms)**	**Time width (ms)**
1	0.0881	0.0163
2	0.1069	0.0213
3	0.1313	0.0275
4	0.1619	0.0338
5	0.2006	0.0437
6	0.2506	0.0562
7	0.3144	0.0712
8	0.3956	0.0913
9	0.4994	0.1163
10	0.6313	0.1475
11	0.7994	0.1888
12	1.0140	0.2400
13	1.2870	0.3063
14	1.6360	0.3913
15	2.0810	0.4988
16	2.6480	0.6363
17	3.3730	0.8125
18	4.2970	1.0360
19	5.4750	1.3210
20	6.9780	1.6850

Field example 1 (6.25Hz)		
Channel	**Delay Time (µs)**	**Time width (µs)**
1	320.0	65.00
2	385.0	85.00
3	470.0	110.0
4	580.0	135.0
5	715.0	175.0
6	890.0	225.0
7	1115	285.0
8	1400	365.0
9	1765	465.0
10	2230	590.0
11	2820	755.0
12	3575	960.0
13	4535	1225
14	5760	1565
15	7325	1995
16	9320	2545
17	11870	3250
18	15120	4145
19	19260	5285
20	24550	6740

Field example 2 (30Hz)		
Channel	**Delay Time (µs)**	**Time width (µs)**
1	80.00	16.25
2	96.25	21.25
3	117.5	27.50
4	145.0	33.75
5	178.8	43.75
6	222.5	56.25
7	278.5	71.25
8	350.0	91.25
9	441.3	116.3
10	557.5	147.5
11	705.0	188.8
12	893.8	240.0
13	1134	306.3
14	1440	391.3
15	1831	498.8
16	2330	636.3
17	2966	812.5
18	3779	1036
19	4815	1321
20	6136	1685

Field example 3 (30Hz)		
Channel	**Delay Time (µs)**	**Time width (µs)**
1	80.00	16.25
2	96.25	21.25
3	117.5	27.50
4	145.0	33.75
5	178.8	43.75
6	222.5	56.25
7	278.5	71.25
8	350.0	91.25
9	441.3	116.3
10	557.5	147.5
11	705.0	188.8
12	893.8	240.0
13	1134	306.3
14	1440	391.3
15	1831	498.8
16	2330	636.3
17	2966	812.5
18	3779	1036
19	4815	1321
20	6136	1685

Field example 4 (6.25Hz)		
Channel	Delay Time (μs)	Time width (μs)
1	320.0	65.00
2	385.0	85.00
3	470.0	110.0
4	580.0	135.0
5	715.0	175.0
6	890.0	225.0
7	1115	285.0
8	1400	365.0
9	1765	465.0
10	2230	590.0
11	2820	755.0
12	3575	960.0
13	4535	1225
14	5760	1565
15	7325	1995
16	9320	2545
17	11870	3250
18	15120	4145
19	19260	5285
20	24550	6740

APPENDIX 2

Enlarged contour maps of field data in Chapter 6.

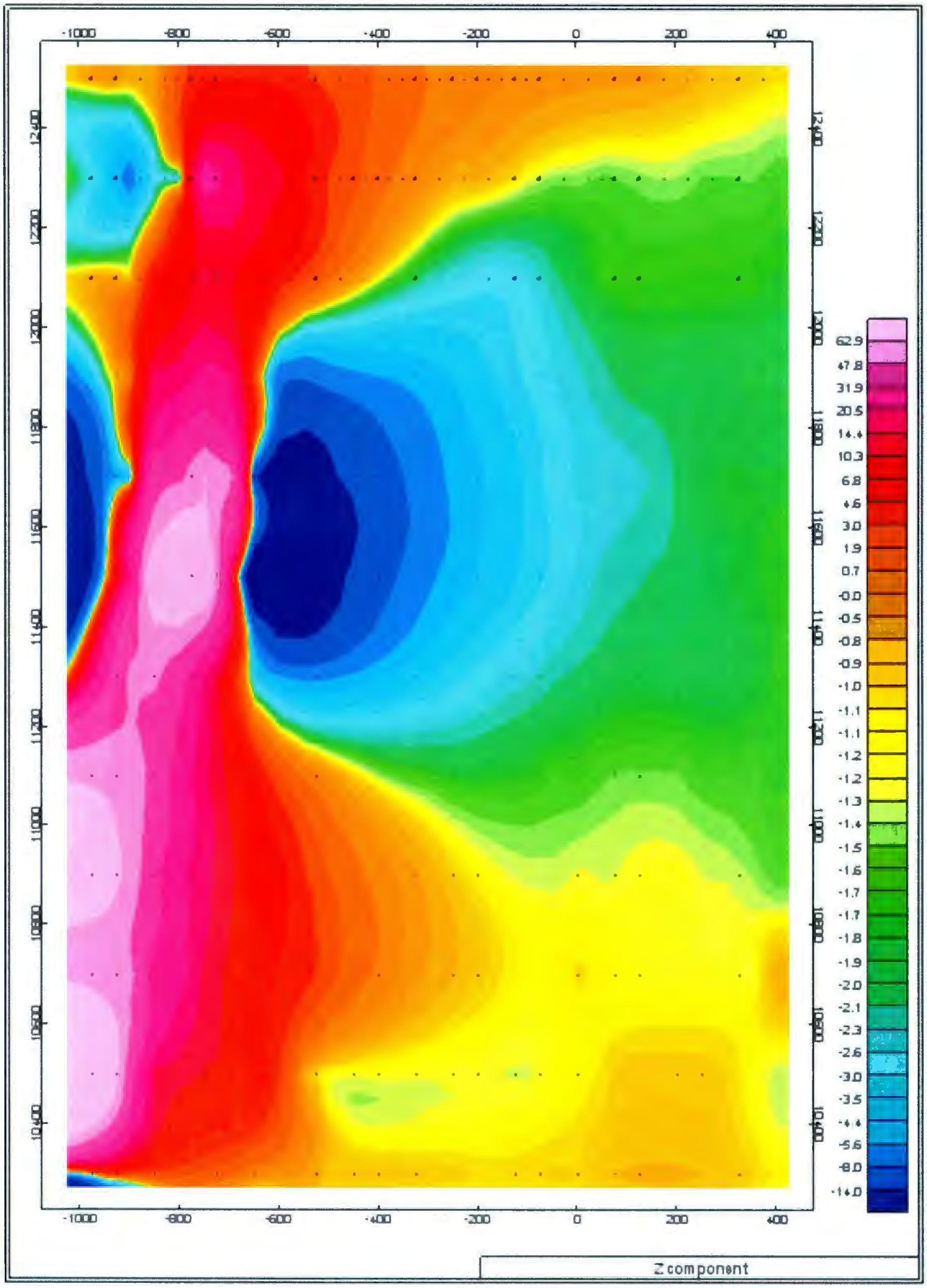

Field Example 1: *z* component

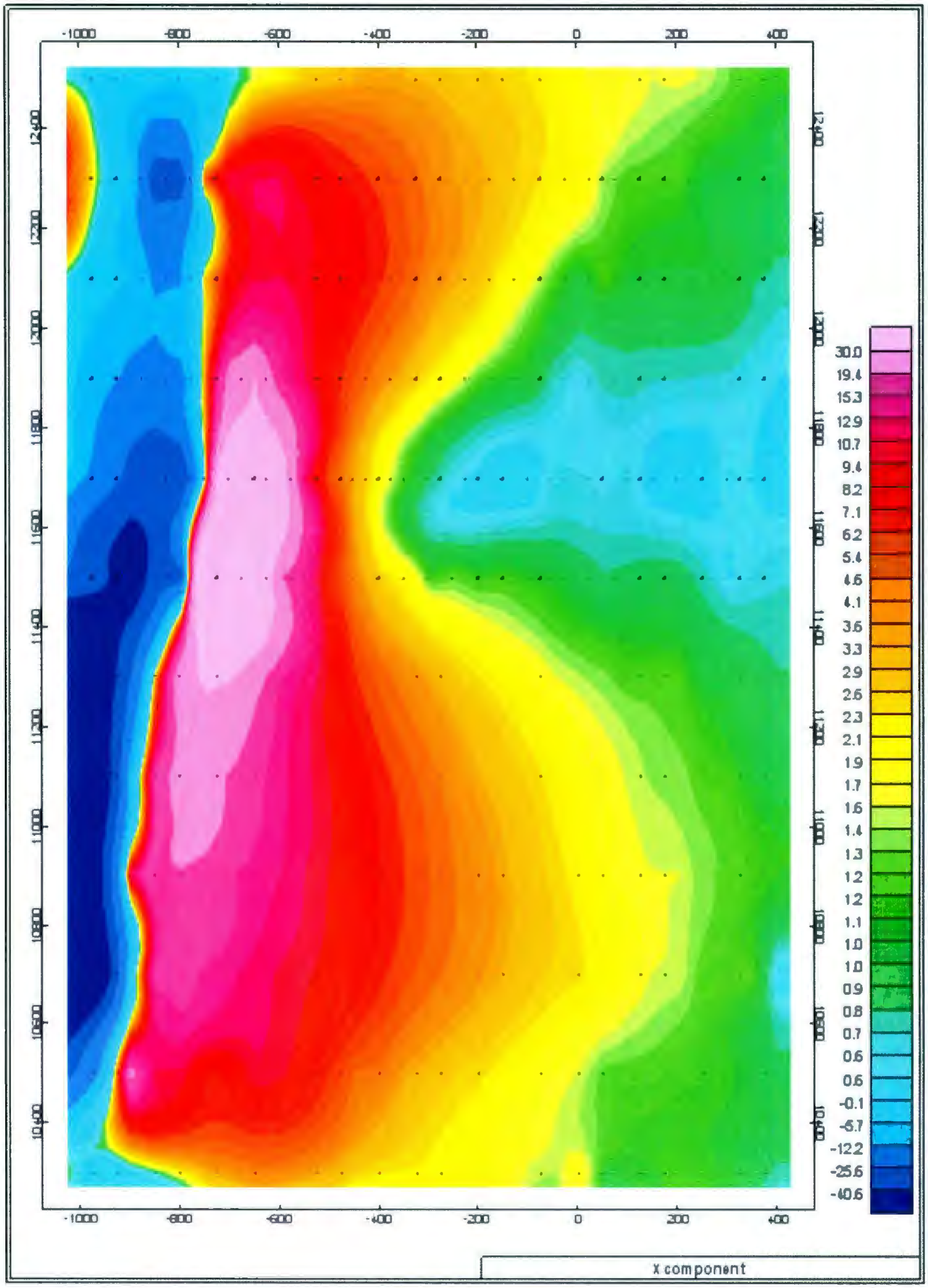

Field Example 1: *x* component

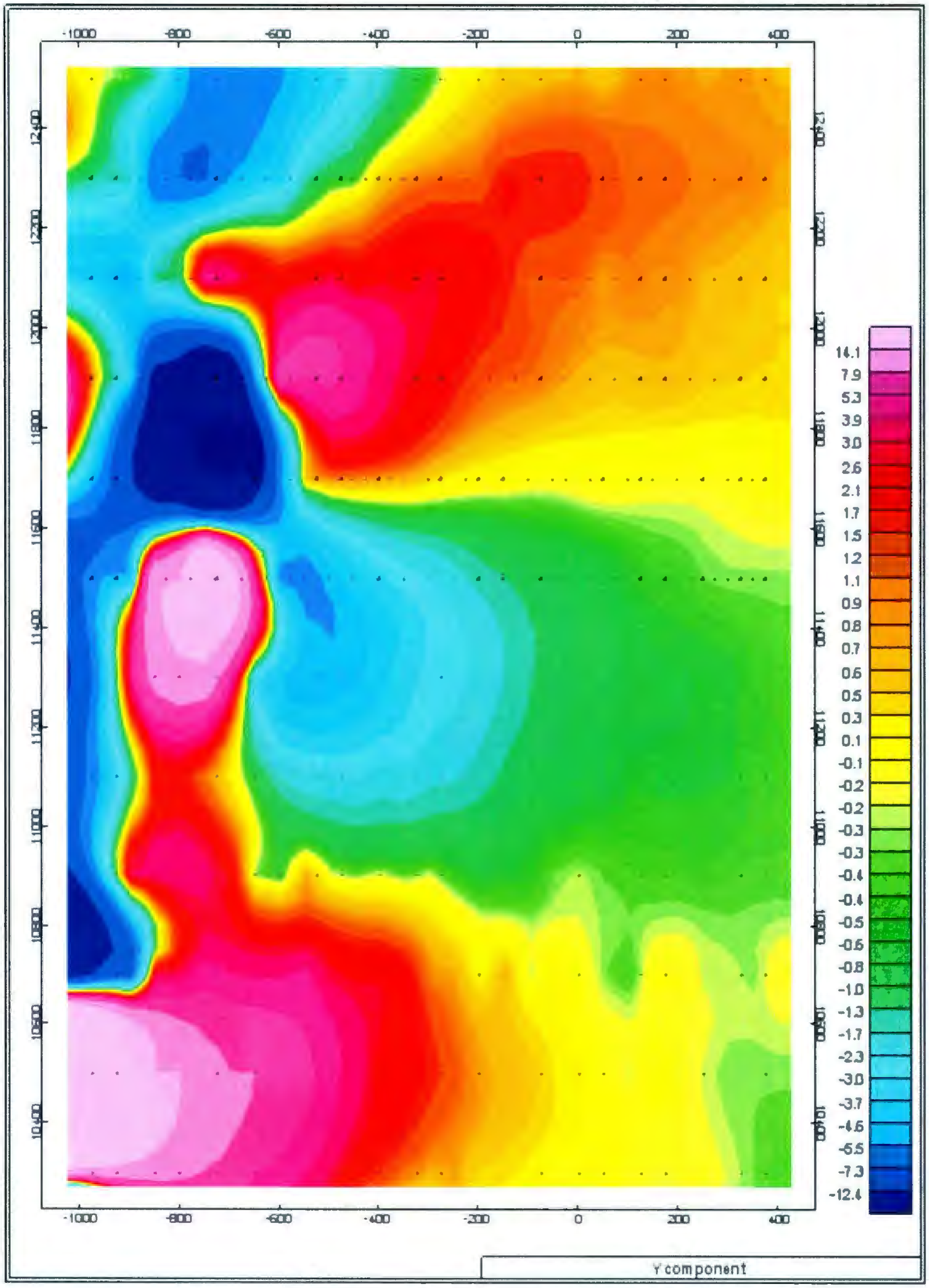

Field Example 1: *y* component

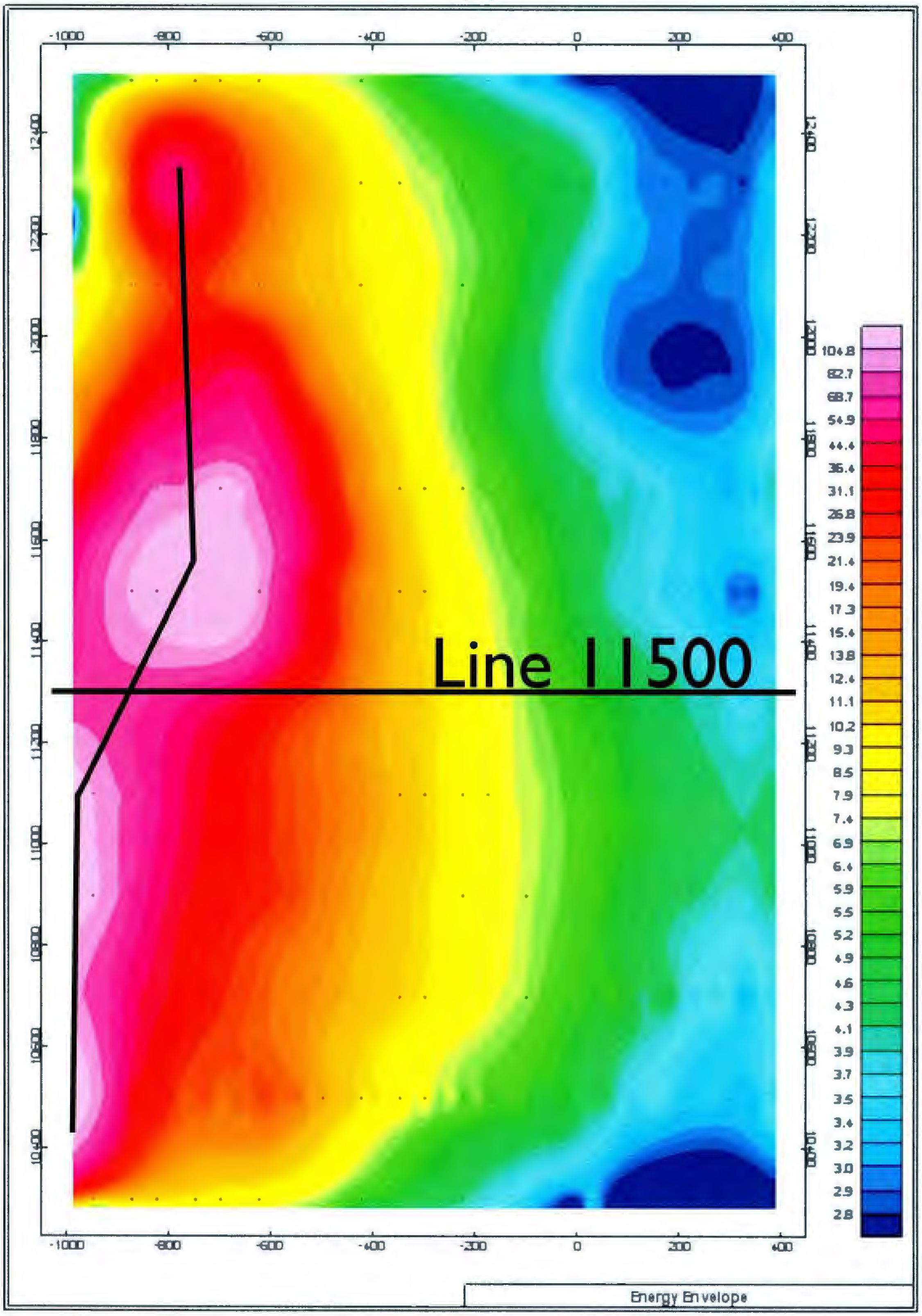

Field Example 1: Energy Envelope

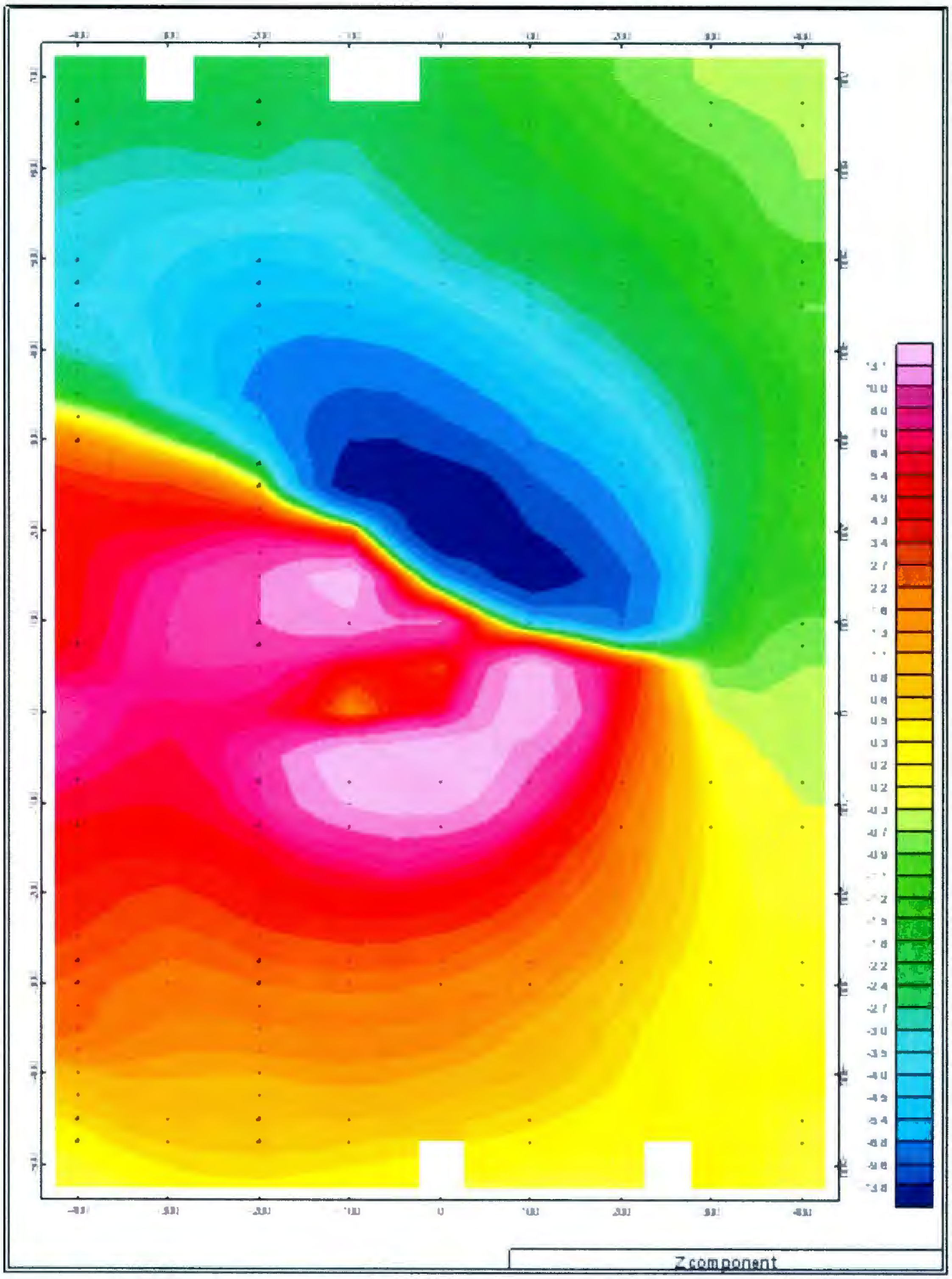

Field Example 2: *z* component

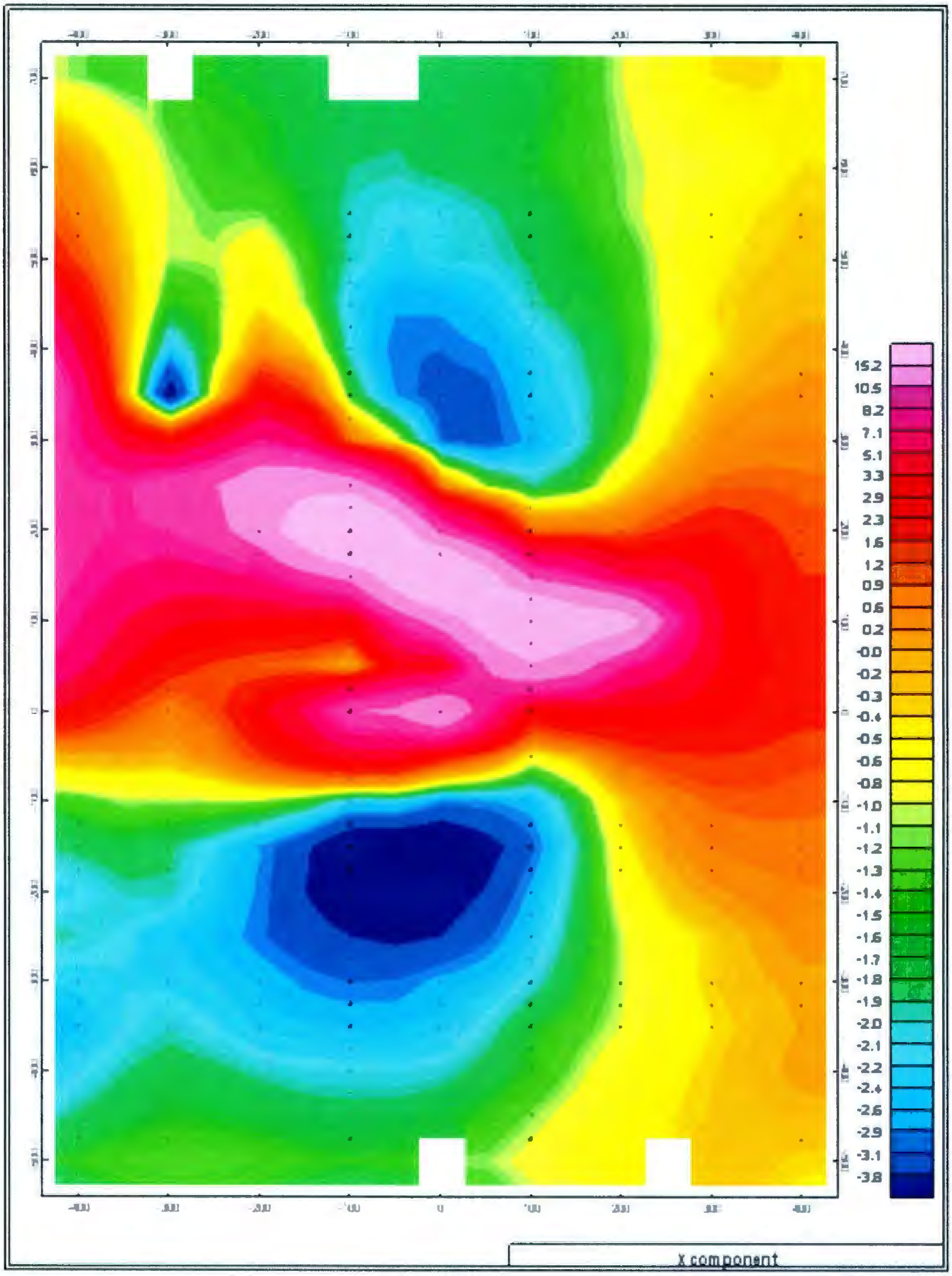

Field Example 2: *x* component

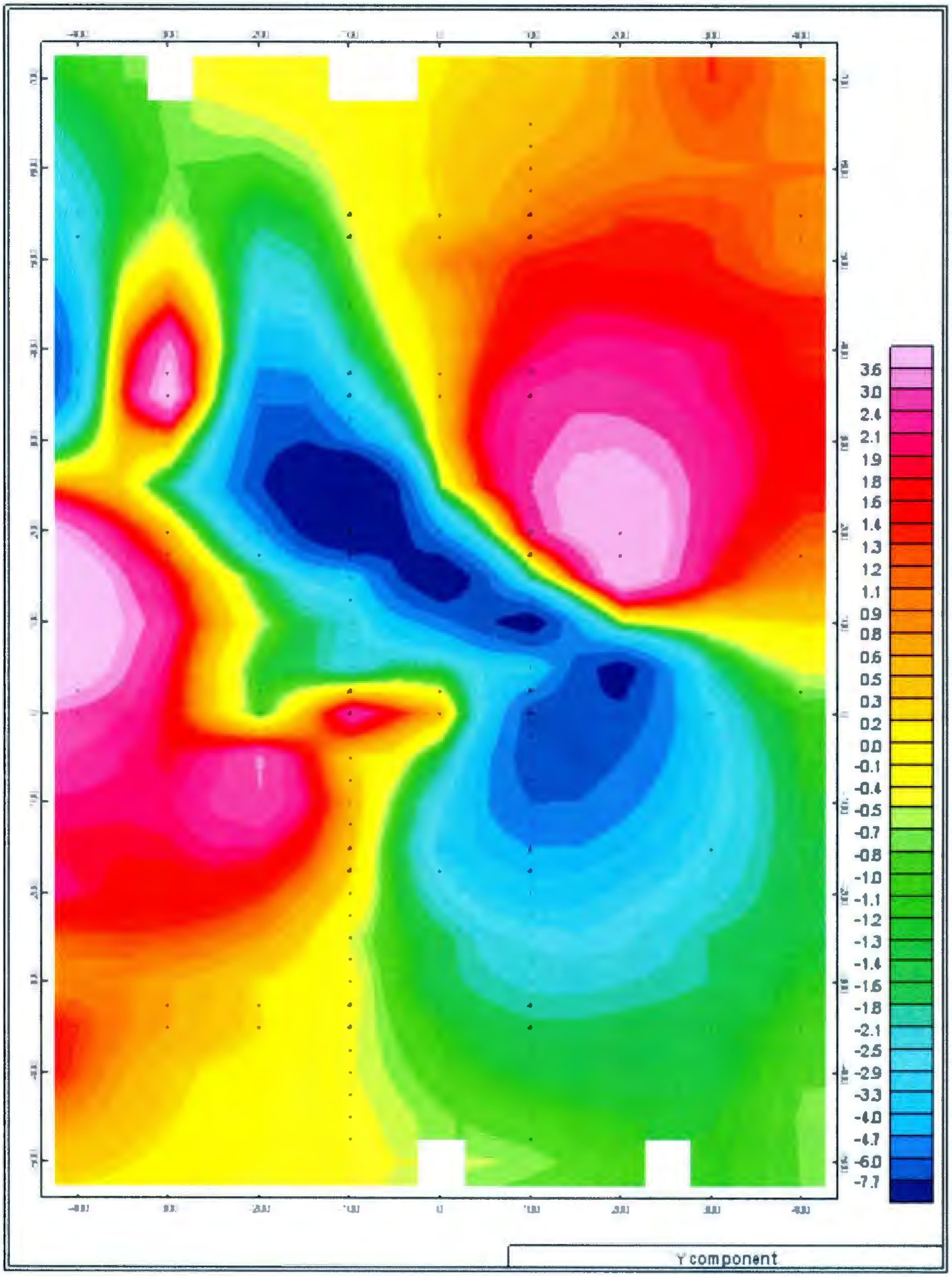

Field Example 2: *y* component

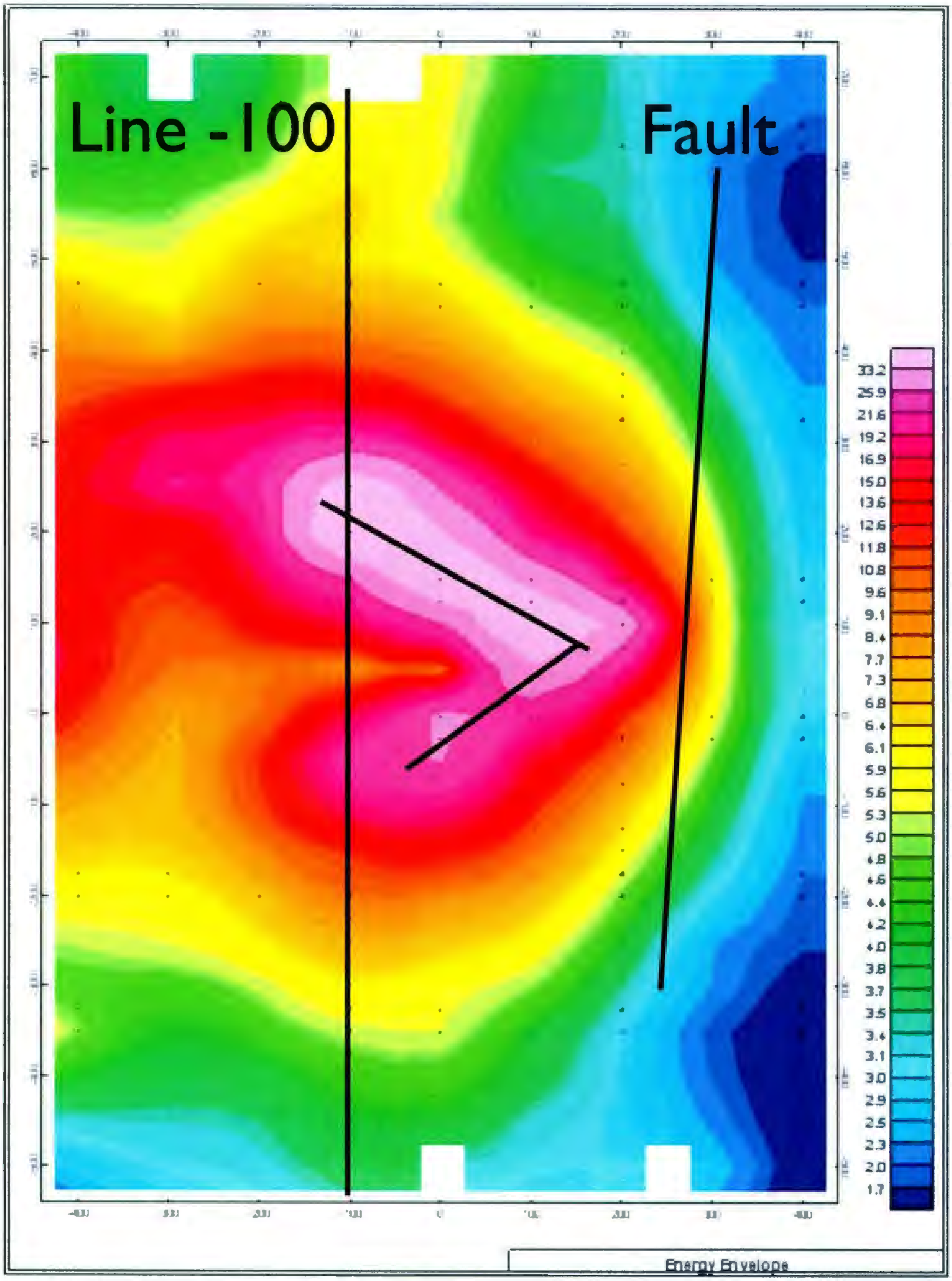

Field Example 2: Energy Envelope

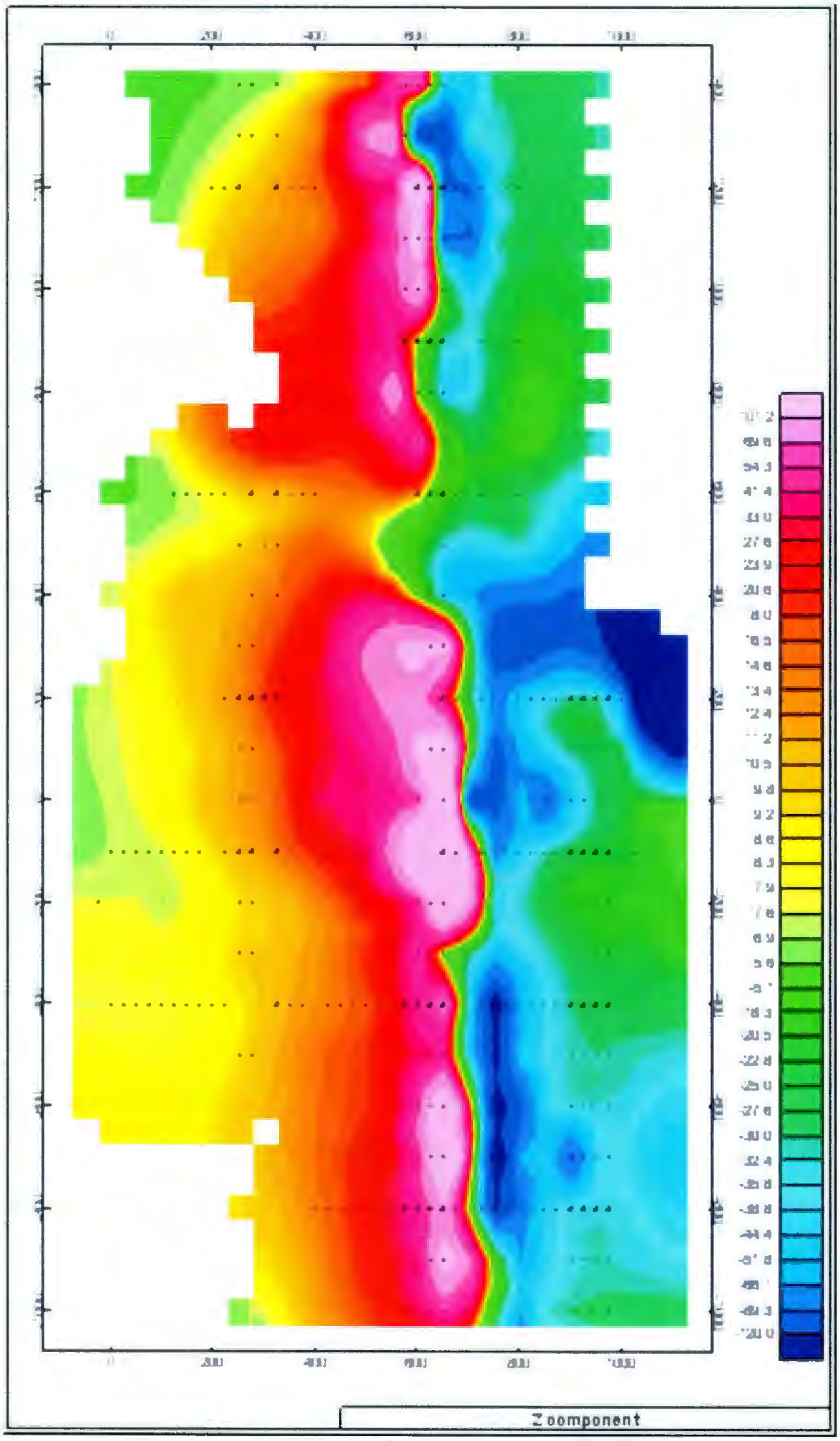

Field Example 3: *z* component

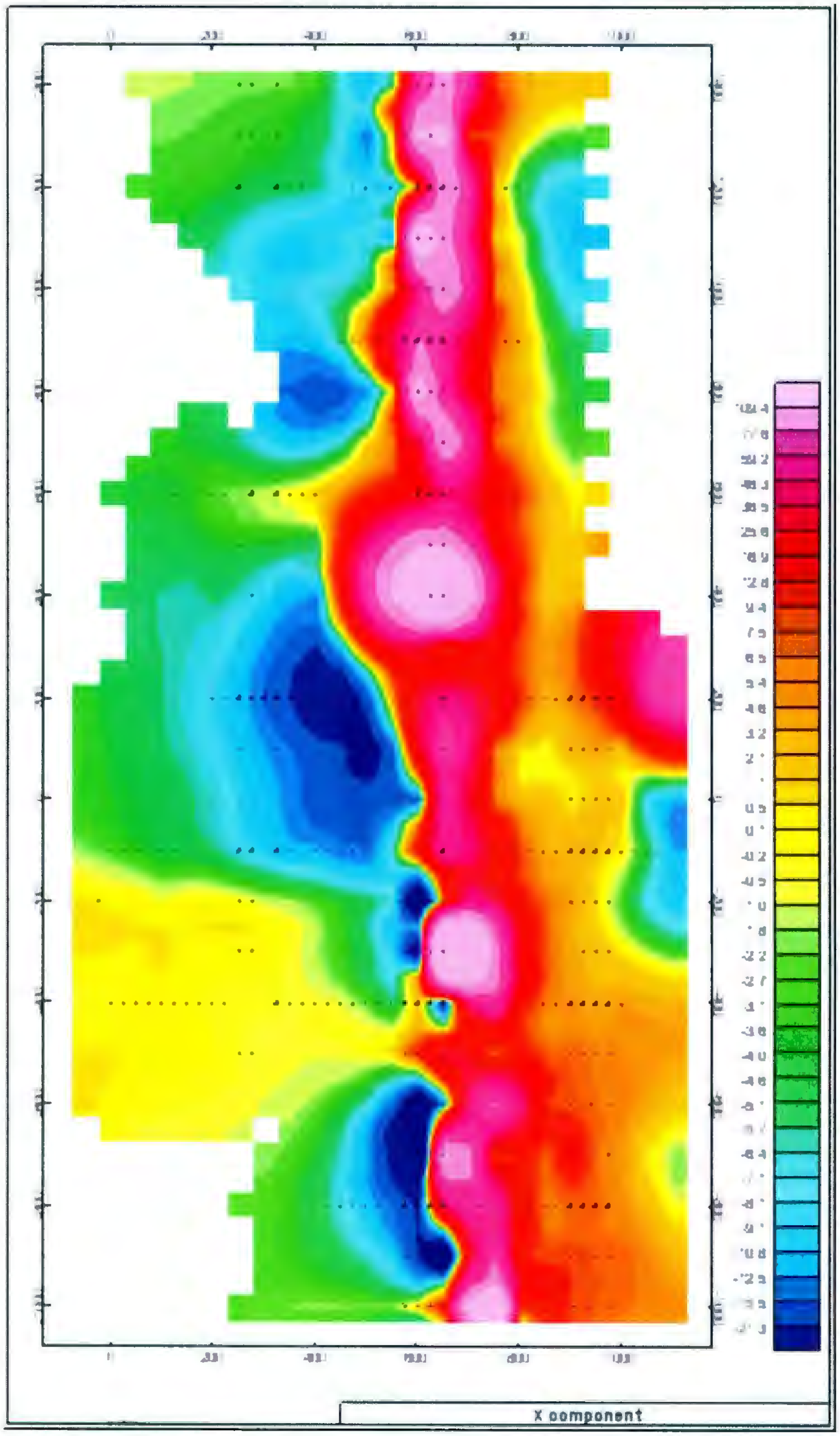

Field Example 3: *x* component

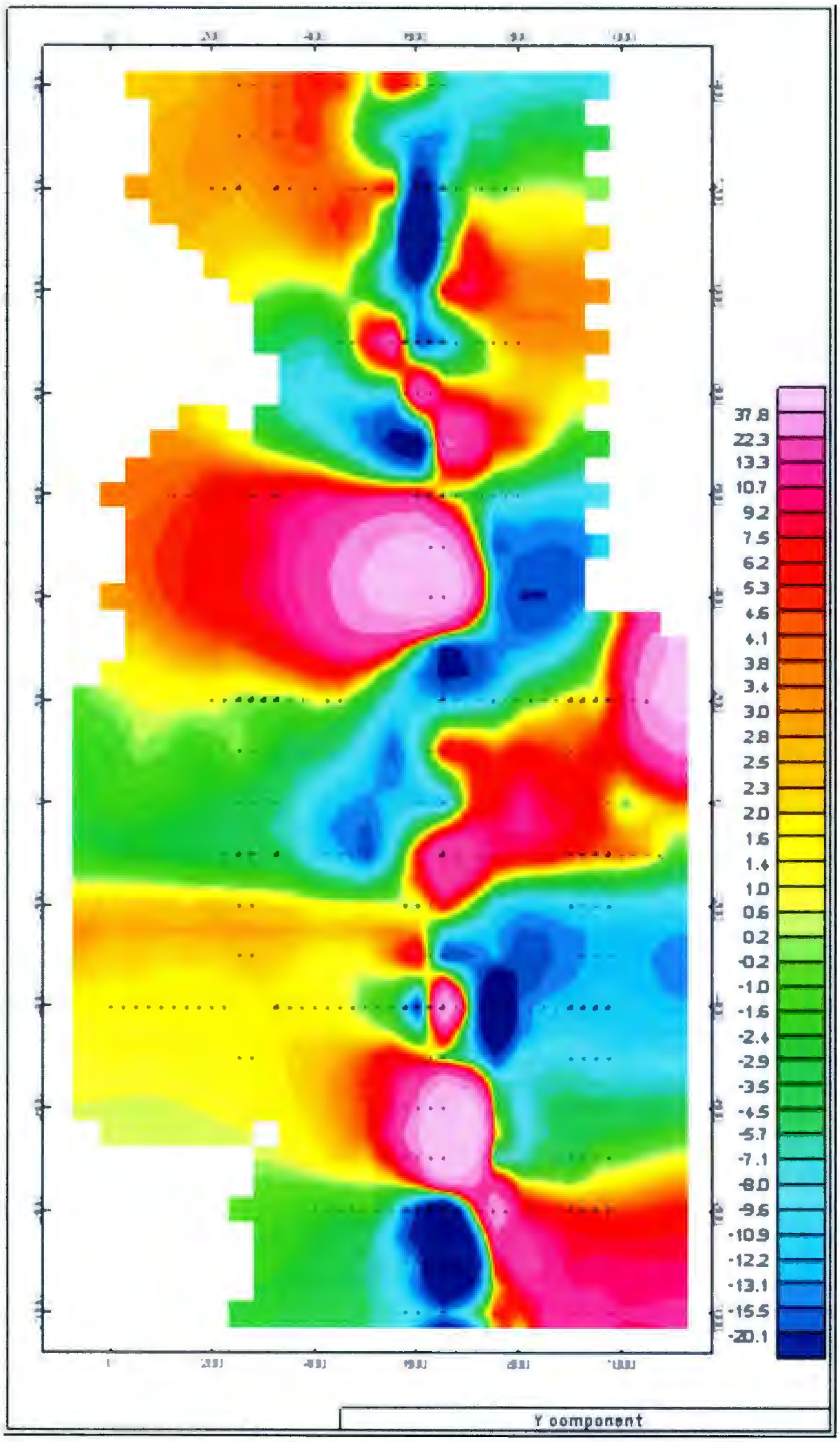

Field Example 3: *y* component

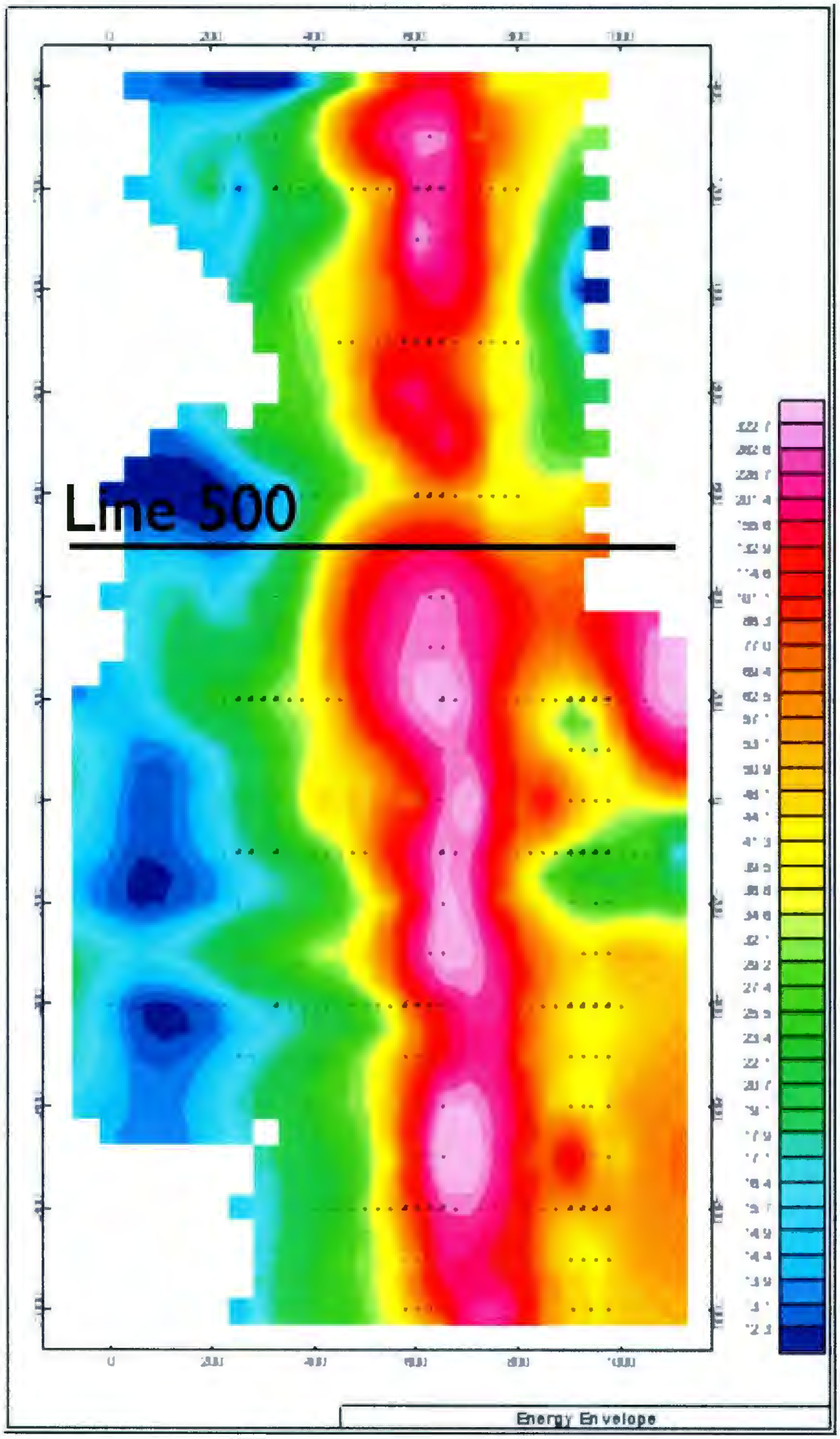

Field Example 3: Energy Envelope

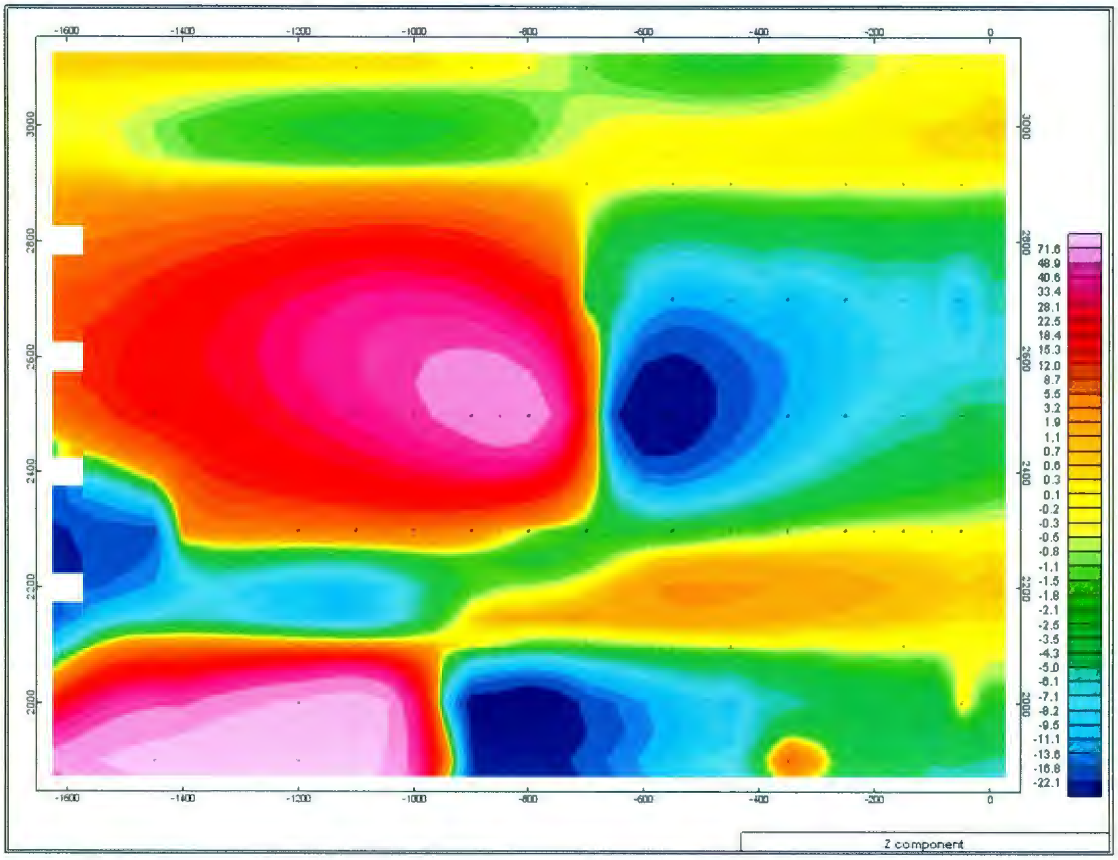

Field Example 4: *z* component

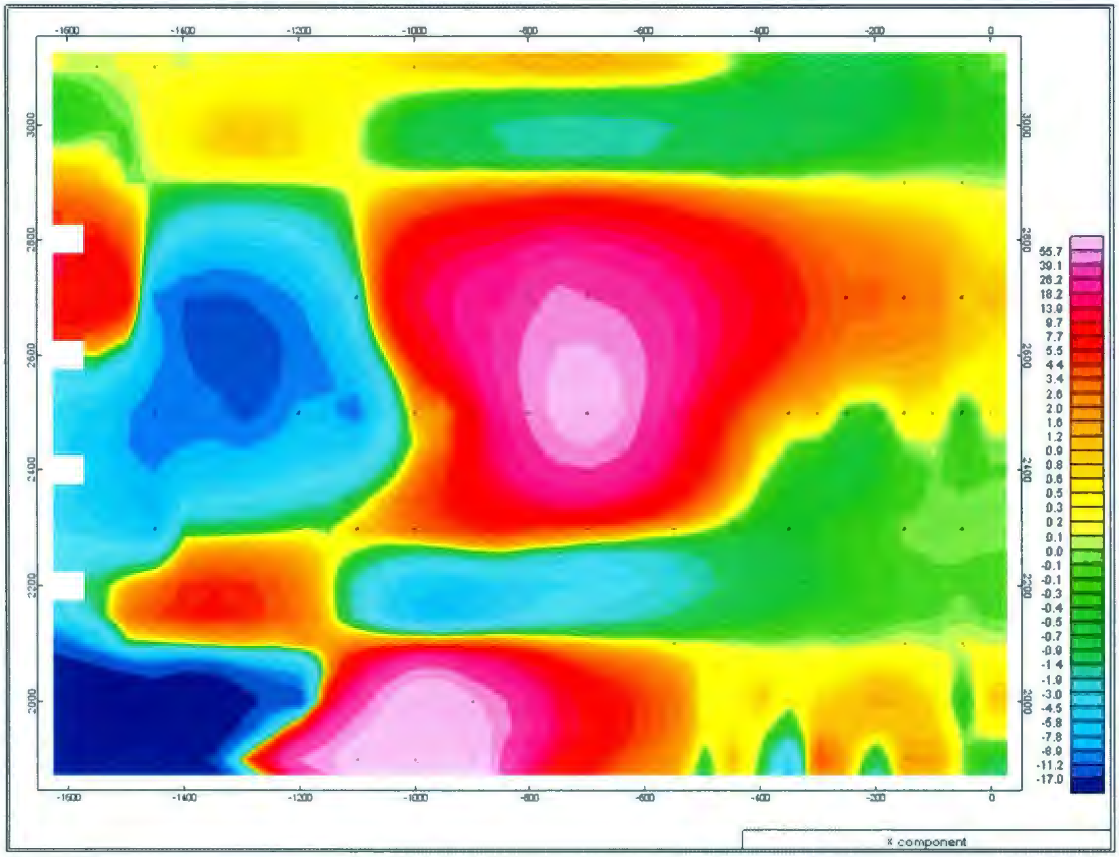

Field Example 4: *x* component

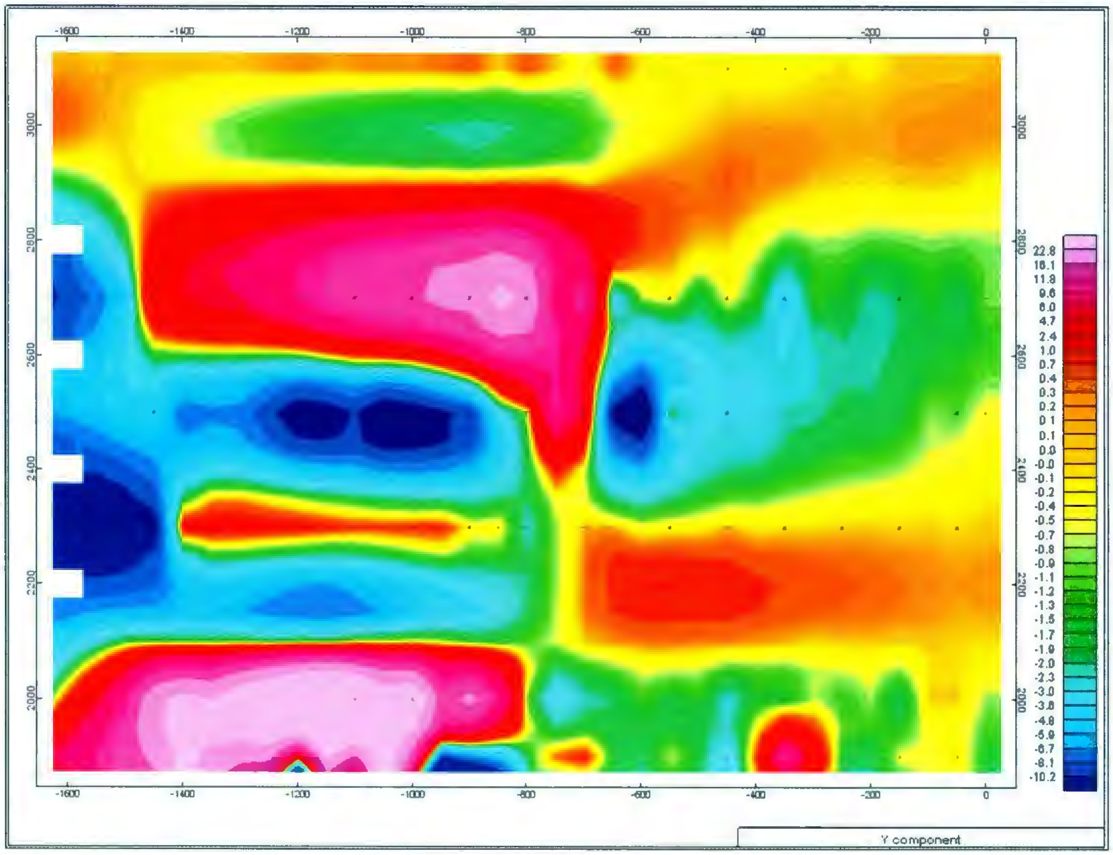

Field Example 4: *y* component

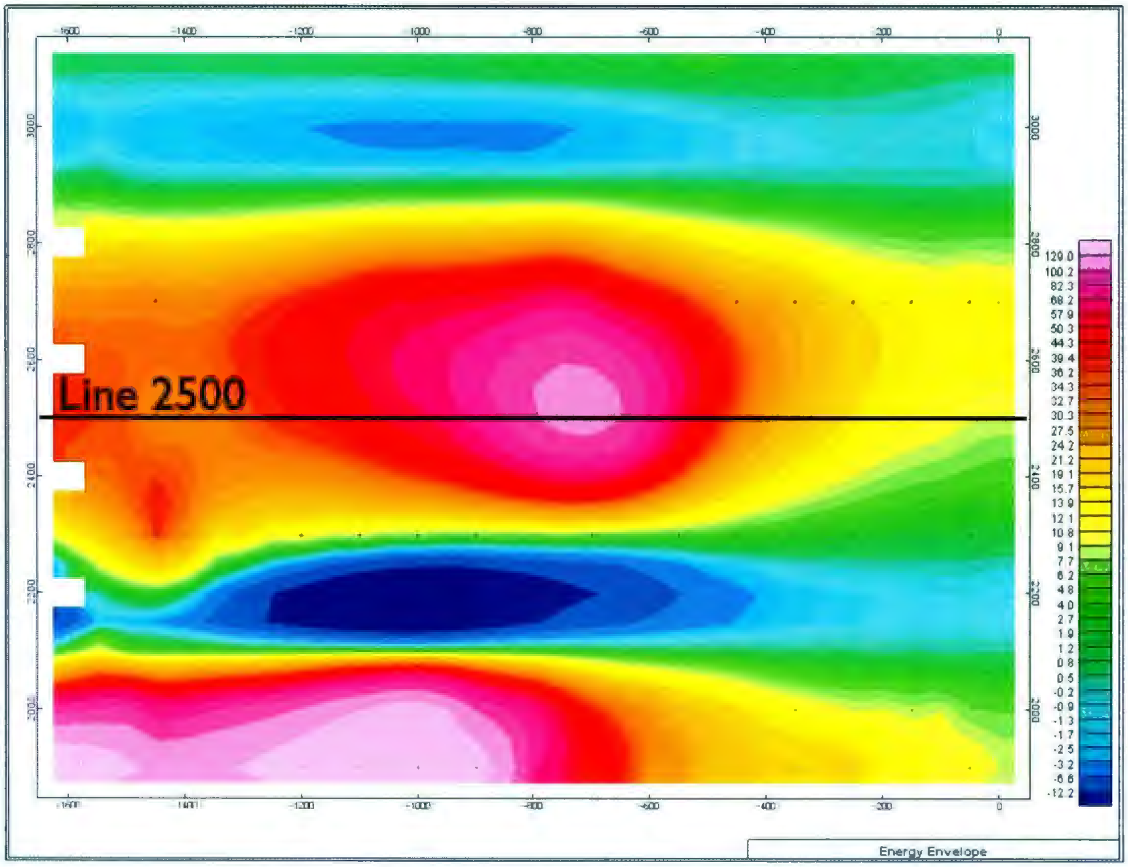

Field Example 4: Energy Envelope

BIBLIOGRAPHY

Akgün, M., 2001. Estimation of some bodies parameters from the self potential method using Hilbert transform. Journal of the Balkan geophysical society. vol. 4, no. 2 , p. 29-44.

Bournas, N. and Baker, H. A.. 2001. Interpretation of magnetic anomalies using the horizontal gradient of the analytical signal. Annali di Geofisica. vol. 44, no. 3, p. 05-526.

Debeglia, N. and Corpel, J., 1997. Automatic 3-D interpretation of potential field data using analytic signal derivatives. Geophysics. vol. 62, no. 1, p. 87-96.

Diniz, P. S., Silva, E. A. and Netto, S. L., 2002. Digital Signal Processing: System Analysis and Design. Cambridge University Press

Gabor, D., 1946. Theory of Communication. Journal of the IEE. vol. 93, p. 429-457

Grant, F. S.. and West, G. F., 1965. Interpretation theory in applied geophysics: New York, McGraw-Hill. Book Co., Inc.

Macnae, J. C., 1978, Primary E&H Fields from a Polygonal Loop, University of Toronto, Master's degree thesis, p. 102.

Nabighian, M. N. and Macnae, J. C., 1987. Time Domain Electromagnetic Prospecting Methods. In: Nabighian, Misac N., Electromagnetic Methods in Applied Geophysics. SEG, Tulsa, OK

Nabighian, M.N., 1984, Toward the three- dimensional automatic interpretation of potential field data via generalized Hilbert transforms: Fundamental relations. Geophysics. vol. 49, no. 3, p. 780-786

Nabighian, M.N., 1974. Additional comments on the analytic signal of two-dimensional magnetic bodies with polygonal cross- section. Geophysics. vol. 39, no. 1, p. 85-92

Nabighian, M. N., 1972. The analytical signal of two-dimensional magnetic bodies with polygonal cross-section: Its properties and use for automated anomaly interpretation. Geophysics, vol. 37, no. 3, p. 507-517.

Roest, W. R.. Verhoef, J. Pilkington, M. 1992. Magnetic interpretation using the 3-D analytic signal. Geophysics, vol 57, no. 1, p. 116-125.

Smith, R. S. and Keating, P. B., 1996. The usefulness of multicomponent, time-domain airborne electromagnetic measurements. Geophysics, vol. 61, no. 1, p. 74-81.

Spies, R., 1975. The dual loop configuration of the transient electromagnetic method. Geophysics, vol. 40, no. 6, p. 1051-1057.